Cryptic diversity in a seemingly paraphyletic lichen genus

A molecular phylogenetic study of *Calvitimela*

Markus Osaland Fjelde

Master Thesis
Biodiversity and Systematics
60 credits

Natural History Museum
Faculty of Mathematics and Natural Sciences

UNIVERSITY OF OSLO

June 2021

Cryptic diversity in a seemingly paraphyletic lichen genus

A molecular phylogenetic study of *Calvitimela*

2021

Cryptic diversity in a seemingly paraphyletic lichen genus

A molecular phylogenetic study of *Calvitimela*

Author: Markus Osaland Fjelde

http://www.duo.uio.no/

Print: Reprosentralen, Universitetet i Oslo

Acknowledgements

I would like to give a huge thanks to my supervisors at NHM Einar Timdal, Mika Bendiksby and Reidar Haugan. You have all inspired me. Einar, this would not have been possible without your limitless knowledge of lichens, their taxonomy, and your contagious curiosity for nature. Mika, your working ethics and eye for detail, critical feedback and phylogenetic expertise has been essential for pushing me in the right direction. Reidar, your unparalleled understanding of lichen diversity and amazing company on field trips have given me both a bad self-esteem (because I understand how little I know) but also memories for life. Somehow, I thought playing in a biology band was the narrowest and niche thing I was ever going to experience, that was before I was introduced to the internal lichen humor at NHM (*Rhizocarpon simillimum*). I would also like to thank Siri Rui for all the nice conversations and for always being kind, and your invaluable assistance with loans and specimens. I am also very grateful to the kind people at the DNA laboratory at NHM for being so eager to help. A special thanks to Lisbeth Thorbek for providing an excellent introduction and training in lab procedures. Thanks to all collaborators for providing material: Dr. Alan Fryday, M.Sc. Jean Gagnon, Dr. Serge Payette, Dr. Jean Carlos Villareal, Dr. Walter Obermayer, Dr. Toby Spribille and Dr. Stefan Ekman. Annie, thanks for all the fruitful conversations and your constant willingness to figure things out (for me!), you have really lifted the lichen group to a new level in your short time being here. Solveig, you truly are a role model for the next generation of systematists, and I really appreciate all the good talks we´ve had about phylogenetics (also thanks for letting me borrow your InDesign account for almost two years!). I am doubtful that any person in the world would be as good a work partner as you Erik, you are irreplaceable. I have really enjoyed our time together in the last couple of years. I hope we can continue to discover the beautiful world of crustose lichens as “boulder brothers” in the future. Vilde, I just could not have done this without you, thank you for always being there and supporting me, through my ups and downs. You mean the world to me. Lastly, I want to express my utmost appreciation to everyone who helped with reading, commenting, and giving feedback on the thesis manuscript, you know who you are, thank you so much!

Abstract

Molecular phylogenetics has revolutionized the taxonomy of crustose lichens and revealed an extensive amount of cryptic diversity. Resolving the relationships between genera in the crustose lichen family Tephromelataceae has proven difficult and the taxon limits within the genus *Calvitimela* are only partly understood. In this study, I tested the monophyly of *Calvitimela* and investigated phylogenetic relationships at different taxonomic levels. To ultimately contribute towards a more natural classification of the genus, I used an integrative taxonomic approach. Freshly collected material from Norway and fungarium specimens of all species currently assigned to *Calvitimela* (including available holotype, isotype and lectotype material) formed the foundations for the study. Additional population sampling of *Calvitimela melaleuca* sensu lato across Norway was performed. Chemical and morphological characters were analyzed to test their diagnostic values in the genus. More than 300 sequences from five different loci (ITS, LSU, MCM7, mtSSU, TEF1-α) were produced and used, together with existing molecular data, to infer phylogenetic relationships in *Calvitimela*. The divergence time estimates from molecular dating were used as an assisting tool to circumscribe natural taxa. Additionally, the potential reasons for non-phylogenetic signal were explored. My molecular phylogenetic results show deeply divergent lineages in *Calvitimela*. Morphological characters are uncovered as overlapping between divergent subgenera in the genus, whereas chemical characters are informative at the level of subgenera, but largely homoplastic at species level. Moreover, the subgenus *Calvitimela* is found to constitute four distinct genetic lineages, and detailed morphological examinations of *C. melaleuca* s. lat. reveal differences between taxa previously assumed to be morphologically cryptic. Population level analyses of *C. melaleuca* s. lat. corroborate the species to be paraphyletic. Furthermore, young evolutionary ages and signs of gene tree discordance indicate a recent divergence and possibly incomplete lineage sorting in the subgenus *Calvitimela*. Phylogenetic analysis of the mtSSU suggests that the Antarctic species *C. uniseptata* belongs in *Lecania* (Ramalinaceae). I also find molecular evidence for *C. septentrionalis* being sister to *C. cuprea*. In the subgenus *Severidea*, one new grouping is recovered as a highly supported sister to *C. aglaea*. Lastly, two fertile specimens are found to be phylogenetically nested within the sorediate species *C. cuprea*. I discuss the need for an updated classification of *Calvitimela* and the role of cryptic diversity in an evolutionary context. Through generic circumscription and species delimitation I argue for a practical taxonomy in *Calvitimela*.

Table of contents

1 Introduction

Calvitimela Hafellner is a circumpolar lichen genus in the family Tephromelataceae (Lecanorales, Lecanoromycetes) inhabiting rocks in primarily alpine and arctic regions. Members of the Tephromelataceae are crustose lichens with green algal (chlorococcoid) photobionts and lecideine or lecanorine (only in *Tephromela* M. Choisy) apothecia. The family consists of the genera *Tephromela*, *Calvitimela*, *Mycoblastus* Norman and *Violella* T. Sprib. Together, these four genera constitute a well-supported monophyletic group, that is, they share a common ancestor (Spribille et al. 2011a; Bendiksby et al. 2015). Historically, however, the species now assigned to *Calvitimela* were placed in the huge, classical genus *Lecidea* Ach., for instance by Fries (1874; as *Lecidea* strips *L. armeniacae*) and Magnusson (1931; as "*Lecidea armeniaca*- und *elata*-Gruppe"). Hertel & Rambold (1985) split the 'calvitimelas' out from *Lecidea* and placed them in the genus *Tephromela*. The generic name *Tephromela* had recently been resurrected by Hafellner (1984) for a small group of species split out from *Lecanora* Ach. Hafellner (1984), at the same time, described the new monotypic family Tephromelataceae. Hence, in the taxonomy of Hertel & Rambold (1985), *Tephromela* contains both species with lecideine and lecanorine apothecia, a character which is often used at the generic or family level. Hafellner and Türk (2001) then removed the species having lecideine apothecia (i.e., the 'calvitimelas') from *Tephromela* and introduced the new genus *Calvitimela*. In the most recent update on ascomycete taxonomy, Lücking et al. (2017) recognized 10 species of *Calvitimela* (Fig. 1A-I, the species *C. septentrionalis* (Hertel & Rambold) McCune is not depicted), 10 of *Mycoblastus*, 30 of *Tephromela*, and two of *Violella*.

In the influential molecular phylogenetic works on the Lecanoromycetes by Miadlikowska et al. (2006; 2014), they found *Mycoblastus* and *Tephromela* grouping together as the sister group to the morphologically diverse families Lecanoraceae and Parmeliaceae. Arup et al. (2007) were the first to show that *Calvitimela* grouped together with these two genera (i.e., *Mycoblastus* and *Tephromela*) while investigating the sister group relations of the Parmeliaceae. Their phylogenetic results, based on DNA sequences of the nuclear ribosomal cistron, the ITS and LSU markers, indicated a heterogeneous clade consisting of the three genera, that is, both *Calvitimela* and *Mycoblastus* were recovered as paraphyletic. In a photobiont study of the *T. atra* group by Muggia et al. (2008), *C. armeniaca* together with *Mycoblastus sanguinarius* were recovered as sister taxa to the core *Tephromela*. A few years later, Spribille et al. (2011a) described the genus *Violella* and found *Calvitimela*, *Tephromela* and *Violella* to constitute a well-supported monophyletic entity with *Mycoblastus* as their closest relative.

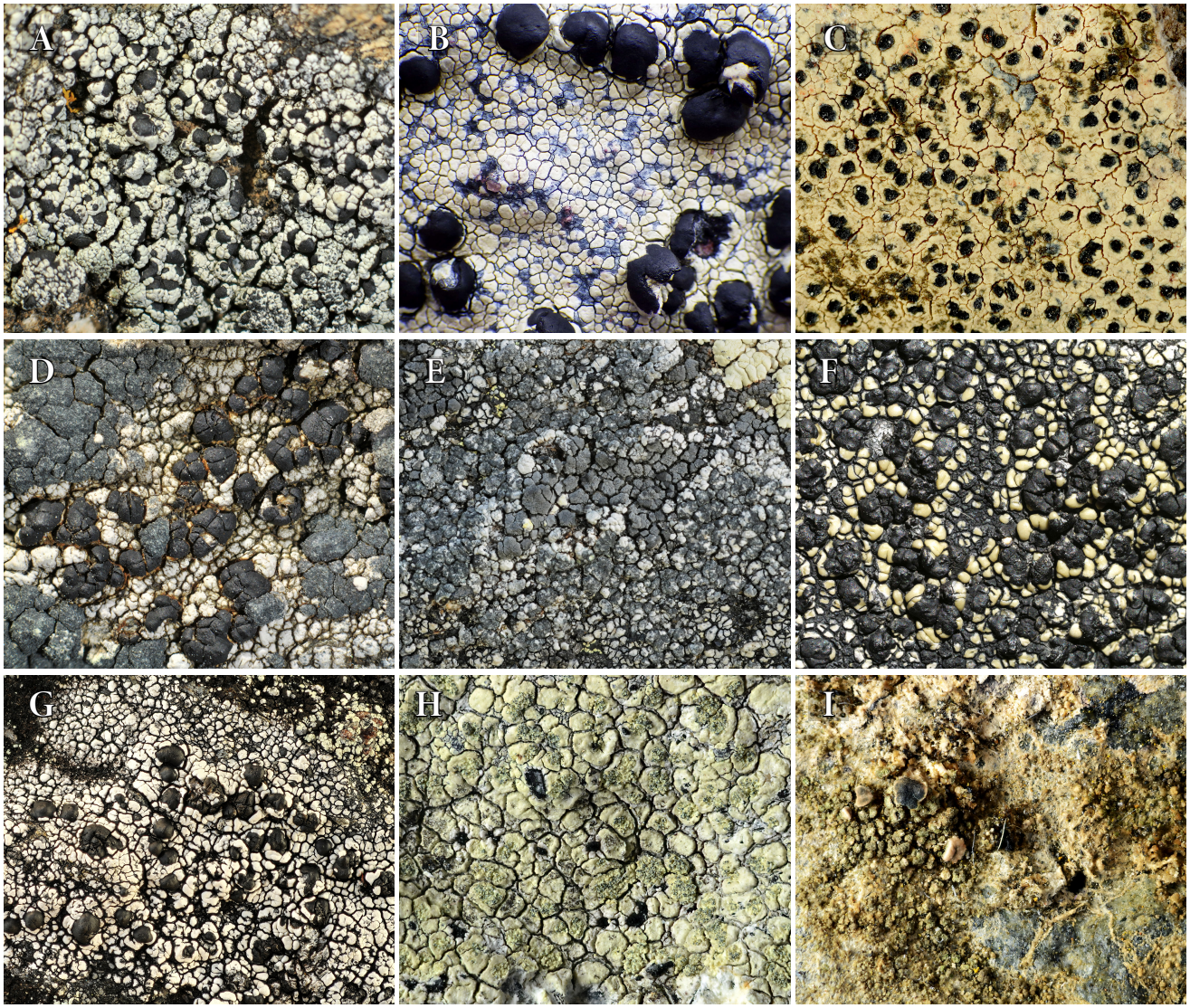

Figure 1. The species currently belonging to *Calvitimela* (except *C. septentrionalis*), **A**: *Calvitimela aglaea* (Sommerf.) Hafellner (O-L-173831), **B**: *C. armeniaca* (DC.) Hafellner (O-L-195741), **C**: *C. austochilensis* Fryday (MSC-0057474), **D**: *C. cuprea* Haugan & Timdal (O-L-179616), **E**: *C. livida* Haugan & Timdal (O-L-163835), **F**: *C. melaleuca* (Sommerf.) R. Sant (O-L-195711) **G**: *C. perlata* (Haugan & Timdal) R. Sant (O-L-163770), **H**: *C. talayana* (Haugan & Timdal) M.P. Andreev (O-L-225289), **I**: *C. uniseptata* G. Thor (UPS-L-838893). Photos: Einar Timdal and Markus O. Fjelde.

In their molecular phylogenetic study of *Calvitimela* sensu lato, based on three nuclear markers (ITS, TEF1-α, MCM7), Bendiksby et al. (2015) pointed to taxonomic challenges at different taxonomic levels in need of more in-depth studies: (1) The largely unresolved phylogenetic relationships between the genera *Tephromela* and *Violella* and the subgenera introduced by Bendiksby et al. (2015) (i.e., *Calvitimela* subgen. *Calomela*, *Calvitimela*, *Paramela*, and *Severidea*) and (2) the taxonomic challenges of the subgenus *Calvitimela* (i.e., *Calvitimela* sensu stricto), which included a paraphyletic *C. melaleuca* (see Fig. 1), uninformative morphology, and a confusing pattern of secondary metabolites.

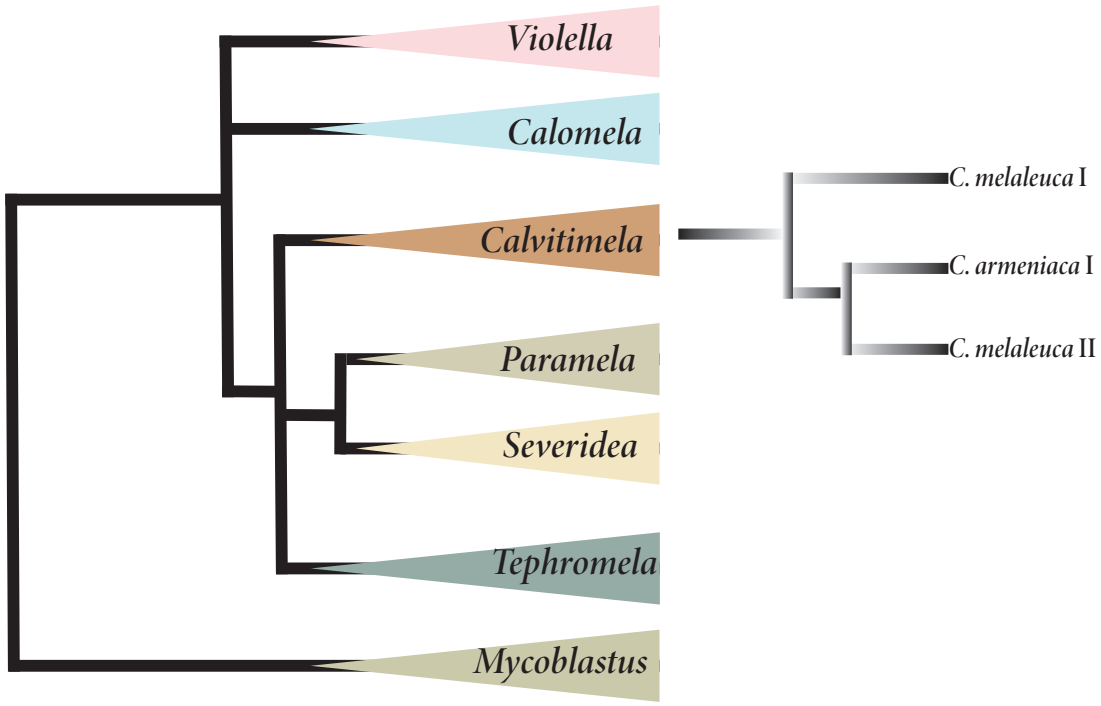

Figure 2. A schematic illustration of the phylogenetic relationships between the genera and subgenera in the Tephromelataceae (left), and between the lineages in the subgenus *Calvitimela* (right), based on results by Bendiksby et al. (2015).

The idea that lichens are symbiotic partnerships has been around since the late 1800s (Schwendener 1869); a symbiosis between one fungal (the mycobiont) and one algal and/or cyanobacterial component (the photobiont). Due to rules by the International Code of Botanical Nomenclature, starting in 1950, the taxonomy of lichens is based on the fungal component. This has come to shape the way lichenologists view and study lichens. That is with a focus on the main (usually ascomycete) fungus of the lichen.

The traditional way of circumscribing lichen species based on morphological and chemical traits are still central in lichen taxonomy. Crustose lichens have few morphological characters on which to base taxonomic conclusions. For this group, therefore, the use of thin layer chromatography (TLC), which is a method for documenting differential expression of secondary metabolites (hereafter referred to as "chemistry"), has been essential for species recognition and delimitation (see e.g., Culberson 1969 and references therein). However, not all lichens have detectable or informative chemistry (see LaGreca et al. 2020 and references therein), and even when including all available morphological and TLC data, the combination may not be enough to reach sensible species hypothesis.

The advent of DNA sequencing and molecular phylogenetics, enabling the analyses of evolutionary relationships based on many more characters, has essentially revolutionized the taxonomy of crustose lichens. Moreover, an extensive amount of so-called cryptic species has been revealed using molecular phylogenetics

(e.g., Crespo and Lumbsch 2010, Singh *et al*. 2015, Schneider *et al*. 2016, Leavitt *et al.* 2016; Haugan & Timdal 2019). Cryptic species are here understood as taxa that cannot readily be distinguished morphologically, with evidence (usually molecular) that suggest they are on different evolutionary trajectories (Struck et al. 2018a). Following the discovery of cryptic species, not rarely, overlooked diagnostic morphology becomes evident (e.g., Frolov et al. 2016). Such species are then often referred to as semi- or pseudocryptic species (e.g., Mann & Evans 2008). Two related concepts in lichenology are the terms "species pair" and "sibling species". The former refers to the phenomenon when two lichens only differ by their reproductive strategy (see Poelt 1970; Mattson & Lumbsch 1989), where a "primary species" produces sexual reproductive structures and a "secondary species" reproduce by asexual propagules or fragmentation. The latter refers to a special case of cryptic species: "…Species recognized primarily by cryptic or non-morphological discontinuities" (Culberson 1986), essentially meaning morphological indistinguishable taxa with for instance different chemistries. Today, a more restricted definition of sibling species refers to cryptic species that are monophyletic (Lumbsch & Leavitt et al. 2011).

The current recommended way to circumscribe fungal species is through a combination of a genealogical, phenotypical, geographical and/or recombinational approach (i.e., integrative taxonomy; Lücking et al. 2020). Practically this process includes first establishing species hypotheses through for instance a phylogenetic species concept and often using a genealogical concordance approach if multiple genes are available (see Taylor et al. 2000). Ultimately, the idea is that collection of data to investigate if other sources of evidence support the initial hypotheses will provide a robust framework for recognizing species.

A wide array of genetically informative markers exists and are frequently used in molecular systematic research. Many important markers are ribosomal, like the nuclear small and large subunits (LSU and SSU) or the mitochondrial small subunit (SSU). The universal barcode for fungi, the nuclear ribosomal internal transcribed spacer region (ITS) is one of the most applied genetic regions for molecular studies of lichens. It is a non-coding multi-copy region of the ribosomal cistron, consisting of the ribosomal RNA 5.8S, which is flanked by the two often highly variable intron regions ITS1 and ITS2 (Schoch et al. 2012). A few protein coding genes have been used in *Calvitimela* and related groups in previous studies (Spribille et al. 2011; Bendiksby et al. 2015) such as the mini-chromosome maintenance factor 7 (MCM7) and the transcription elongation factor 1-α (TEF1-α). TEF1-α has been shown to be quite variable and sufficient at resolving species to generic relationships in the Tephromelataceae. Where MCM7 also partly shares these characteristics, Spribille et al. (2011b) showed a detectable level of substitution saturation with MCM7 when investigating the species *Mycoblastus sanguinarius*. When multiple changes have occurred along a string of DNA sequence that leads to underestimation of genetic distances, saturation of substitution is said to have happened (Philippe et al. 2011). This can result in unrelated taxa to be wrongly inferred as closely related through homoplasy. In the data used for phylogenetic reconstruction, structured noise like this is often referred to as non-phylogenetic signal (Philippe et al. 2011).

The efforts to decipher the tree of life lies more and more in the hands of molecular phylogeneticists. The probabilistic methods for phylogenetic tree inference such as Maximum Likelihood (ML) and Bayesian

inference have become increasingly important tools for phylogenetics in the last few decades. With new and faster algorithms, like those implemented in RAxML-NG (Kozlov et al. 2019) and the access to high performance computing clusters, it has become faster and easier to reconstruct hypotheses about the evolutionary past. Population genetics is also a useful tool for investigating the genetic differentiation between, and within, populations of lichen forming fungi (review: Werth 2010). When taxa are morphologically cryptic, population genetics can help quantify evolutionary change that can uncover underlying differences between them.

Molecular dating has become increasingly popular and is a valuable technique for understanding at which time scales evolutionary processes occur. It has even been proposed that a temporal approach to classify lichen groups could serve as an objective way of circumscribing taxonomic units (Divakar et al. 2017). Many methods for performing molecular dating analyses now exist with the different implementations in the software BEAST (Bouckaert et. al 2019) being widely used.

In this study, I use an integrative taxonomic approach to reach a better understanding of *Calvitimela*; the ultimate aim being to contribute towards a more natural classification of the genus. I combine molecular phylogenetics with studies of morphology and chemistry to study *Calvitimela* from the level of genus circumscription, through species delimitation and phylogenetic interrelationships, to population structure in *C. melaleuca*. The study is based on a broad and global taxon sampling with additional population sampling of *C. melaleuca* s. lat. from Norway. Much effort has been put into identifying phylogenetically informative morphological and chemical characters, including in-depth investigations of seemingly cryptic species. Lastly, I explore the sources of non-phylogenetic signal in the molecular data, and asses the genetic marker's ability to resolve phylogenetic relationships at different taxonomic levels.

2 Material and Methods

2.1 Taxon sampling

For this study I have investigated all currently recognized *Calvitimela* species through a global sampling approach. I have included both freshly collected material and fungarium specimens from various institutions (O, GZU, KGLO, MSC, QFA, UPS, WIS; Figs. 3 and 4; Table S1). In the summers of 2019 and 2020, the lichen group at O conducted fieldwork at a wide range of localities in Norway. Around 200 *Calvitimela* specimens were collected during this field work. I collected samples by hammer and chisel and dried them in paper bags before they were brought to O for further investigation. Two independent sampling schemes of *C. melaleuca* were performed. First, connected with the global sampling as described above, extensive collection of fresh material in Norway and fungaria material from around the world. Secondly, a population level sampling of *C. melaleuca* in Norway. Population samples were collected at four different localities (Fig. 11; Table S2). Small thallus fragments were taken from 20 individuals at each locality within a radius of up to 5 meters using a sterile knife. Throughout this thesis, I explicitly use the taxonomy of Bendiksby et al. (2015), referring to the subgenera they introduced.

2.2 Morphology and Chemistry

I examined the material morphologically under dissecting microscopes and compared against expert-controlled fungarium specimens. When available, type material was included (Table 1). Spore size was measured for selected specimens (Table S1). Thin cross sections of apothecia showing individual asci were cut and placed in a drop of 5% potassium hydroxide (KOH), and spore sizes were measured under light microscopes using immersion oil and 100X magnification. The spore size measurements were based on a single and suitable cross section (i.e., with at least 15 visible spores) from one apothecium per individual. All anatomically studied specimens were checked for crystals under polarized light. Amyloid reactions were tested after pretreatment with KOH, with a modified Lugol's solution, where water was replaced by 50% lactic acid.

Thin-layer chromatography (TLC) was performed on nearly all included specimens of *Calvitimela* (see Table S1) in accordance with the methods of Culberson (1972), Menlove (1974), and Culberson & Johnson (1982). Secondary chemistry was examined using the solvent systems A, B' and C and run-on glass plates for identifying fatty acids.

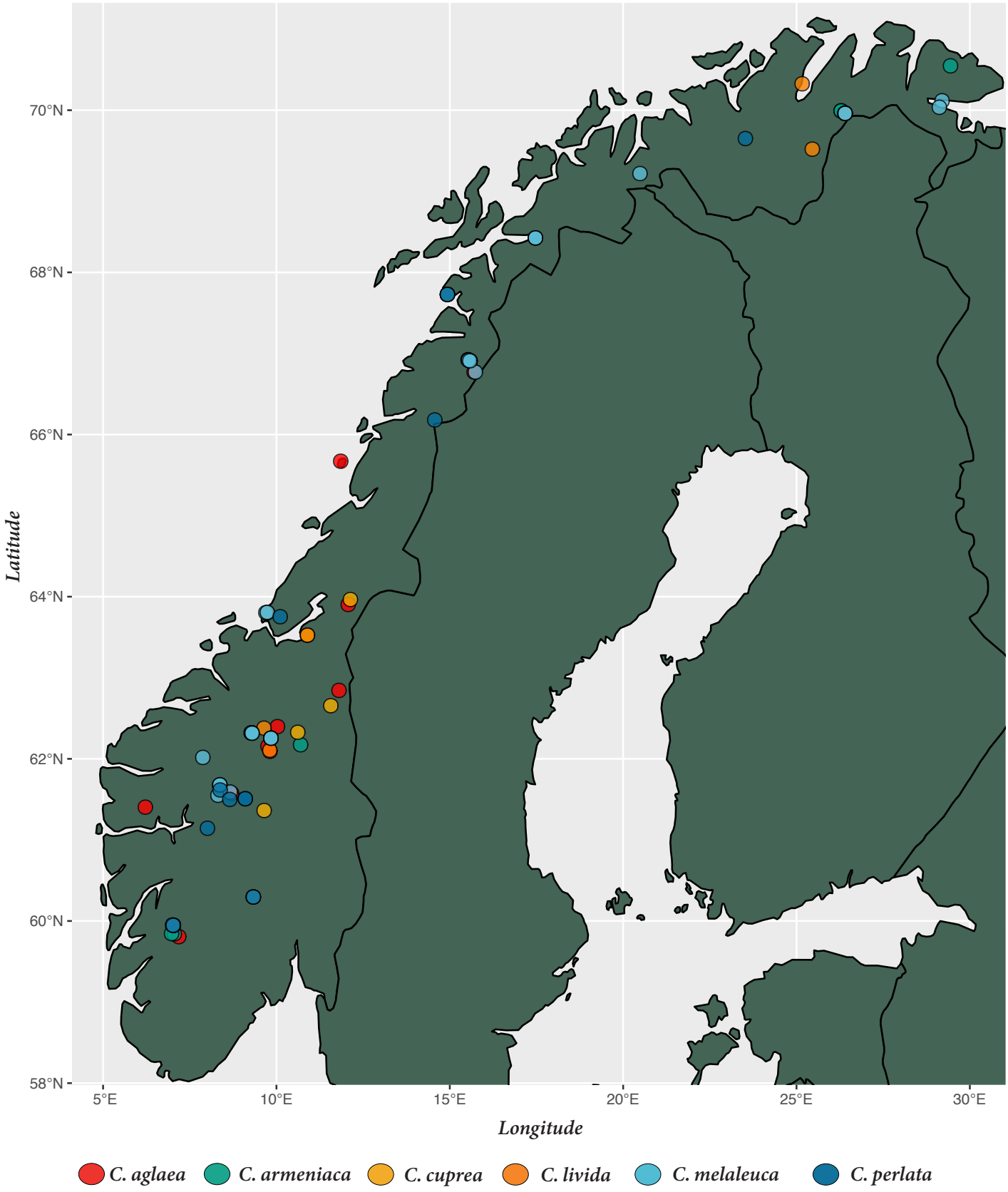

Figure 3. Map showing my taxon sampling of *Calvitimela* in Norway, including existing records at O, and records from field-work in the summers of 2019 and 2020. Colored points representing the six different species known to Norway. The distribution map was made in R using the packages *rnaturalearth* (South 2017) and *sp* (Pebesma & Bivand 2005; Bivand et al. 2013).

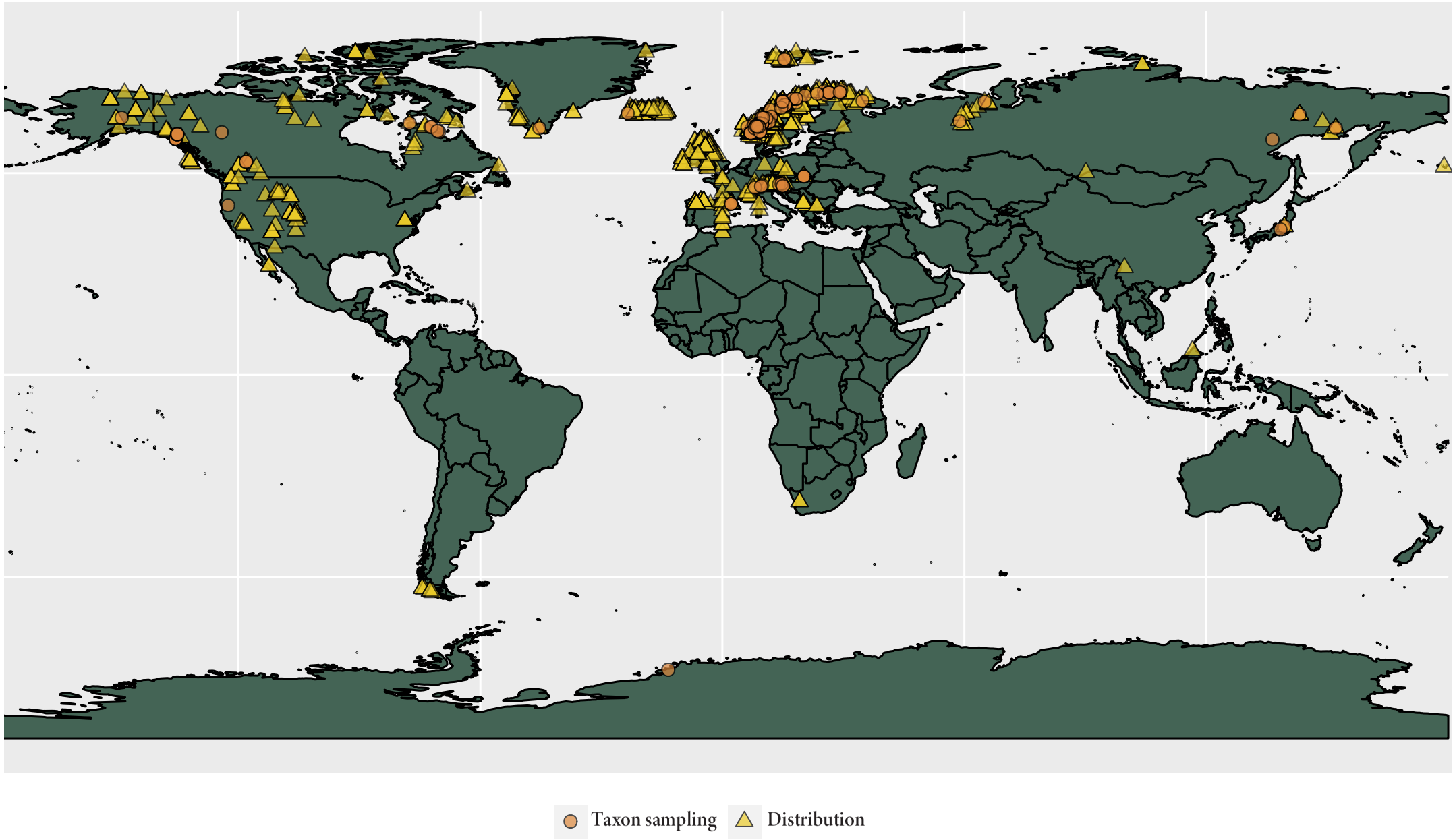

Figure 4. The world distribution of *Calvitimela* based on occurrence data downloaded from GBIF (as of May 2021; yellow triangles). Orange circles represent my taxon sampling for the current study. The distribution map was made using the R packages *rnaturalearth* (South 2017), *sp* (Pebesma & Bivand 2005; Bivand et al. 2013), and *rgbif* (Chamberlain & Boettiger 2017; Chamberlain et al. 2021) and mapped together with records produced during this study (Table S1).

Table 1. All type specimens observed during this study. The fungarium and voucher number, type identity, locality information, collection date, and collector are shown for the different types.

Taxon	Fungarium and voucher	Type	Country	Locality	Date	Collector
C. aglaea	O-L-000131	Holotype	NORWAY	NORDLAND, BODØ: Bodøe	June, 1826	S.C. Sommerfelt
C. austochilensis	MSC-0016623	Holotype	CHILE	MAGALLANES: Moorland on hill, S side of Caleta San José, Bahía 52˚51'S, 74˚28'W	October, 1969	H. Imshaug & K. Ohlsson
C. cuprea	O-L-179566	Holotype	NORWAY	HEDMARK, TYNSET: Fådalsgruva, old mine in Mt Gruvkletten 62˚19.63'N, 10˚36.88'E	June, 2012	M. Bendiksby et al.
C. livida	O-L-163835	Holotype	NORWAY	BUSKERUD, SIGDAL: Mt Holmevassnatten 60˚17.79'N, 9˚19.95'E	August, 2010	E. Timdal
C. melaleuca	O-L-001273	Lectotype	NORWAY	NORDLAND, SALTDAL: Saltd. in saxis alpis Baadfjeld	July, 1822	S.C. Sommerfelt
C. perlata	O-L-000125	Holotype	NORWAY	SØR-TRØNDELAG, OPPDAL Drivdalen, by the rapids in the lower parts of the river Kaldvella 62˚17'N, 9˚34'E	July, 1993	E. Timdal
C. talayana	O-L-000126	Holotype	RUSSIA	MAGADANSKAYA OBLAST: Khacynskii region: c. 26 km S of Myakit (=top of the pass on the road to Talaya) 61°11'N, 152°06'E	July, 1992	R. Haugan & E. Timdal
C. uniseptata	UPS-838893	Isotype	ANTARCTICA	DRONNING MAUD LAND: Vestfjella, the nunatak Basen, 1000 m NW of the Swedish station Wasa 73°02'S, 13°25'W	February, 1992	G. Thor

2.3 Molecular work

2.3.1 DNA extraction, PCR, and sanger sequencing

I extracted genomic DNA from dried tissue (apothecia and/or thallus) using the E.Z.N.A plant kit (Omega Bio-tek, Inc., Norcross, Georgia, U.S.A.), following the manufacturers guidelines except for a few modifications (as described by Bendiksby & Timdal 2013). I continued with polymerase chain reaction (PCR) using Illustra PuReTaq Ready-To-Go beads (GE Healthcare, Buckinghamshire, UK) following the protocol described by Kistenich et al. (2018), with modified volumes for each reaction: 0.3 µl of both primers and a total mixture volume of 11.8 µl, to which 0.7 µl DNA template was added. Primers are listed in Table 2. The following nuclear genetic regions were amplified: the internal transcribed spacer region (ITS1, 5.8S, ITS2), and the large subunit (LSU) of the nuclear ribosomal rRNA, the DNA replication licensing factor mini-chromosome maintenance factor 7 (MCM7), and the translation elongation factor 1-α (TEF1-α). Additionally, I amplified the mitochondrial ribosomal small subunit (mtSSU) using internal primers (mtSSU-RhiF, mtSSU-RhiR) when amplification was poor. The following PCR cycling conditions were used: 95 °C for 7 min, 35 cycles of 95 °C for 30 s, 58 °C for 30 s, 72 °C for 1 min, followed by 72 °C for 7 min. For the LSU marker slightly different cycling conditions were used: 95 °C for 7 min, 35 cycles of 95 °C for 30 s, 68-58 °C (touch down) for 30 s, 72 °C for 1 min, followed by 72 °C for 5 min.

Table 2. All primers used in the study and their associated loci, their nucleotide sequences (in 5'-3' direction), and their references.

Primer	Locus	Sequence	Reference
ITS1F	*ITS*	5'-CTTGGTCATTTAGAGGAAGTAA-3'	White *et al*. 1990
ITS4	*ITS*	5'-TCCTCCGCTTATTGATATGC-3'	–
LRlecF	*LSU*	5'-CCTCAGTAACGGCGAG-3'	Schneider *et al*. (2015)
LRlecR	*LSU*	5'- AGGCTTCGTCACGGAC-3'	–
mitSSU1	*mtSSU*[a]	5'- AGCAGTGAGGAATATTGGTC -3'	Zoller *et al*. (1999)
mitSSU3R	*mtSSU*[a]	5'- ATGTGGCACGTCTATAGCCC -3'	–
mtSSU-RhiF	*mtSSU*[b]	5'-ACCAGTAGTGAAGTATGTTATT-3'	Unpublished Möller *et al*. (2021)
mtSSU-RhiR	*mtSSU*[b]	5'-AATAACATACTTCACTACTGGT-3'	–
Tephr_mcm7F1	*MCM7*	5'- GCGGTTGCGAGATMTTYCARCC-3'	Bendiksby *et al*. (2015)
Tephr_mcm7R2	*MCM7*	5'- TTRATRTCYCCMCGDATHCGCA-3'	–
Tephr_tefF1	*TEF1-α*	5'- GGTGARTTCGARGCTGGTATCTC-3'	–
Tephr_tefR1	*TEF1-α*	5'- GACTTGAYRAAYTTDGGDGC-3'	–

I cleaned PCR products as described in Kistenich et al. (2018), with Illustra ExoProStar Clean-Up Kit (GE Healthcare, Buckinghamshire, UK), following the manufacturers guidelines, expect using a 10× dilution

of enzymes. The cleaned PCR products were sent for Sanger sequencing at Macrogen Europe (Amsterdam, The Netherlands) and the sample preparation was performed in line with the company's instructions.

2.4 Analyses

2.4.1 Assembly, alignment, and model testing

I assembled the sequences using Geneious Prime version 2020.1.2 (https://www.geneious.com/). An initial identity control was performed by searching our local BLASTn database (all lichen sequences in GenBank downloaded 2020-05-14 merged with all lichen sequences produced at O). I aligned sequences using Muscle (Edgar 2004) in Aliview (Larson 2014). To remove poorly aligned regions and make the trimming process reproducible I trimmed the alignments with Gblocks (Castresana, 2000; Talavera & Castresana, 2007) using the option for less stringent selection: allow gap position within the final blocks. The ITS sequences of the *C. melaleuca* populations aligned easily, and only the ends were manually trimmed away. Moreover, the alignments used for haplotype network construction and calculating population genetic metrics were reduced (see 2.4.3). Model testing was performed using PartitionFinder2 (Lanfear et al. 2016) applying the greedy algorithm (Lanfear et al. 2012), linked branch lengths and the starting Maximum Likelihood (ML) tree by PhyML (Guindon et al. 2010). Best fitting evolutionary substitution models were selected based on the small sample size corrected Akaike Information Criterion (AICc). The alignments of protein coding genes (MCM7 and TEF1-α) were partitioned according to codon positions, and the ribosomal marker (ITS) by the introns and ribosomal part (i.e., ITS1, 5.8S, ITS2). The alignments of the nuclear regions ITS, MCM7 and TEF1-α were concatenated applying the same partitions as described above.

2.4.2 Phylogenetic inference

I constructed ML phylogenetic trees of individual alignments (ITS, LSU, MCM7, mtSSU, TEF1-α) and concatenated alignments (ITS + MCM7 + TEF1-α) with 10 random starting trees and 1000 bootstrap replicates using RAxML-NG-MPI v. 1.0.2. (https://github.com/amkozlov/raxml-ng/releases/tag/1.0.2; Kozlov et al. 2019). All gene alignments (except LSU and mtSSU) were also subjected to Bayesian inference using the mpi version of MrBayes 3.2.7a (github.com/NBISweden/MrBayes/ tree/v3.2.7a; Ronquist et al. 2012). Phylogenetic analyses were carried out on the computer cluster Bioint01 (bioint01.hpc.uio.no) at the University of Oslo. For the separate gene trees, the Metropolis-Coupled Markov Chain Monte Carlo (MC^3) was run for 10 million generations (12 for the concatenated and 8 for the population alignment) with 4 separate chains and 4 individual runs sampling every 100th tree. Convergence and proper parameter mixing were assessed by inspecting trace plots in Tracer 1.7.1 (Rambaut et. al 2018), and by monitoring the value of the Average Standard Deviation of Split Frequencies (ASDSF) as the chains progressed. I assumed

convergence of the chains when a value of ASDSF < 0.01 was reached. The burnin values for tree summarization were set manually at the nearest round generation (e.g., 1 million or 2.5 million) after the ASDSF value had dropped under 0.01. Bayesian gene trees were summarized using the *contype* option *allcompat*, whereas the trees inferred from the concatenated dataset were summarized using the *halfcompat* option to get a 50 % majority rule consensus tree.

Molecular dating was performed using a two-step secondary calibration. Firstly, a molecular dating was performed on a dataset of the major groups in the Lecanoromycetes using the DNA sequences of LSU and mtSSU retrieved from GenBank (see Fig. S4). Secondly, I performed a dating analysis on a subset of the Tephromelataceae data (see Table S1) excluding the outgroup and reducing the number of accessions in well sampled groups (i.e., *Severidea* and subgenus *Calvitimela*). In both calibration steps, ML phylogenies were inferred using the same methods as described above, except only partitioning by each genetic region (i.e., LSU, mtSSU and ITS, MCM7, TEF1-α). The ML topologies were transposed to ultrametric using the function *chronopl ()* in the package *ape* (Paradis & Schliep 2019) in R version 4.0.3. (R Core Team 2020) applying the calibrations described below. The software BEAUTi implemented in BEAST 2.6.3 (Bouckaert et. al 2019) was used for setting up all the molecular dating analyses. The different gene partitions were defined with unlinked substitution models, unlinked clock models and linked trees. The following substitution models were used for the Tephromelataceae data ITS: GTR+G, MCM7: TVMef+G and TEF1-α: SYM+I+G, setting the number of gamma categories to 4 and the number of invariant sites to be estimated (for substitution models used for the Lecanoromycetes data see Fig. S4). The ultrametric ML topologies were used as guiding tree topologies. I used four calibration points from Nelsen et al. (2019) in the initial analysis of the Lecanoromycetes dataset (Fig. S4). Calibration priors were set by using the 95% highest posterior density (HPD) intervals for the crown age estimates inferred by Nelsen et al. (2019). These were used as upper and lower bounds on uniformly distributed priors. The following initial secondary calibration priors were set: Lecanoromycetes 199.7–303.0 million years ago (Ma), Telochistales 76.9–151.8 Ma, Caliciales 50.3–167.1 Ma and Cladoniineae 36.8–85.8 Ma. Most recent common ancestor (MRCA) priors were applied to the crown node of the Tephromelataceae in the first analysis and to the ingroup (all taxa except *Mycoblastus*) in the second analysis. I carried out two independent runs in BEAST 2.6.3 (Bouckaert et. al 2019) for both the Lecanoromycetes and Tephromelataceae data; one run with a log normal relaxed clock and one with a strict molecular clock. The age estimation (41.7–116.5 Ma) from the relaxed clock analysis on the crown node of Tephromelateaceae was used to calibrate the root node on the subset of the Tephromelataceae data (Table S1). For the Lecanoromycetes data the posterior was summarized with a maximum clade credibility (MCC) tree and median heights, using the software TreeAnnotator implemented in BEAST 2.6.3. Moreover, for the Tephromelataceae data, summarization was done onto the ultrametric ML topologies (see above) with both median and common ancestor heights (CA). All MCMC runs were run for 50 million generations, logging the trace and trees every 10^{4th} generation. I only discuss nodes relevant for answering the questions set in this thesis, specifically, excluding *Mycoblastus* and *Tephromela*.

I visualized phylogenetic trees in Dendroscope 3.7.5 (Huson & Scornavacca 2012) to confirm outgroup relationships and use the collapse function to inspect topologies with collapsed branches (with a cutoff bootstrap value of 75). I used Figtree 1.4.4 (http://tree.bio.ed.ac.uk/software/figtree/) to visualize and export tree files and pdfs for later editing in Adobe InDesign (Adobe Inc. 2021). Chemical and geographical characters were manually mapped on to the resulting phylogeny of the concatenated data, in addition to bootstrap values from the ML analysis of the same dataset. Chemical data was manually mapped on to the ITS topology of the *C. melaleuca* populations.

2.4.3 Population genetics

The haplotype network was constructed based on the parsimony criterion using the function *haploNet ()* in the R package *pegas* (Paradis 2010). The nucleotide diversity (π) was calculated in R using the function *nuc.div ()* in *pegas*. The measures of population divergence (d_{XY} and F_{ST}) were obtained by creating an object of class "genome" of the population alignment and retrieving the relevant summary statistics using the R package *PopGenome* (Pfeifer et al. 2014). Aiming to only capture the haplotypes of *C. melaleuca*, the outgroup, and accessions of *C. armeniaca* were removed from the alignment before haplotype network construction. Five data points (1_3, 1_14, 1_20, 3_7, 3_10; see Table S2) were excluded from the calculation of population genetic statistics, since they were seemingly not a part of the true populations sampled at each locality (see section 3.4). However, they were included in the haplotype network construction to assess the total number of haplotypes across all sampled individuals of the *C. melaleuca* populations.

2.4.4 Data exploration

The R environment was used for exploration of both the phenotypic (1) and molecular (2) data, respectively. (1) Spore size variation was investigated by plotting the mean width against the mean length for each observation (i.e., the mean of all 15 measurements for every individual measured) and fitting a line with the *stat_smooth ()* function implemented in *ggplot2* (Wickham 2016) using the method "*loess*", and a value of 1.5 for *span*. To search for potential taxon specific patterns ascribed to just spore length or spore width, boxplots for each were made by plotting the widths and lengths against taxa using *ggplot2* (Wickham 2016). (2) Substitution saturation plots were created by calculating the number of transitions and transversions at the third codon positions (MCM7 and TEF1-α) and the variable regions of ITS (ITS1 and ITS2) using the *titv ()* function in the package *Spider* (Brown et al. 2012) and plotting against the F84 distance calculated with *dist.dna ()* in the package *ape*. The rationale behind including a saturation plot of ITS was to compare, between the nuclear markers, at which level of genetic distance substitutions occur. Segregating sites and base frequencies were calculated with the functions *seg.sites ()* and *base.freqs ()*, respectively, in the package *ape*.

3 Results

3.1 Morphology and chemistry

I obtained spore sizes for 33 individuals from different fertile *Calvitimela* specimens with five individuals per taxon, except *C. cuprea* (N = 3), *C. melaleuca* clade III (N = 2) and *C. perlata* (N = 4), including the lectotype of *C. melaleuca* (Fig. 5; Table 1; Table S1). The largest differences in spore size occurred between *C. perlata* and all other taxa (Fig. 5). In addition, a difference between *C. melaleuca* I and *C. melaleuca* II was observed. The sister taxa *C. melaleuca* II and *C. armeniaca* had smaller spore sizes compared to *C. melaleuca* I and III, where spore width was the most distinguishing measure. The rest of the taxa had a general tendency to overlap in both spore length and width.

A morphological comparison between lineages in the subgenus *Calvitimela* uncovered a difference in thallus color between the two taxa *C. melaleuca* I and II (Fig. 6). The taxon *C. melaleuca* I exhibited white to occasionally light brown thallus color, whereas *C. melaleuca* II showed yellow to sometimes brownish-yellow thallus color. Only two specimens, one freshly collected (O-L-228122; Table S1; Fig. 6E), and one slightly older (QFA-0635917; Table S1) specimen of the clade *C. melaleuca* III were observed, and both had a thallus morphology resembling *C. armeniaca* (Fig. 6A-B) more than *C. melaleuca* s. lat (i.e., *C. melaleuca* I, II and III), with beige colored thallus (not observed for the older specimen due to color degradation) with areolae edges becoming “melanin” pigmented and appearing black to dark gray. Other morphological traits did not show any potential of predicting the phylogenetic clade in the subgenus *Calvitimela*. Some specimens were misidentified in the field, or had incorrect names in GenBank, see the footnotes of Table S1 for a full list of these vouchers. Members of *C. melaleuca* s. lat. showed a general tendency to grow in similar habitats when collected in the field.

One newly discovered clade, *C.* sp., in *Severidea* (Fig. 7A) was collected multiple times and in the field identified as *C. perlata*. In addition, two specimens (OL-228131; Fig. 7C and OL-228193) collected as *C. melaleuca* and *C. aglaea* respectively, were both fertile with whitish areolae, and they likely represent a new morphotype of the sorediate *C. cuprea* (Fig. 7B-C).

Chemistry profiles were acquired from selected specimens (Fig. 10; Table 3; Table S1). I identified the aromatic substances alectorialic acid, atranorin, norstictic acid, protocetraric acid, psoromic acid, stictic acid and usnic acid; the triterpene zeorin; and the fatty acids bourgeanic acid, norrangiformic acid, rangiformic acid, roccellic acid, and two unknown fatty acids; and two unknown acids.

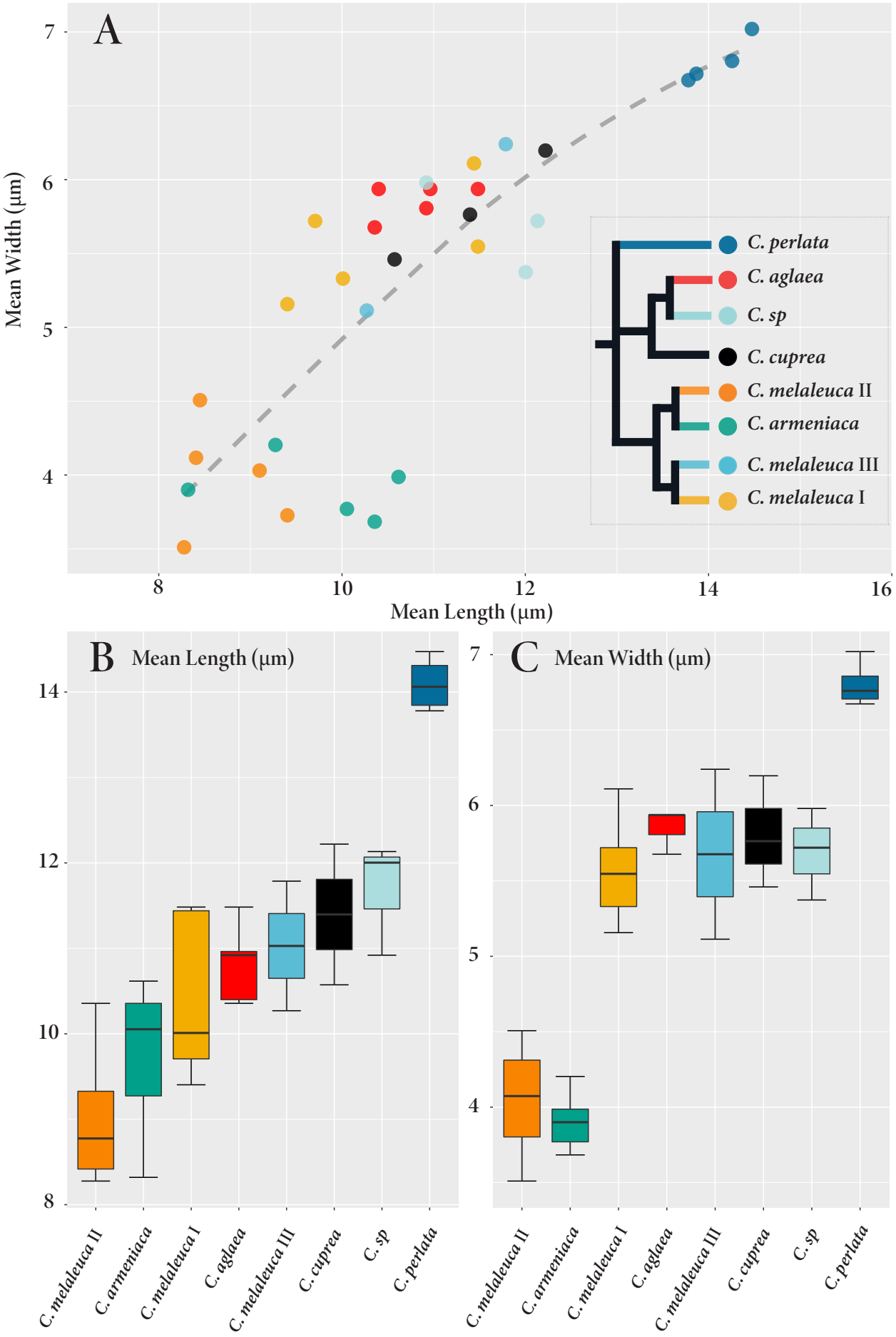

Figure 5. Spore size variation in *Calvitimela*. (**A**) Spore widths plotted against spore lengths from the mean of individual specimens measured, with a schematic topology of the relationships between taxa. (**B**) Spore length, and (**C**) spore width boxplots showing the interquartile range of the data, with whiskers corresponding to the maximum and minimum values, and the centered black line corresponding to the median. The color coding indicate the different taxa.

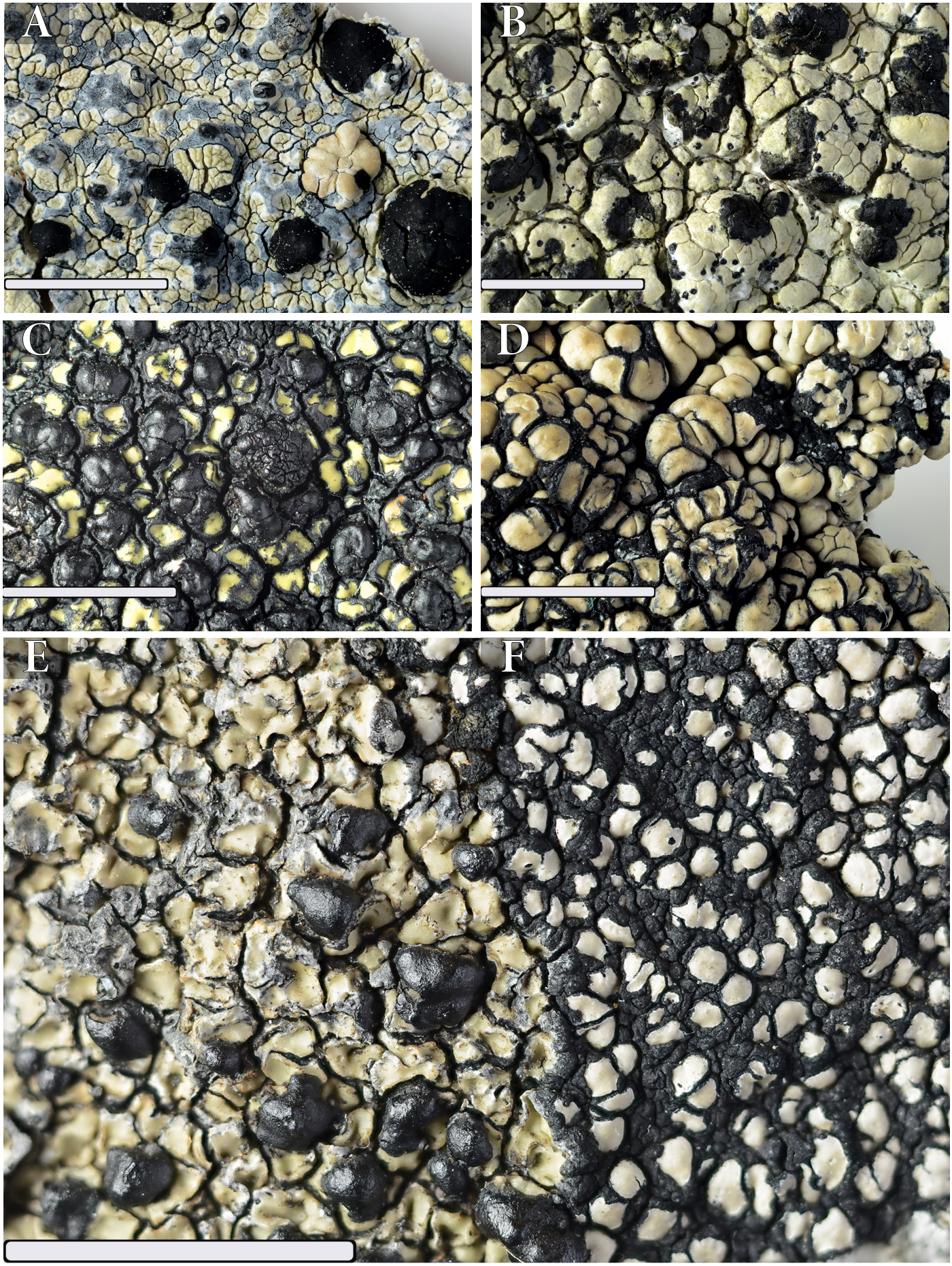

Figure 6. The different morphologies occurring in the subgenus *Calvitimela*, **A**: *C. armeniaca* (O-L-228166), **B**: *C. armeniaca* (O-L-228197) **C**: *C. melaleuca* II (O-L-225749), **D**: *C. melaleuca* I (O-L-225809) E: **C**. *melaleuca* III (O-L-228122) **F**: *C. melaleuca* I (O-L-228123). Scale bars = 5 mm. Photos: Einar Timdal and Markus O. Fjelde.

Figure 7. Curiosities from *Severidea*. **A**: the newly discovered clade *C.* sp. from Sigdal, Norway (O-L-200938). **B**: The sorediate *C. cuprea* (O-L-208192) from Gammalgruvan copper mine in Sweden **C**: The fertile *C. cuprea* (O-L-228131) from Saltdalen, Norway. Scale bars = 5 mm. Photos: Einar Timdal.

Table 3. Overview of the secondary metabolites occurring in *Calvitimela*. Abbreviations: ALE = Alectorialic acid, ATR = Atranorin, BOU = Bourgeanic acid, NOR = Norstictic acid, NRA = Norrangiformic acid, PRO = Protocetraric acid, PSO = Psoromic acid, RAN = Rangiformic acid, ROC = Roccellic acid, STI = Stictic acid, UF1 = Unknown fatty acid 1, UF2 = Unknown fatty acid 2, USN = Usnic acid, UN1 = Unknown substance 1, UN2 = Unknown substance 2. The following abbreviations indicate the degree of presence for the different lichen substances: M = major, m = minor, t = trace, ± = partly occurring, parentheses indicating rare occurrences and exclamation mark indicating very rare. [1]A single specimen of *C. livida* (O-L-228138) was found to contain norstictic acid, and [2]one specimen of *C. cuprea* (O-L- 228124) found to lack norstictic acid.

Species	ALE	ATR	BOU	NOR	NRA	PRO	PSO	RAN	ROC	STI	UF1	UF2	USN	UN1	UN2	ZEO	N
C. aglaea	–	**M**	**(±)M**	–	–	–	**(±!)**	–	–	**(±)**	–	–	**(±)M**	–	–	–	**26**
C. austochilensis	–	**M**		–	–	–	–	–	–	–	–	–	–	–	–	–	**2**
C. armeniaca	**M**	–	–	–	–	**(±)**	**±m**	–	**M**	–	–	–	–	–	–	–	**19**
C. cuprea	–	**M**	–	**t/m**[1]	–	–	–	–	–	**M**	–	–	–	–	–	–	**12**
C. livida	–	**M**	–	**(±!)**[2]	–	–	–	–	–	**M**	–	–	–	–	–	–	**10**
C. melaleuca I	**(±!)**	**(±)M/m**	–	**(±)**	–	**(±)**	**(±)M**	**(±)**	**(±)M**	–	**±**	**±**	–	–	–	–	**18**
C. melaleuca II	**±M**	–	–	**±**	**±**	–	**±**	**±**	**±**	–	**±**	**±**	–	–	–	–	**28**
C. melaleuca III	–	–	–	–	–	–	–	–	**M**	–	–	–	–	–	–	–	**2**
C. perlata	–	**M**	–	–	**M**	–	–	**M**	–	–	–	–	–	**±t/m**	**±t/m**	**(±)**	**12**
C. sp.	–	**M**	–	–	–	–	–	–	–	**M**	–	–	–	–	–	–	**4**
C. septentrionalis	–	**M**	–	–	–	–	–	–	–	**M**	–	–	–	–	–	–	**2**
C. talayana	–	**M**	**(±)t**	–	**M**	–	–	**M**	–	–	–	–	**M**	–	–	–	**5**
C. uniseptata	–	–	–	–	–	–	–	–	–	–	–	–	–	–	–	–	**1**

The two specimens that likely represent a new fertile morphotype of *C. cuprea* had the same chemistry as *C. cuprea* (atranorin, norstictic acid and stictic acid) and were recovered as nested within the *C. cuprea* clade (Fig. 10). The combination of atranorin, bourgeanic acid and usnic acid commonly occurred in *C. aglaea*. Stictic acid was also recorded in specimens of *C. aglaea* even with the absence of bourgeanic acid and usnic acid. *Calvitimela perlata* contained norrangiformic and rangiformic acid, two unknown substances, and zeorin (single occurrence). *Calvitimela talayana* exhibited atranorin, bourgeanic (single occurrence), norrangiformic acid, rangiformic acid and usnic acid. The subgenus *Calvitimela* displayed a lot of variation in chemistry. *Calvitimela armeniaca* usually contained alectorialic acid and roccellic acid, psoromic acid (single occurrence) and rarely protocetraric acid. In *C. melaleuca* I psoromic acid, roccellic acid, alectorialic acid (rare), protocetraric acid (rare), and a few occurrences of two unknown fatty acids were recorded. *Calvitimela melaleuca* II contained alectorialic acid, norstictic acid, norrangiformic acid, psoromic acid, rangiformic acid and roccellic acid to varying degrees, plus some rare occurrences of two unknown fatty acids. *Calvitimela melaleuca* III only displayed roccellic acid.

In total eight different substances were recorded from the population samples of *C. melaleuca*, five fatty acids: norrangiformic acid, rangiformic acid, roccellic acid and two unknown fatty acids, and three aromatic substances: atranorin, norstictic acid, and psoromic acid (Fig. 11; Table S2). In addition, a few occurrences of unknown acids were recorded (Table S2). In general, there was a lack of correlation between chemistries and phylogenetic clades (Fig. 10). However, individuals from population 1 tended to contain norstictic acid, norrangiformic acid, and rangiformic acid, and an unknown fatty acid (UNF2), whereas these substances were rare for the rest of the populations.

3.2 Molecular data

3.2.1 Genetic markers and amplification

I obtained 301 sequences: 171 from ITS (including 75 from the *C. melaleuca* populations), 12 from LSU, 51 from MCM7, 13 from mtSSU, and 54 from TEF1-α (Table S1). I experienced multiple copies of the LSU in the PCR products during gel electrophoresis with all *Calvitimela* amplicons. Due to low PCR success rate and the unclear phylogenetic signal from the mtSSU, I was unable to present a reasonable interpretation of these sequences (Fig. S2). Despite multiple attempts, I was not able to obtain sequence data for the species *C. austochilensis*. I was however able to acquire one mtSSU sequence from the Antarctic *C. uniseptata* and my phylogenetic analyses strongly support *C. uniseptata* to belong in the genus *Lecania* (Ramalinaceae; Fig. S3).

3.2.2 Alignments and substitution models

The alignments consisted of the sequences produced during this study and existing sequences mined from GenBank (Table S1). After the trimming of the different alignments, they consisted of the following number of accessions and total sequence lengths: ITS 181 and 501, MCM7 113 and 489, TEF1-α 110 and 804, population alignment (ITS) 81 and 588. The inferred substitution models differed amongst the loci and their partitions (Table 4).

Table 4. Metrics of the three nuclear loci (ITS, MCM7, TEF1-α) with number of accessions and the separate partitions used, where CP = Codon Position. Number of sites and segregating sites (including outgroup), base frequencies, and selected substitution models are shown for each partition and locus. The same information is shown for the alignment of population samples used for phylogenetic inference.

Locus	Data	Partition	# Accessions	# Sites	# Segregating sites	Base frequencies				Model
						A	C	G	T	
ITS	All	ITS1		177	166	0.147	0.329	0.291	0.233	GTR+I+G
		5.8S		157	36	0.272	0.233	0.240	0.255	GTR+I+G
		ITS2		167	124	0.222	0.273	0.273	0.232	GTR+I+G
Total		Full alignment	**181**	**501**	**326**	**0.213**	**0.279**	**0.268**	**0.240**	GTR+I+G
MCM7	All	CP 1		163	41	0.275	0.250	0.307	0.169	GTR+I+G
		CP 2		163	21	0.346	0.219	0.142	0.293	GTR+I+G
		CP 3		163	156	0.230	0.239	0.246	0.284	K80+I+G
Total		Full alignment	**115**	**489**	**218**	**0.284**	**0.236**	**0.232**	**0.249**	TVMEF+G
TEF1-α	All	CP 1		268	120	0.316	0.192	0.350	0.142	TRN+I+G
		CP 2		268	111	0.325	0.245	0.159	0.270	TRN+I+G
		CP 3		268	252	0.093	0.407	0.204	0.296	GTR+I+G
Total		Full alignment	**110**	**804**	**483**	**0.245**	**0.281**	**0.238**	**0.236**	SYM+I+G
ITS	Population	ITS1		242	89	0.186	0.285	0.280	0.248	GTR
		5.8S		157	4	0.274	0.223	0.242	0.261	TRNEF+I
		ITS2		189	55	0.231	0.282	0.253	0.234	GTR
Total		Full alignment	**81**	**588**	**148**	**0.224**	**0.268**	**0.261**	**0.247**	SYM+I

The amount of segregating sites decreased from ITS (65%) through TEF1-α (60%) with the lowest amount of segregating sites present in MCM7 (45%). The amounts of missing data (Fig. 8) for the different markers increased from MCM7 (2.04%) through TEF1-α (5.81%), with the highest amount present in ITS (18.68%).

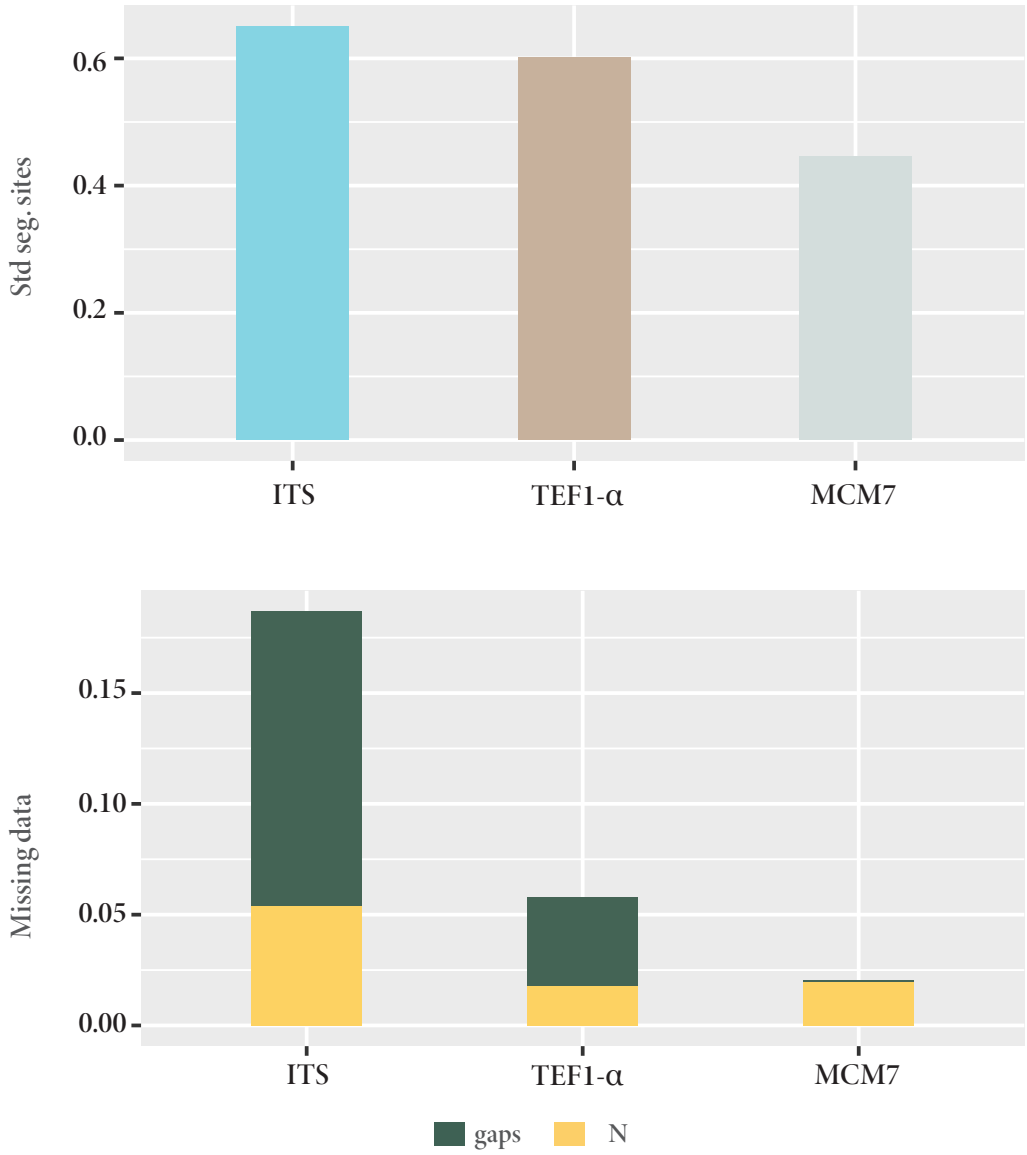

Figure 8. Missing data and nucleotide variability for the different alignments. The top diagram shows the amount of standardized segregating sites (number of segregating sites divided by sequence length) for each of the three nuclear loci. The bottom diagram indicates the amount of missing data (between 0 and 1) where yellow displays the amount of actual missing sites, and green displays percentage of gaps.

The saturation plots show a transition and transversion saturation plateau reached at a F84 distance of around 1 for the MCM7 gene (Fig. 9A). For the TEF1-α gene, an approximate linear increase of both substitution types over the F84 distance was observed (Fig. 9B). TEF1-α also showed an absence of substitutions in the range of approximately 0.15 and 0.25 F84 distance. Little to no difference was observed between outgroup inclusion/exclusion for the different saturation plots, and only plots excluding the outgroup taxa are shown. Substitutions were distributed within F84 distances of 0 and 0.5 for ITS, 0 and 3 for MCM7 (the majority within 0 to 1) and between 0 and 1 for TEF1-α.

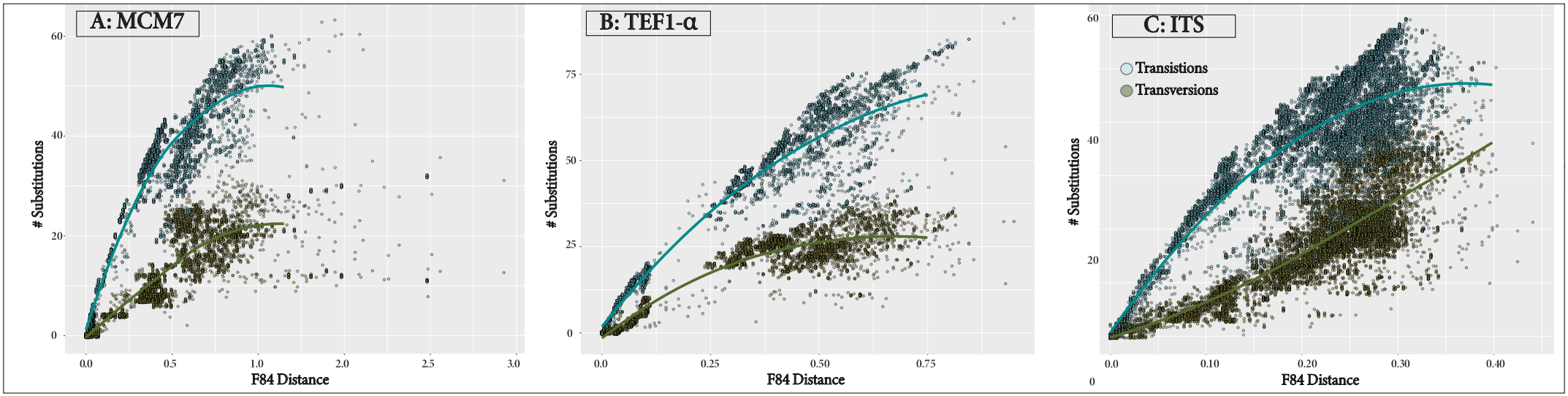

Figure 9. Saturation plots of the two nuclear alignments with outgroup taxa excluded (**A**) MCM7 (**B**) TEF1-α. The plots (**A** and **B**) show the number of third position transversions and transitions as a function of the F84 distance. The nuclear marker ITS (**C**), showing the number of transversions and transitions for the entire variable regions ITS1 and ITS2 against the F84 distance. ITS was included to indicate at which level of genetic distance substitutions occur for this marker.

3.3 Phylogenetic relationships

3.3.1 Gene tree topologies

The bayesian MC^3 runs for the separate gene trees converged at slightly above 3 million generations (for ITS), slightly above 1.6 (for MCM7) and just below 1 million (for TEF1-α), all with effective sample size (ESS) values well above 200 for all parameters. The different gene trees (ITS, MCM7, TEF1-α) showed congruent topologies with respect to the major diverging lineages (Fig. S1) using ML, with no supported (>75 BS) incongruencies (Fig. S1). However, one TEF1-α sequence of *C. melaleuca* III grouped as supported sister to *C. armeniaca* and *C. melaleuca* II. Whereas the three ITS sequences from the same clade grouped as supported sister to *C. melaleuca* I. ITS had poor bootstrap support values (< 60) in all deeper nodes of the topology. MCM7 had strong support for the ingroup/outgroup relationship (BS = 97) and intermediate support (BS = 75) for a monophyletic Tephromelataceae. TEF1-α showed near robust support (BS = 85) for ingroup/outgroup and low support (BS = 68) for a monophyletic Tephromelataceae. All gene trees share an important feature, intermediate branch lengths are short and generally low supported by bootstrap resampling. Comparatively, the bayesian gene trees of ITS and TEF1-α showed much higher support (PP) among these short branches at intermediate to deep topological levels. MCM7 however, showed similar branch support (PP) to bootstrap resampling with only a small to moderate overall increase in PP's at all internodes.

3.3.2 Concatenated topology

The Bayesian MC^3 runs converged at just below 8 million generations, with ESS values well above 200 for all parameters. The deeper nodes in the Tephromelataceae were unresolved (Fig. 10). All included genera and subgenera were highly supported, respectively, except for a moderately supported *Mycoblastus* (BS = 64). Their interrelations, however, remain largely unresolved and unsupported by bootstrapping. A clade of *Calvitimela* subgenera *Calomela*, *Paramela*, and *Severidea*, and the genus *Violella*, was supported only moderately by posterior probability (PP = 0.92). A sister-relation between *Calomela* and *Violella* was only marginally supported by posterior probability (PP = 0.5).

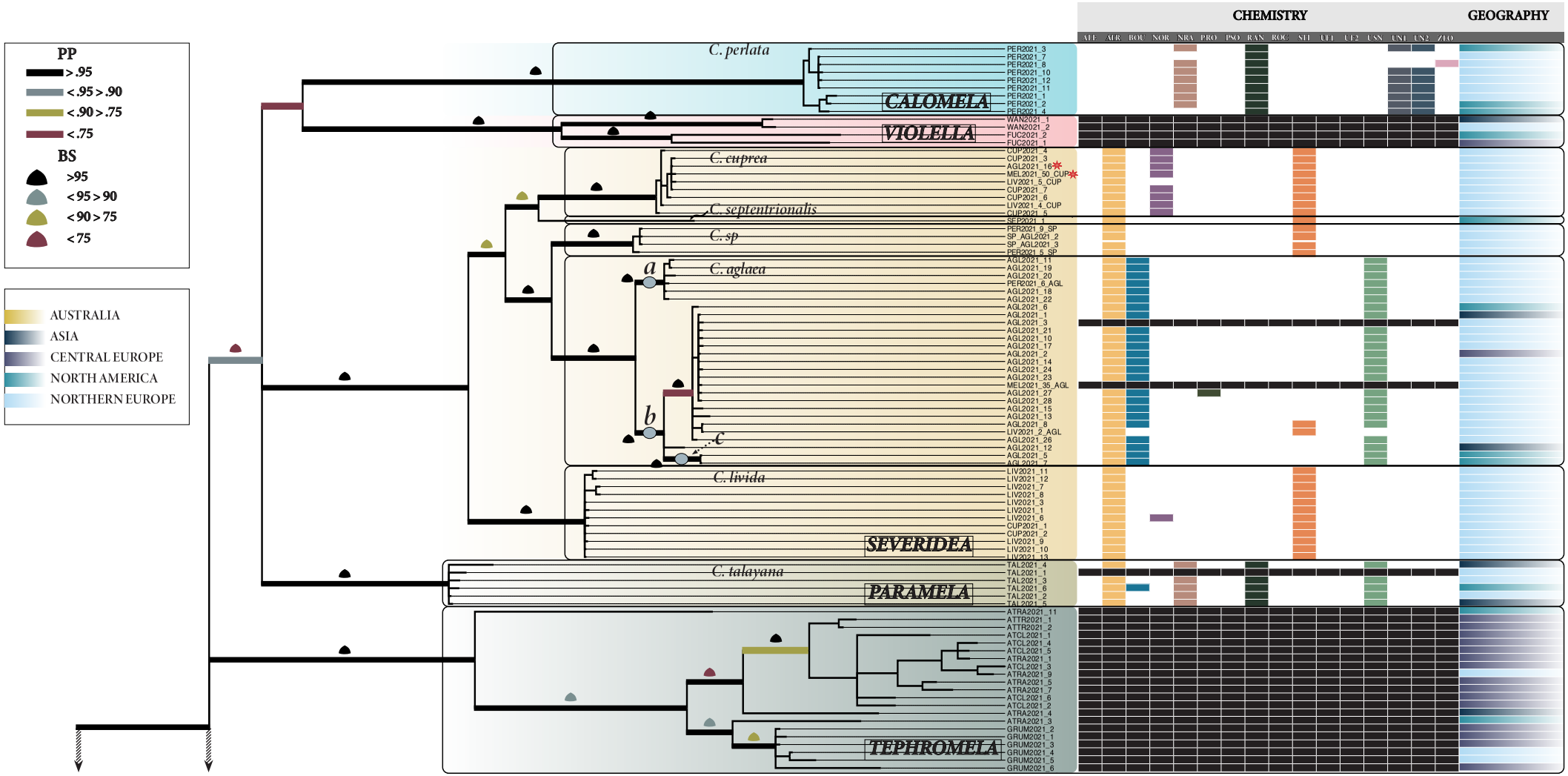
PP
> .95
< .95 > .90
< .90 > .75
< .75
BS
>95
< 95 > 90
< 90 > 75
< 75
AUSTRALIA
ASIA
CENTRAL EUROPE
NORTH AMERICA
NORTHERN EUROPE
CHEMISTRY
GEOGRAPHY
ATE AIR BOU NOR NRA PRO PSO RAN ROG SEI UE1 UE2 USN UN1 UN2 ZEO
C. perlata
CALOMELA
VIOLELLA
C. cuprea
C. septentrionalis
C. sp
C. aglaea
a
b
c
C. livida
SEVERIDEA
C. talayana
PARAMELA
TEPHROMELA

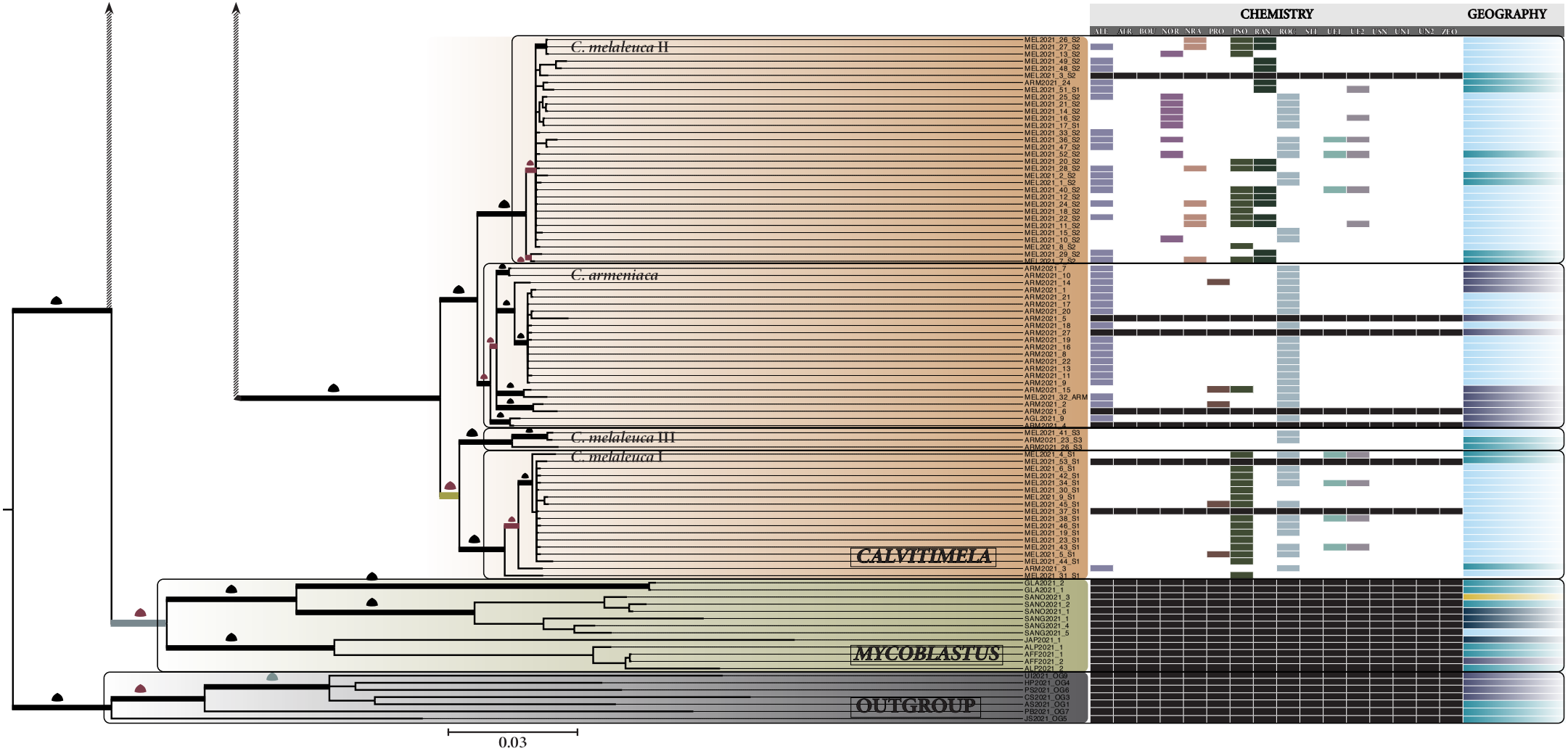
CHEMISTRY
GEOGRAPHY
ALE AUR BOU NOR NRA PRO PSO RAN ROC STE UE1 UE2 USN UN1 UN2 ZEO
C. melaleuca II
C. armeniaca
C. melaleuca III
C. melaleuca I
CALVITIMELA
MYCOBLASTUS
OUTGROUP
0.03

Figure 10. Bayesian 50% majority rule consensus tree based on 183 accessions and 1794 aligned characters from the concatenated nuclear regions (ITS, MCM7, TEF1-α). Thick branches with different colors indicate posterior probabilities (PP; see figure legend). Bootstrap values from 1000 replicates are shown with colored triangles (see figure legend). Triangles for short branches in the subgenus *Calvitimela* are scaled down to reduce overplotting. The different color codes indicate the separate genera and subgenera in the Tephromelataceae. Major geographical zones are manually mapped on the phylogeny with different colors (see figure legend). The nodes "a", "b", and "c" highlight three supported groupings within the species *C. aglaea*. The chemistry of vouchers from *Calvitimela* are mapped onto the phylogeny with different colors in the right-hand matrix. The black squares indicate vouchers for which no TLC data was obtained. Abbreviations for the different lichen substances: ALE = Alectorialic acid, ATR = Atranorin, BOU = Bourgeanic acid, NOR = Norstictic acid, NRA = Norrangiformic acid, PRO = Protocetraric acid, PSO = Psoromic acid, RAN = Rangiformic acid, ROC = Roccellic acid, STI = Stictic acid, UF1 = Unknown fatty acid 1, UF2 = Unknown fatty acid 2, US = Usnic acid, UN1 = Unknown substance 1, UN2 = Unknown substance 2. The scale bar indicates the number of substitutions per site. The two accessions of the fertile morphotype of *C. cuprea* are marked with red stars.

My phylogenetic analyses of the concatenated data showed four independent lineages in the subgenus *Calvitimela* (Fig. 10). Firstly, a new highly supported clade *C. melaleuca* III (BS = 100, PP = 1), was recovered as sister to *C. melaleuca* I (BS = 100, PP = 1) with marginal to moderate support (BS = 55, PP = 0.85). Secondly, the partly supported clade *C. armeniaca* (BS = 61, PP = 0.96) was indicated as sister to the *C. melaleuca* II clade (BS = 100, PP = 1) with high support (BS = 99, PP = 1). Within C. *armeniaca* six fully supported (BS = 100, PP = 1), relatively short to intermediate length branches were recovered. There was a topological discordance between the gene trees and the tree based on the concatenated data in the subgenus *Calvitimela*. However, only one relationship was supported (see above: 3.3.1). Another highly supported lineage (*C.* sp; BS = 100, PP = 1) was recovered as a sister taxon to *C. aglaea* (BS = 100, PP = 1) with high support (BS = 97, PP = 1). Within *C. aglaea*, three groupings were recovered with high support (BS = 100, PP = 1; Fig. 10 node "a", "b" and "c"). A single accession of *C. septentrionalis* grouped as a moderately to highly supported sister (BS = 84, PP = 1) to *C. cuprea*. With collapsed topological edges of the ML tree, based on the concatenated data (setting a cutoff at bootstrap values < 75), the backbone of the lineages *Calvitimela*, *Calomela*, *Tephromela*, *Severidea*, *Paramela* and *Violella* were reduced to a polytomy.

3.4 Populations of *C. melaleuca*

The Bayesian MC^3 runs for the population (ITS) analysis converged at approximately 500 000 generations, with ESS values above 200 for all parameters. The two main lineages of *C. melaleuca* (mel I and mel II; (corresponding to the clades *C. melaleuca* I and II in Fig. 10)) were recovered with robust support by both Bayesian and ML phylogenetic analyses (Fig. 11). The lineage representing *C. armeniaca* was recovered as the sister taxon to *C. melaleuc*a II (mel II). However, the monophyly of *C. armeniaca* + *C. melaleuca* II was only partially robust (P P= 0.97, BS = 71), as also indicated in the concatenated topology (Fig. 10). Sixteen different haplotypes of ITS were recovered in the populations with the two most abundant (II and VII) were

exclusive to mel I. Relatively high estimates of d_{XY} and F_{ST} (Table 5) were seen between population 1 and the rest of the populations. From the estimated nucleotide diversity (π), there was low within population diversity in all the sampled populations (>= 0.004). A total of five samples from population 1 and 3 (1_3, 1_14, 1_20, 3_7, 3_10; See Table S2; Fig. 11) showed unexpected phylogenetic placements. The three individuals from population 1 represented a divergent sister clade to the lineage mel I (Fig. 11: I**) and not mel II as the rest of the samples from the same locality. The ITS sequences of these three individuals showed 37 shared characters (nucleotides out of 556 – 6.7% difference) that differed from the three individuals compromising *C. melaleuca* III (in Fig. 10). In population 2, there were two individuals recovered as outlier lineages in mel I and mel II respectively (Fig. 11: I* and II*).

Table 5. Population genetic metrics of the ITS alignment based on populations of *C. melaleuca*. The population identity (1–4) is indicated with the number of individuals per population and the number of haplotypes recovered. Population 1 from Snøhetta (Innlandet), population 2 from Kopparen (Trøndelag), population 3 from Storengdalen (Nordland), and population 4 from Dárjohčohkka (Finnmark). The total number of sites in the alignment, the total number of segregating sites per population and between all populations are shown. Nucleotide diversity (π) is shown for each population. The F_{ST} and d_{XY} estimates between all pairs of populations (PopX, PopY) are shown at the bottom.

Population	**# Individuals**	**# Haplotypes**	**# Sites**	**# Segregating sites**	**Base frequencies**				**π**
					A	**C**	**G**	**T**	
1	16	7	502	4	0.211	0.280	0.264	0.243	0.00301
2	16	3	502	4	0.206	0.277	0.266	0.252	0.00375
3	18	6	502	4	0.206	0.277	0.265	0.252	0.00378
4	20	6	502	4	0.206	0.277	0.265	0.252	0.00359
All	**70**	**16**	**502**	**43**	**0.207**	**0.278**	**0.265**	**0.250**	–

Divergence between populations					
PopX		**PopY**	**F_{ST}**	**D_{XY}**	
1	~	**2**	0.9565	0.0773	
1	~	**3**	0.9539	0.0771	
1	~	**4**	0.9548	0.0772	
2	~	**3**	0.0522	0.0041	
2	~	**4**	0.0924	0.0042	
3	~	**4**	0	0.0038	

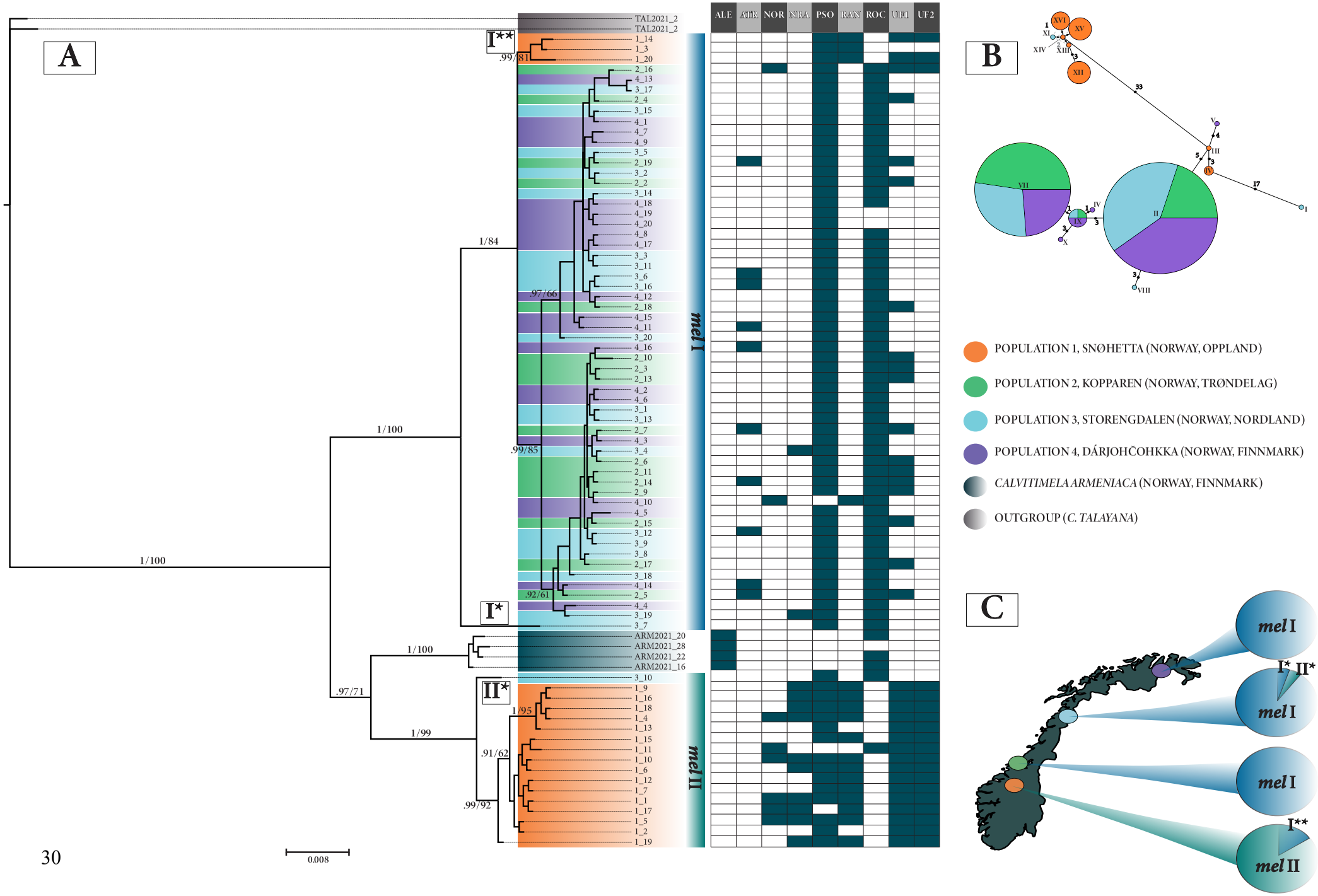
A
TAL2021_2
TAL2021_2
I**
1_14
1_3
1_20
.99/81
2_16
4_13
3_17
2_4
3_15
4_1
4_7
4_9
3_5
2_19
3_2
2_2
3_14
4_18
4_19
4_20
4_8
4_17
3_3
3_11
3_6
3_16
4_12
2_18
4_15
4_11
3_20
4_16
2_10
2_3
2_13
4_2
4_6
3_1
3_13
2_7
4_3
3_4
2_6
2_11
2_14
2_9
4_10
4_5
2_15
3_12
3_9
3_8
2_17
3_18
4_14
2_5
4_4
3_19
3_7
1/84
.97/66
.99/85
.92/61
1/100
1/100
I*
ARM2021_20
ARM2021_28
ARM2021_22
ARM2021_16
3_10
1/100
.97/71
II*
1_9
1_16
1_18
1_4
1_13
1_15
1_11
1_10
1_6
1_12
1_7
1_1
1_17
1_5
1_2
1_19
1/95
1/99
.91/62
.99/92
mel I
mel II
ALE
ATR
NOR
NRA
PSO
RAN
ROC
UF1
UF2
0.008
B
XVI
XV
XI
XIV
XIII
XII
33
V
4
III
5
3
IV
17
I
VII
1
IV
1
IX
3
II
3
X
3
VIII
POPULATION 1, SNØHETTA (NORWAY, OPPLAND)
POPULATION 2, KOPPAREN (NORWAY, TRØNDELAG)
POPULATION 3, STORENGDALEN (NORWAY, NORDLAND)
POPULATION 4, DÁRJOHČOHKKA (NORWAY, FINNMARK)
CALVITIMELA ARMENIACA (NORWAY, FINNMARK)
OUTGROUP (C. TALAYANA)
C
mel I
I* II*
mel I
mel I
I**
mel II

Figure 11. (**A**) A Bayesian majority rule consensus phylogram of the ITS from four different populations of *C. melaleuca* across Norway (see figure legend). Branch support values are shown above branches in the order of posterior probabilities (PP)/Bootstrap support (BS; manually mapped onto the Bayesian topology) with the scale bar indicating number of substitutions per site. Branches are colored with respect to population identity (see figure legend), and the two clades of *C. melaleuca* (mel I and II) are indicated (**B**) Haplotype network of the *C. melaleuca* populations based on the ITS. There were 16 haplotypes recovered in the analysis, each circle representing a unique haplotype with corresponding roman numerals, and size indicating haplotype frequency. Distances between nodes indicate the number of mutations. Circles are colored by population (see figure legend). (**C**) Map showing the sampling localities for the different populations of *C. melaleuca*. Pie charts indicating the phylogenetic identity of the samples within each population corresponding to mel I and mel II. In population 1, three individuals represent a sub clade within mel I, namely I**. In population 3, two individuals represent outliers in mel I (= I*) and mel II (= II*) respectively. The chemistry of individual population samples is mapped onto the phylogeny. Abbreviations for the different lichen substances: ALE = Alectorialic acid, ATR = Atranorin, NOR = Norstictic acid, NRA = Norrangiformic acid, PSO = Psoromic acid, RAN = Rangiformic acid, ROC = Roccellic acid, UF1 = Unknown fatty acid 1, UF2 = Unknown fatty acid 2.

3.5 Molecular dating

The two MCMC runs from one strict and one relaxed molecular clock analysis, converged with ESS values above 200 for all parameters. The two different dating analyses showed incongruent backbone topologies with differences in supported branches (Table 6). Negative branch lengths were observed at the short branches leading up to *Calomela*, *Paramela* and *Violella* in the resulting tree from the strict molecular clock analysis. These were mitigated with CA height summarization. The median age estimates differed between the strict and relaxed molecular clock analysis, but 95% HPD intervals were overlapping (Table 6). From the relaxed molecular clock analysis, the estimated median age for the split leading up to *Calvitimela* s. lat and *Violella* was 34.85 Ma (26.14–58.70 Ma 95% HPD). While the divergence between *Severidea* and the lineages *Calomela*, *Paramela* and *Violella* was 32.79 Ma (24.40–54.30 Ma 95% HPD).

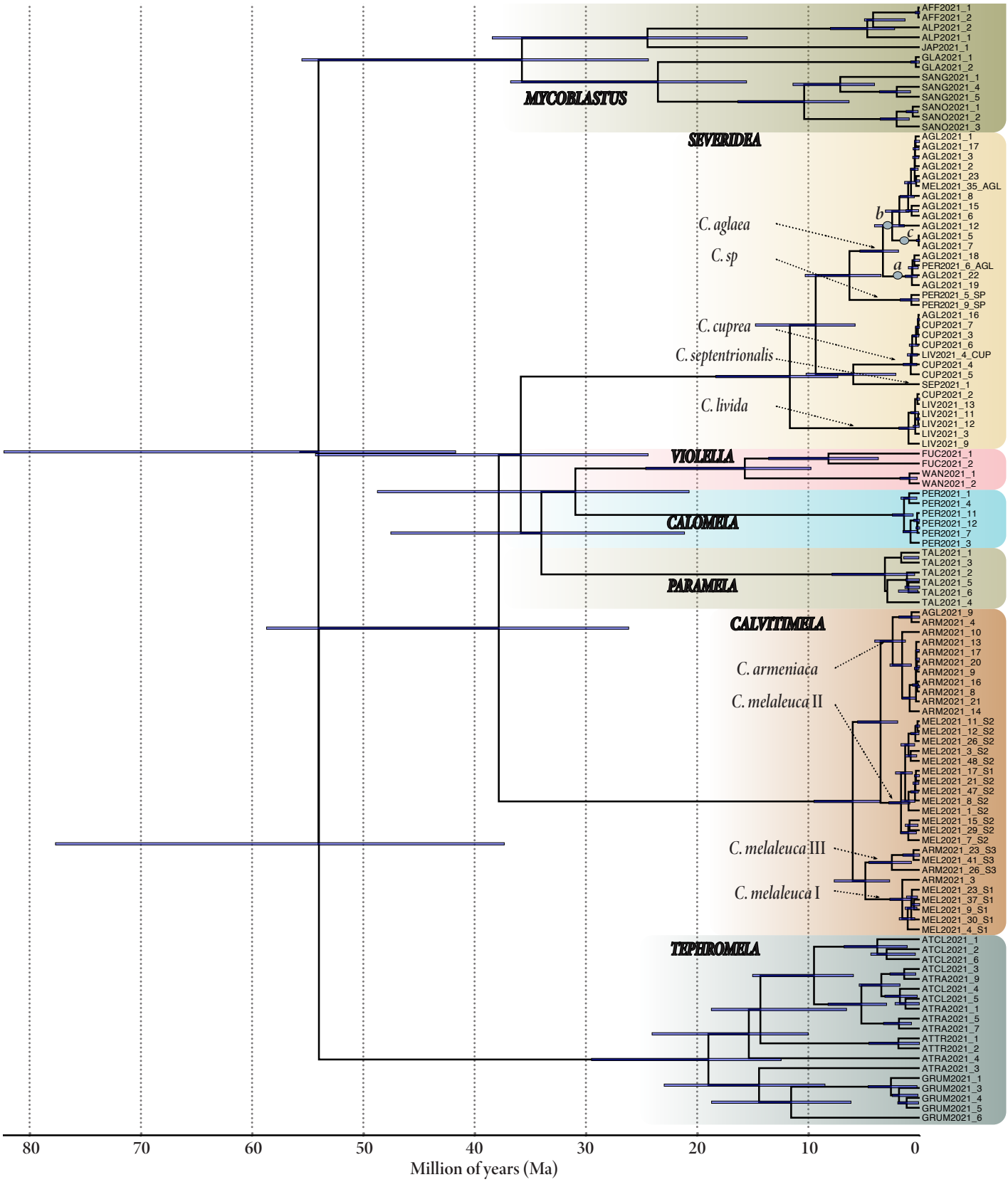

Figure 12. Time calibrated phylogeny of the Tephromelataceae. A Bayesian common ancestor chronogram from the log normal relaxed clock molecular dating analyses of three nuclear loci ITS, MCM7 and TEF1-α. Clade coloring represents the different genera and subgenera in the Tephromelataceae. The different clades of *Calvitimela* are indicated with arrows, and the three groupings in *C. aglaea* are represented with ”a”, ”b” and ”c”. The scale axis at the bottom represents age in millions of years (Ma). Node bars indicate the 95% highest density posterior interval (95% HPD) for estimated node ages (Ma).

Within *Severidea*, *C. livida* was estimated to have diverged from the rest of the taxa in this subgenus 10.83 Ma (7.35–18.33 Ma 95% HPD). The subsequent split between *C. cuprea* and *C. aglaea* + *C.* sp. was estimated at 8.68 Ma (5.81–14.76 Ma 95% HPD). Furthermore, the split between *C. aglaea* + *C.* sp. was estimated at 5.89 Ma (3.47–10.29 Ma 95% HPD), and the estimated time between *C. cuprea* and *C. septentrionalis* 5.65 Ma (2.14–10.21 Ma 95% HPD). Between the two groupings "a" and "b" within *C. aglaea* the estimated node age was 3.08 Ma (1.91–5.38 Ma 95% HPD).

The estimated node age for the ancestral node to the lineages within the subgenus *Calvitimela* was 5.61 Ma (3.58–9.50 Ma 95% HPD). Whereas the split between *C. armeniaca* and *C. melaleuca* II was estimated to 3.28 Ma (1.97–5.59 Ma 95% HPD). The split between *C. melaleuca* I and III was estimated to 4.44 Ma (2.70–7.68 Ma 95% HPD). The two different molecular dating analyses showed high support for the monophyly of *Calvitimela* s. lat + *Violella*. All major lineages corresponding to genera and subgenera were recovered as in previous analyses (see Table 6).

Table 6. The different clades of interest in the Tephromelataceae are shown with median node ages and 95% HPD intervals from one strict and one relaxed molecular clock analysis. Branch support is given for the branches leading up to the different clades. The three clades indicated in bold are only marginally to moderately supported in both analyses, where the two first are effectively non-existing in the strict analysis (indicated with ~ 0).

Clade	Crown age (Ma)		95% HPD interval		Branch support	
	Strict	Relaxed	Strict	Relaxed	Strict	Relaxed
Calvitimela s. lat + *Violella*	39.09	34.85	30.20 – 65.14	26.14 – 58.70	0.99	1
Calomela + *Paramela* + *Severidea* + *Violella*	**33.34**	**32.69**	**28.33 – 36.47**	**24.40 – 54.30**	**~ 0**	**0.87**
Calomela + *Paramela* + *Violella*	**34.84**	**28.77**	**29.36 – 51.91**	**21.13 – 47.52**	**~ 0**	**0.45**
Calomela + *Violella*	**35.79**	**28.67**	**27.17 – 59.77**	**20.72 – 48.73**	**0.90**	**0.74**
Violella	19.28	14.56	13.90 – 32.52	9.78 – 24.62	1	1
Severidea	14.62	10.83	10.65 – 24.48	7.35 – 18.33	1	1
C. aglaea + *C. cuprea*	12.71	8.68	9.13 – 21.24	5.81 – 14.76	0.99	0.99
C. aglaea + *C. sp*	9.34	5.89	6.21 – 15.76	3.47 – 10.29	1	1
C. cuprea +*C. septentrionalis*	10.35	5.65	6.72 – 17.48	2.14 – 10.21	1	0.99
C. aglaea a + b	4.39	3.08	2.87 – 7.49	1.91 – 5.38	1	1
Calvitimela (subgen.)	8.76	5.61	6.21 – 14.82	3.57 – 9.50	1	1
C. melaleuca I + III	7.32	4.44	4.87 – 12.37	2.70 – 7.68	0.58	0.90
C. armeniaca + *C. melaleuca* II	4.78	3.28	3.09 – 8.11	1.97 – 5.59	1	1

4 Discussion

With this study, I have gained a better understanding of the phylogeny and natural taxon limits in the genus *Calvitimela* through an integrative taxonomic approach. My investigations cover various taxonomic levels and geographic scales, from genus through species levels on a global scale, to populations of *C. melaleuca* s. lat. in Norway. Together with in-depth studies of morphological and chemical characters, I have uncovered characters that appear to be phylogenetically informative for species previously considered cryptic. Finally, I have explored the potential sources of non-phylogenetic signals in the molecular data.

4.1 Generic circumscription

The difficulty of circumscribing genera in the Tephromelataceae is evident, from Hertel & Rambold (1985) through Bendiksby et al. (2015). My phylogenetic analyses of the three nuclear loci (ITS, MCM7, TEF1-α) reveal deeply divergent clades with unclear relationships to each other in the family Tephromelataceae (Figs. 10 and 12), echoing the findings by Spribille et al. (2011a) and Bendiksby et al. (2015). The clades correspond to the subgenera *Calvitimela*, *Calomela*, *Severidea*, and *Paramela*, and the genera *Mycoblastus, Tephromela*, and *Violella*, respectively. Although with low bootstrap support, the genus *Mycoblastus* is recovered as the phylogenetic sister to the rest of the abovementioned taxa (Fig. 10), as previously shown by Spribille et al. (2011a) and Bendiksby et al. (2015). My results show a non-concordance between the molecular phylogeny and morphological characters and provide evidence for the insufficiency of chemical characters as diagnostic tools in *Calvitimela* (Figs. 5–7 and 10).

The strongly supported and long-branched subgenera within *Calvitimela* s. lat. and the genus *Violella* are inferred to have diverged between 26 and 58 Ma (Fig. 12; Table 6), suggesting that they represent relatively old evolutionary lineages. Moreover, the secondary chemistry appears largely homoplastic at species level in the molecular phylogeny (Fig. 10). At the level of subgenera, however, the chemistry seems to be phylogenetically informative, corresponding with the strongly supported and long-branched clades in the molecular phylogenetic hypothesis. In the subgenera *Severidea* and *Paramela*, the combination of atranorin and usnic acid is common, where stictic acid seems to be restricted to *Severidea* (Fig. 10; Table 3). The substances alectorialic acid, norstictic acid, psoromic acid and roccellic acid appear to be good indicators of the subgenus *Calvitimela* (Fig. 10; Table 3); atranorin may also occur (Fig. 11). Moreover, norrangiformic- and rangiformic acid are common in *Calomela* and *Paramela* but can also occur in parts of the subgenus *Calvitimela* (Figs. 10-11). The black, shiny and lecideine apothecia, and the blue-green color of the epithecium in the members of *Calvitimela* s. lat. (e.g., Haugan & Timdal 1994) makes them distinct from members of *Mycoblastus*, *Violella* and *Tephromela*. Although, species of the genera *Mycoblastus* and *Violella* also have lecideine apothecia, they are epiphytic and have several anatomical traits that distinguish them from *Calvitimela* s. lat (see Spribille et al. 2011a, 2011b). Moreover, monophyly of the genus *Calvitimela* is not

supported by the molecular phylogeny, nor is there any strong evidence for the contrary. As such, whether these characters could represent synapomorphies for the genus or not remains an open question, as the phylogenetic interrelationships between *Calvitimela* s. lat. and the genera *Tephromela* and *Violella* remain unresolved. The process of independent evolution of a phenotype in different lineages (by i.e., convergence; Swift et al. 2016), might produce character state discordances with DNA-based phylogenies. Recently it has even been suggested that an inherent mismatch between the lichen phenotype and its corresponding fungal molecular phylogeny exists, as discussed by Spribille et al. (2018). This stems from the realization that lichens achieve their phenotype through the symbiotic state (see Spribille et al. 2018 and references therein). The evolution of one symbiont (the fungal component) seems to not always explain the observable phenotypic outcome of a lichen.

From my results, it seems that capturing deep phylogenetic relationships of the Tephromelataceae, using three nuclear loci and a dichotomous tree-like model of evolution, is not possible. This can relate to a substantial amount of change during the evolutionary history of the Tephromelataceae, through for instance, a rapid diversification event. Another possibility is that actual genetic distances at deeper phylogenetic levels are underestimated and effectively erased by substitutional saturation (Philippe et al. 2011; Widhelm et al. 2019; see methods and troubleshooting below). However, in general, weak phylogenetic signals are not uncommon for ancient divergences (Delsuc et al. 2005).

Since *Calvitimela* cannot be shown monophyletic with the current data, any taxonomic decision at the generic level includes either accepting a seemingly paraphyletic genus or reaccepting a *Tephromela* sensu Hertel & Rambold (1985). This implies circumscribing all species in *Calvitimela*, *Tephromela* and *Violella* into one large genus (see Spribille et al. 2011a). A third solution would be to recognize all the strongly supported clades as separate genera and thereby raise the taxonomic rank of the current *Calvitimela* subgenera. None of the alternative solutions seem persuasive in that they all imply a degree of arbitrary reassignment of ranks. The strongest argument against any of these alternatives is of practical nature. The genus circumscription of *Calvitimela* was originally based on details of anatomical characters (e.g., ascus, paraphyses and excipulum; Hertel & Rambold 1985). This is practical as it is possible to morphologically, and to some degree chemically, distinguish the *Calvitimela* species from species in *Mycoblastus*, *Tephromela* and *Violella.* Furthermore, acknowledging a circumscription of *Calvitimela* sensu Hafellner & Türk (2001), essentially including all species with lecideine apothecia (not considering *Mycoblastus* and *Violella*), will reduce confusion compared to introducing several new genera only discernible from molecular phylogenies. On the other hand, Divakar et al. (2017) argue for a temporal band around 30 Ma as an objective time frame for generic circumscription in the Parmeliaceae. Applying the same logic in the Tephromelataceae, this would, with my molecular dating results, call for elevating the *Calvitimela* subgenera to generic rank.

Calvitimela uniseptata, and potentially also *C. austrochilensis*, appear to be extraneous in the Tephromelataceae. The mtSSU from the single accession of *C. uniseptata* did group (with high support) in the genus *Lecania* (Fig. S3), more specifically close to a clade of *Lecania gerlachei* (Vain.) Darb. and *L. brialmontii* (Vain.) Zahlbr. These two species, together with *L. racovitzae* (Vain.) Darb., comprise a nested

Antarctic clade within *Lecania* A. Massal., previously referred to as *Thamnolecania* (Vain.) Gyeln. (see Næsborg et al. 2007 and references therein). From its description in Lumbsch et al. (2011), *C. uniseptata* has a squamulose thallus and a single septum in its ascospores. These morphological features fall within the concept of *Lecania* s. lat. Taken together, I suggest that either a combination into *Lecania* or alternatively synonymizing it with *L. brialmontii*, is suitable for *C. uniseptata*. The inability to amplify the markers TEF1-α and MCM7 from *C. austochilensis* using Tephromelataceae specific primers supports this taxon not being closely affiliated with the Tephromelataceae. In general, amplification was difficult with most primers for specimens of old age. I therefore suspect the amplification difficulties could be caused by old age (*C. austochilensis*: 1969) and poor quality of the material. Hence, no conclusions can be drawn based on amplification failure alone.

4.2 Species delimitations in the subgenus *Calvitimela*

The name *C. melaleuca* currently refers to three distinct evolutionary lineages; *C. melaleuca* I, *C. melaleuca* II (Bendiksby et al. 2015) and *C. melaleuca* III (recognized here; Fig. 10), making it a paraphyletic species with respect to *C. armeniaca*. My phylogenetic analyses confirm four independent clades in the subgenus *Calvitimela* (Fig. 10). The clades have to some extent overlapping chemistries and morphologies (Figs. 5–6; Table 3). However, they correlate with thallus morphology and to some degree with spore size (Figs. 5–6). The spore measurements for the lectotype of *C. melaleuca* are overlapping with those of *C. armeniaca* and *C. melaleuca* II (Fig. 5). This suggests that the name *C. melaleuca* is not applicable to the *C. melaleuca* I clade previously thought to represent the "true *C. melaleuca*" by Bendiksby et al. (2015). The thallus color of the clade *C. melaleuca* I is white, *C. melaleuca* II is yellow, and the new clade *C. melaleuca* III reported herein, is beige with a slightly different thallus morphology (Figs. 6C–F). This indicates that thallus color represents a possible diagnostic character for these clades. The major patterns of chemistry in the *subgenus Calvitimela* (Figs. 10–11; Table 3), is the regular to irregular presence of norstictic acid, rangiformic acid and norrangiformic acid in *C. melaleuca* II and an absence of these substances in *C. melaleuca* I. Alectorialic acid is rare in *C. melaleuca* I, whereas it is more common in *C. melaleuca* II. Roccelic acid and psoromic acid are common in both clades, and roccellic acid is the only detected substance from *C. melaleuca* III. This unclear association between chemistry and genotypes in *C. melaleuca* s. lat. indicates that secondary metabolite production does not follow any clade specific pattern for these groups. In *C. armeniaca*, detectable lichen substances are more homogenous (i.e., alectorialic acid, roccellic acid and rarely protocetraric acid). In addition, the thallus of *C. armeniaca* is recognizably more matte than in *C. melaleuca* s. lat. (Fig. 6A–B).

In the subgenus *Calvitimela*, the clade *C. melaleuca* III was already collected by McCune et al. (2020) as *C. armeniaca* (McCune 36825). The authors did mention unusual chemical spot tests for this specimen, which indicated a presence of norstictic acid (medulla K+ orange). From the two specimens seen (O-L-228122 and QFA-0635917) only roccellic acid was confirmed by TLC (Fig. 10, Table 3). With the complex chemistry reported herein, and as previously shown (i.e., Bendiksby et al. 2015) for *C. melaleuca* s. lat., I do not assume this clade to have diagnostic chemistry.

Morphological and chemical characters can be rather obscure in the subgenus *Calvitimela* (Fig. 6; Table 3). The problem of differentiating between *C. armeniaca* and *C. melaleuca* based on morphology or chemistry is indeed evident from all the mislabeled sequences in GenBank and inconsistent use of the two names, as already mentioned by Bendiksby et al. (2015). The concept of *C. armeniaca* is a well-established one going back to the third edition of the classic work *Flore française* (Lamarck & De Candolle 1805) with the description as *Rhizocarpon armeniacum*. Still, different morphotypes exist, which can resemble morphotypes in the sister lineage *C. melaleuca* II. The discovery of a third clade *C. melaleuca* III further complicates this (Fig. 6E).

The divergence time estimates of the subgenus *Calvitimela* suggest that the common ancestor of the four groupings (*C. armeniaca* and *C. melaleuca* I, II, and III) diverged between 3.6–9.5 Ma (Fig. 12; Table 6). Moreover, the clades *C. armeniaca* and *C. melaleuca* II are indicated to have split between 2–5.6 Ma, and *C. melaleuca* I and II between 2.7–7.7 Ma. The distinction between the four genetic lineages in this subgenus as separate species, however, is less straightforward considering the short length of the branch leading to *C. armeniaca*, overlapping morphologies, and diffuse chemical patterns. Furthermore, the moderately supported sister relationships between *C. melaleuca* I and III and the poor bootstrap support for the *C. armeniaca* clade, introduce uncertainties regarding the phylogenetic relationships between these clades. In addition, the six highly supported clades within *C. armeniaca*, point to this being a more genetically variable species compared to the results by Bendiksby et al. (2015). In the case of a recent divergence, the unclear phylogenetic signals, as observed in my gene trees, would be expected (Philippe et al. 2011). The different gene trees (Fig. S2) showed slight incongruences with the phylogenetic hypothesis based on the concatenated data (Fig. 10). More specifically, this was only observed for the different genetic lineages in the subgenus *Calvitimela*. Taken together, this may suggest an incompatible evolution between genes and species (Maddison 1997).

From my population level analysis, the four populations fall within two divergent evolutionary lineages, namely *C. melaleuca* I and *C. melaleuca* II (mel I and mel II; Fig. 11). *C. melaleuca* I seems to be the most widely distributed genotype in Norway (Fig. 11). Haplotypes are largely shared across the geographically spread-out populations of *C. melaleuc*a I (Fig. 11A), indicating that they may be connected through gene flow. *Calvitimela melaleuca* II, represented by a single population (population 1), is recovered as sister to *C. armeniaca* in the phylogenetic analysis of ITS. Out of the four populations, population 1 is the only one collected at high altitudes (Snøhetta; Table S2). My results might imply that this is a clade connected to greater elevations, but with a sample size of one for this population the discussion on distribution patterns for *C. melaleuca* s. lat is not possible at this point. Furthermore, the relatively high estimates of divergence

(d_{XY} and F_{ST}) between the populations (i.e., population 1 compared to the rest) further point to *C. melaleuca* I and II being separate evolutionary lineages. A less extreme value of d_{XY} likely reflects that the individual populations are genetically homogeneous (Table 5). Values of F_{ST} can be high when within population variance is low, but due to d_{XY} being standardized across length it is not affected by the properties of relative measure (Sætre & Ravinet 2019, p. 159). Only a few polymorphisms are present in the ITS region within each population (Table 5), as also shown by the low nucleotide diversity (π). This further corroborates that the populations are genetically homogenous.

Three individuals from population 1 (I**; Fig. 11) were supported as either sister to *C. melaleuca* I or as belonging within *C. melaleuca* I. The distance (~7%; see section 3.4.1) between the sequences from I** and sequences of *C. melaleuca* III indicates that they might not belong in *C. melaleuca* III, but rather *C. melaleuca* I. Moreover, if the lineages of *C. melaleuca* s. lat. have undergone recent speciation events, the odd placement of both I** and II*, could equally well be explained by incomplete lineage sorting (i.e., the retention of ancestral polymorphism; see Garrido-Benavent et al. 2021 and references therein). Taken together with the subtle morphological disparity between the different clades in the subgenus *Calvitimela*, this might point to the beginning of local adaptation after a recent divergence.

On a last note, the presence of diagnostic phenotypic characters that are possible to observe in old type specimens has been hard to pinpoint for *C. melaleuca* s. lat. and pose a serious problem for connecting the types to the species hypotheses. Thallus color and spore size do, however, show promise as diagnostic characters. We propose that the lineages (I and III) in *C. melaleuca* should be given names subsequent to type studies of the currently regarded synonyms of *C. melaleuca*; *Lecidea arctogena* (Th. Fr.) H. Olivier, *L. leucomelaena* (Vain.) Vain., *C. testaceoatra* (Vain.) Hafellner.

4.3 Novelties in *Severidea*

The subgenus *Severidea* consists of the species *C. aglaea*, *C. cuprea*, *C. livida*, *C. septentrionalis*, and one new clade, *C.* sp., reported herein (Fig. 10). From my phylogenetic analysis, the new clade is recovered as a highly supported sister to *C. aglaea* but resembles *C. perlata* morphologically. Chemical analyses also show that *C.* sp. contain stictic acid and atranorin, which judging from phylogenetic relationships is the plesiomorphic chemotype in *Severidea*. Moreover, the clade is indicated to have diverged from *C. aglaea* between 3.5 and 10.3 Ma (Fig. 12; Table 6), strengthening the conception of this as a distinct evolutionary lineage. Even though the phenotypic similarity with *C. perlata* is evident, the spore size is overlapping with that of *C. aglaea* (Fig. 5).

Three highly supported clades ("a", "b" and "c") are reported within *C. aglaea* from my phylogenetic analysis (Fig. 10), in line with Bendiksby et al. (2015). The divergence time estimate between the two groupings "a" and "b" in *C. aglaea* is between 1.91–5.38 Ma (Table 6), suggesting that these two clades might be distinct species. However, a thorough morphological investigation of these genetic lineages is needed to

elucidate potential differences between them, but such investigation was out of scope for the current study.

A newly discovered fertile morphotype is found to be nested within the species *C. cuprea* (Figs. 10 and 7C). This implies an extension of the previously known morphological range of this species (see Bendiksby et al. 2015). Different morphotypes with respect to reproductive characters are not uncommon for lichen species (see Lumbsch & Leavitt et al. 2011 and references therein), and dispersion by vegetative propagules, such as soredia, is thought to represent selective advantages in stable environments and during population establishment (Singh et al. 2015). In the *C. cuprea* case, the acquisition of reproductive characters can be related to ecological adaptation, considering that some individuals can have both soredia and apothecia, and some only one of the above. The concept of species pairs (see Poelt 1970; Mattson & Lumbsch 1989) might be relevant for these two morphotypes. Although, with a continuum like presence of reproductive characters and the fact that they are highly nested phylogenetically (i.e., not strictly monophyletic) this is not believed to be the case.

My molecular dating analyses suggest that the two species *C. cuprea* and *C. livida* shared a common ancestor between 7.4 and 18.3 Ma ago (Fig. 12; Table 6). As also shown by Bendiksby et al. (2015) they have near indistinguishable morphologies and are not monophyletic with respect to each other. However, they differ slightly in chemistry with *C. cuprea* having a trace of norstictic acid (Bendiksby et al., 2015). Surprisingly, herein, one specimen of *C. cuprea* (O-L-228124) was found to lack norstictic acid, and one specimen of *C. livida* (O-L-228138) to contain norstictic acid (Fig. 10; Table S1). This questions the chemical distinction previously held between *C. cuprea* and *C. livida* by Bendiksby et al. (2015). Their ecologies are also different, with *C. cuprea* being associated with heavy metal rocks in old copper or nickel mines, and *C. livida* having a wider habitat range. Although this ecological distinction may be important, it is not fully diagnostic, as one record from North America (see Lendemer & Harris 2016), and both the newly discovered fertile morphotype of *C. cuprea* and two specimens (O-L-228124 and O-L-228168) from this study were collected outside of mining habitats. With that said, *C. cuprea* seems to have a greater affinity towards growing on rocks rich in heavy metals.

The placement of *Calomela*, *Paramela* and *Violella* are indicated to be closer to *Severidea* than other lineages in the Tephromelataceae, but their phylogenetic interrelationships are still unresolved (Fig. 10). The species belonging to *Severidea* was treated by Haugan and Timdal (1994), and subsequently Andreev (2004), both predicting the species *C. perlata* and *C. talayana* to be related to *C. aglaea*. Haugan & Timdal (1994) also reported longer spores for *C. perlata* compared to *C. aglaea*, whereas generally larger spores (length and width) compared to *Calvitimela* s. lat. is reported herein (Fig. 5). Furthermore, Spribille et al. (2011a) expected members of *Severidea* to be placed in its own genus. Seeing that *Severidea* is clearly distinct both phylogenetically and chemically from the other subgenera of *Calvitimela*, one might argue for raising *Severidea* from subgenus to genus. Essentially, three solutions exist: keep the current taxonomy of Bendiksby et al. (2015), raise all subgenera to genera, or alternatively include *Calomela*, *Paramela*, *Severidea* and *Violella* into one large genus. The same argument (see above) about practicality applies just as much in *Severidea*. Until phylogenetic relationships can be fully resolved, I recommend the retention of practical

circumscriptions at generic and subgeneric levels.

The taxon *C. septentrionalis* group as sister to *C. cuprea*. The species *C. septentrionalis* has been mysterious since its description from Greenland by Hertel & Rambold (1985) and is only known from the type-material. In this study, *C. septentrionalis* was represented by a single specimen (with one accession of ITS: McCune 36285) from North America, and the application of the name here follows McCune (2017). Without having seen the type, I cannot be certain about the identity of this specimen, however. Due to the lack of data for this taxon, I must leave further discussions to later taxonomic treatments.

The species *C. talayana* is herein reported as new to Canada with one record from Quebec (QFA-0635921). *Calvitimela talayana* is a rarely collected sorediate species making up the subgenus *Paramela* (see Fjelde et al. 2020). The new record provides evidence for the North American and Russian populations of *C. talayana* being conspecific.

4.4 Taxonomic implications and cryptic species

The concept of cryptic species has been under much recent debate (e.g., Struck et al. 2018a, 2018b; Heethoff 2018). The debate is due to the important distinction between the cryptic species as a taxonomic artifact and the true cryptic diversity occurring in nature. Even if two species, seemingly identical in morphology, are found as distinct genetic lineages, it does not necessarily imply that they are cryptic. As proposed by Struck et al. (2018a), a quantitative assessment of phenotypic similarity should be applied in an evolutionary context. In crustose lichens, such assessments of phenotypic similarities are often difficult to obtain. Morphological traits are frequently delicate, and even if differences can be observed, words to explain them often fall short. As shown herein, however, after the establishment of sound phylogenetic hypotheses, and the following close inspection of morphological and chemical characters, diagnostic tools might be uncovered.

The term sibling species may be relevant for clades that are closely related, monophyletic, but genetically distinct and seemingly not phenotypically different (e.g., clade “a” and “b” in *C. aglaea*). The phenotypic similarity between sibling species is thought to arise through morphological stasis (Lumbsch & Leavitt et al. 2011). As described by Struck et al. (2018a), the lack of morphological diversification can be due to low standing genetic variation and/or developmental constraints. The authors also point out that the ecology of taxa showing stasis can have remained constant through time, thereby causing stabilizing selection to retain a common morphology.

The observed phenotypic similarity between non-monophyletic and more distantly related clades (i.e., *C. cuprea* vs. *C. livida*, *C. sp.* vs. *C. perlata*, *C. sp.* vs. the fertile morphotype of *C. cuprea*, *C. melaleuca* I vs. II; Fig. 5–7, 10) can represent adaptations to similar environments (Lumbsch & Leavitt et al. 2011). An interesting observation for the abovementioned clades is that even if they are similar in morphology, they seem to differ at some level between pairs. Take for example the larger spore size between *C. perlata* and the other taxa in *Calvitimela* s. lat. This suggest that *C. perlata* is not a cryptic species compared to

morphologically similar clades (e.g., *C.* sp.). Moreover, subtle differences in chemistry, such as those between *C. cuprea* and *C. livida*, or in thallus morphology like the ones between *C. melaleuca* I and II, seemingly argues against the presence of cryptic diversity in *Calvitimela*. However, the degree of obscurity and overlap in chemistry and morphology at species level in general, increase the chances of misidentifications, especially in the field. Therefore, terms like semi- or pseudocryptic might be suitable. In a practical setting, without the necessary tools to distinguish between similar species in *Calvitimela*, they remain cryptic.

This study has corroborated an unresolved *Calvitimela* with a substantial increase in molecular data compared to Bendiksby et al. (2015). In a broad sense, a few but recognizable morphological traits connect the subgenera of *Calvitimela* together. Chemically, species belonging to *Calvitimela* are distinguishable from the other genera in the Tephromelataceae, but not always within the subgenera. To reach any satisfying circumscription of genera in the Tephromelataceae, my results strongly suggest that additional molecular data is needed. However, a step towards a more natural classification of *Calvitimela* comes through the discovery that *C. uniseptata* belongs in *Lecania*.

In essence, the three genetically divergent clades of *C. melaleuca* s. lat. coexist and share similar ecological niches. They have overlapping chemistries and to some extent morphologies, however spore size and thallus color seem to be diagnostic characters. I suggest that the four genetic lineages in the subgenus *Calvitimela* should be treated as separate taxa. In *Severidea* both morphological and chemical characters are overlapping, but phylogenetic evidence suggest that the clearly divergent clade *C.* sp. also should be recognized as an independent taxon. In line with Bendiksby et al. (2015) I leave the taxonomic treatment of the three groupings “a”, ”b” and “c” within *C. aglaea* to further in-depth morphological studies has been undertaken. The fertile morphotype of *C. cuprea* is conspecific with the sorediate morphotype. Lastly, the taxonomic novelties discovered in this study require names, and a proper nomenclatural treatment.

4.5 Methods and troubleshooting

4.5.1 Morphology and chemistry

Some specimens of *C. melaleuca* s. lat were wrongly determined (i.e., C. *melaleuca* I as *C. melaleuca* II but not vice versa), and I suspect this to be explained by the change in color of fungarium specimens over time (from white to orange and brown) for one specimen (QFA-0623869), and a lack of pigmentation for the other (O-L-225834). The known *C. cuprea* is sorediate and rarely fertile (Bendiksby et al. 2015) and the newly discovered variety of *C. cuprea* is exclusively fertile. Even if sequence cross-contamination cannot be excluded, the two different morphotypes possibly represent unique responses to different ecologies. Sequence cross-contamination could also explain the chemistry seen for the two specimens of *C. cuprea* (O-L-228124) and *C. livida* (O-L-228138). Even though TLC runs were replicated multiple times and gave the same results, more examples are needed to fully confirm this pattern. During this study, a lot of effort was put into a broad

sampling of *C. melaleuca* s. lat. From this sampling, it was evident that the different clades of *C. melaleuca* s. lat. often grew side by side, occupying similar niches (e.g., Fig. 6E–F). Throughout the population sampling, fragments were carefully taken from only one individual thallus at the time, with sterilization of the knife between samples. However, the unintended sampling of a mistaken clade could have occurred. This could have led to contamination and subsequently wrong chemistries inferred during TLC.

4.5.2 Molecular data and phylogenetic inference

The genetic markers used in this study showed variability in their resolution ability at different taxonomic levels. The ITS provided by far the highest resolution at species level and below. Interspecific variation in regions such as the ITS can be maintained because of a non-selective constraint on non-coding regions (Ganley & Kobayashi 2007). This is perhaps the most important reason for the elevated level of variability in ITS, compared to the two other nuclear markers (MCM7, TEF1-α), which I imagine can be subjected to purifying selection at their first and second codon positions to maintain protein function. If intragenomic variability in the ribosomal DNA (e.g., in ITS and LSU) is present, due to multiple different copies, it can lead to comparison of non-homologous characters in the sequence alignment process (Maddison 1997; Stadler et. al 2020). I did not experience any significant problems when aligning sequences of ITS and believe that the probability of comparing non-homologous characters was low.

The higher terminal resolution of ITS corresponded to the high occurrence of substitutions at relatively short F84 distances (Figs. 9 and S1). The idea of including ITS when constructing saturation plots (Fig. 9) was to assess at which level of distance substitutions occurred across the different markers. The distribution of substitutions over F84 distances for the three nuclear loci reflected their level of variability. The two other markers (MCM7 and TEF1-α) had substitutions distributed over a larger interval of distances and had slightly more resolved backbones, but lower terminal resolution (Fig. 9; Fig. S1). In addition, the absence of substitutions observed for TEF1-α (see section 3.2.2) seem to be connected to the short and poorly supported branches leading up to the subgenus *Calvitimela*, *Severidea* and *Tephromela* (Fig. S1E-F). The differences in saturation plots when excluding the outgroup taxa was almost none. This suggests that the main lineages in the Tephromelataceae are quite divergent, also compared to the outgroup, and that the selected outgroup taxa could be reconsidered in future work.

The protein coding gene MCM7 was found to have lower resolution at terminal levels compared to ITS (Fig. S1). Schoch et al. (2012) reported high resolving power at species level across the fungal kingdom for this gene. The comparatively low percentage of segregating sites across MCM7 likely contributes to the slightly reduced terminal resolution. My results also show saturation of substitution for MCM7 (Fig. 9), suggesting that this is a less favorable gene for phylogenetic inference in the Tephromelataceae. Substitutional saturation is a source of non-phylogenetic signal and can cause phylogenetic results to be unreliable (Philippe et al. 2011). Therefore, in parallel with the findings of Spribille et al. (2011b) in *Mycoblastus*, I recommend

that careful measures should be taken when using this gene in the Tephromelataceae in future studies.

TEF1-α showed a moderate resolution power at all topological levels but not exceeding ITS (Fig. S1). Single-copy protein coding genes are valuable markers for inferring phylogenetic relationships (see Pizarro et al. 2018 and references therein). One advantage includes bypassing the issue of potential non-homologous comparison that can occur when comparing multi-copy regions like the ITS (Stadler et. al 2020). Nonetheless, as shown herein, substitutional saturation can occur at third codon positions of some protein coding genes, and the detection of such processes should be incorporated into pre-analysis and data exploration steps when performing phylogenetic analysis.

The mtSSU marker is expected to be a conserved region, and therefore, the amplification and subsequent phylogenetic issues (Fig. S2A) experienced with this marker might suggest primer mismatch, or the amplification of a non-desired fungal contaminant or symbiont. Uniparental inheritance of mitochondria might also have caused incongruence with the nuclear phylogenies (Anderson & Kohn 2007). The small number of accessions for the nuclear LSU marker and the resulting ML topology (Fig. S2B) showed similar phylogenetic relationships as the gene trees of the three other nuclear markers (ITS, MCM7, TEF1-α; Fig. S1).

The use of a few and informative genetic markers is common practice in molecular systematics. However, it is not unusual with backbone resolution problems, and difficulties in resolving deeper taxon boundaries. It has been shown that very large data sets are needed to render fully supported backbone topologies (e.g., Pizzaro et al. 2018), but this is not always the case (Widhelm et al. 2019), seeing that just adding more data to solve your problem is not necessarily the best systematic solution (Philippe et al. 2011; Lemmon & Lemmon 2013). Phylogenomic approaches should be considered when dealing with troubled backbone support, since including a larger amount of the genome might improve the phylogenetic signal. Nevertheless, a careful selection of suitable genetic markers and phylogenetic tools are at least as important in systematic research. In addition, assessing the quality of molecular data is essential to avoid non-phylogenetic signals disrupting phylogenetic outcome (Delsuc et al. 2005).

I experienced a discrepancy between obtained bootstrap support values and bayesian posterior probabilities for all separate gene trees, most notably in ITS and TEF1-α (Figure S1). This highlights a known issue with Bayesian posterior probabilities, that is, sensitivity to signal in the data, and ability to attach high support to branches with small amounts of character change (Alfaro et al. 2003). The recurring low bootstrap values in deeper and intermediate branches can point to internal conflicting signals within the separate alignments (i.e., multiple equally probable topological alternatives in the resampled bootstrap trees; Fig. S1). Which in turn can be a result of a complex evolutionary history in the Tephromelataceae not possible to capture using a dichotomous tree-like model of evolution. Strictly speaking, no supported incongruencies between the gene trees was observed judging from the ML analyses (Fig. S1A, C and E), except a minor case involving one sequence (see section 3.3.1). However, if the relatively highly supported short branches from the bayesian gene trees were interpreted as measures of reliable support and not as a methodological artifact, these would imply incongruent gene trees (Fig. S1B, D and F). In that case, concatenation would not have been justifiable. Thus, analyzing the partitions independently in a multispecies coalescent framework should

be considered in future work. A potential pitfall with concatenation is that the phylogenetic signal from one marker can be overrepresented in the resulting topology. For example, the strong terminal signals in ITS could convey intraspecific as opposed to interspecific variation. Which in turn would imply a resulting delimitation of populations and not species. Furthermore, the true species tree may not always be reflected by single gene trees and including such genes in a concatenated super matrix may cause non-phylogenetic signals to distort the genuine phylogenetic signal (Phillipe et al. 2011).

Different information criteria can sometimes select different models and might be sensitive to overfitting like AICc (Dziak et al. 2020). This could explain the complexity of the substitution models in this study (Table 4). Another issue concerns the number of parameters in the evolutionary model; the more parameters, the easier it is to violate some of the underlying assumptions of the model. The non-phylogenetic signal inferred from probabilistic methods mainly stems from the molecular data violating the model assumptions (Delsuc et al. 2005; Philippe et al. 2011). Therefore, explicitly assessing if and how the data violates assumptions is essential for avoiding wrong inferences of phylogenetic relationships.

4.5.3 Molecular dating

The major clades in the Tephromelataceae (i.e., genera and subgenera) were topologically congruent and 95% HPD age estimate intervals were overlapping between the strict and relaxed analyses (Table 6). However, the strict clock always had consistently older median estimates compared to the relaxed clock (Table 6). Summarizing trees from the posterior of the strict and relaxed analysis yielded different backbone topologies, which may have affected node age estimations because of topological uncertainties (Table 6). The lack of fossil records for lichens (Honegger et al. 2013) is a major obstacle for obtaining accurate estimates of divergence times. The fossil calibration scheme used by Nelsen et al. (2019) is one of the most extensive to date, with thorough justification of the different calibrations used and a broad sampling across the fungal kingdom. Still, there can be severe effects in the estimated node ages from which type of calibrations (e.g., fossils or prior distributions) are used, and how they are set (e.g., fixed ages, or constrained ages; Sauquet 2013). The taxon sampling can also affect the outcome by for example introducing larger intervals of node age estimates with smaller sample sizes (Soares & Schrago 2012).

In general, there are many uncertainties when performing molecular dating analyses, particularly when applying secondary calibrations (see Sauquet 2013 and reference therein) and the results should be interpreted with caution. One could argue that my calibration priors could have been set with log normal distributions, when considering that estimates of divergence time follow a log normal distribution (Morrison 2008). Also, the analysis may have been run by explicitly sampling from the prior, to assess the prior setting effect on the output. With a relatively short time frame and only aiming to provide an initial framework for discussing evolutionary histories in *Calvitimela*, these options were left out, but should be considered in future studies. The study by Divakar et al. (2017) is one of the few studies including sequences of *Mycoblastus* and *Tephromela* in a molecular dating framework. I did not set out to discuss the divergence time of these two

genera and seeing that the sampling schemes between this study and Divakar et al (2017) are very different, it is not meaningful to discuss potential discrepancies between age estimates.

4.6 Future perspectives

Technological advancements evolve and our tools for understanding biological diversity are continuously operating at finer scales of precision. This is an invaluable asset for systematists as we are increasingly able to represent more realistic hypotheses of nature through our classification systems. Dealing with difficult phylogenetic problems, like the one in *Calvitimela*, requires time and rigorous inspection. If questions about deep phylogenetic relationships in the Tephromelataceae are to be understood, more and new, preferably highly conserved markers, are needed. Potentially, whole genome data could reveal interesting results about the ancient evolutionary history of the genus and the family.

The problem of cryptic species is evident in taxonomy and in many ways reflects the current scientific transitions. We are now able to probe more aspects of biology than ever before with for example modern sequencing, advanced microscopy, and powerful analytical tools. Moving from morphological species concepts to complex integrative taxonomic concepts it is no surprise that we find more characters, and thus can describe more species. In *Calvitimela*, the distinction between cryptic and non-cryptic diversity is not consistently clear-cut, with the varying degrees of character obscurity and mismatch to the DNA based phylogeny. To further elucidate species in the subgenus *Calvitimela* a more extensive population sampling would be beneficial. For instance, a broad sampling (including vouchers) of all four clades in the subgenus *Calvitimela*, from a wider geographic range could be used to quantitatively assess chemical, genetic, and phenotypic variation. In general, increased sampling together with studies of ecological factors and geographical distribution patterns is recommended to reach a better understanding of the species in *Calvitimela* s. lat.

Moving forward, a molecular investigation of photobionts or other symbionts could uncover unknown patterns between observable traits (morphological and chemical) and genetic lineages. Signs of incongruence between the different gene trees and the concatenated tree were observed in the subgenus *Calvitimela*. Therefore, an independent analysis of different genetic markers in a multispecies coalescent framework is encouraged to account for incompatible evolution between genes and species. To further explore the potential of more complex evolutionary histories, a phylogenetic network approach could be useful to account for processes such as reticulation, hybridization, horizontal gene transfer and gene duplication.

On one hand the taxonomy and nomenclature of organisms should reflect hypothesis of evolution, but on the other hand be accessible and practical for users such as conservationists, hobbyist, and biologists in general. Inviting the idea that practical taxonomic circumscriptions and true representations of evolutionary histories do not always go hand in hand is essential for a continuation of sound classification and meaningful communication of biodiversity.

References

Adobe Inc. 2020. Adobe InDesign. Retrieved from https://adobe.com/products/indesign.

Alfaro, M. E., Zoller, S., & Lutzoni, F. 2003. Bayes or bootstrap? A simulation study comparing the performance of Bayesian Markov chain Monte Carlo sampling and bootstrapping in assessing phylogenetic confidence. *Molecular Biology and Evolution* **20**: 255-266. https://doi.org/10.1093/molbev/msg028.

Anderson, J. B., & Kohn, L. M. 2007. Dikaryons, diploids, and evolution. In *Sex in fungi: molecular determination and evolutionary implications* p. 333-348. American Society of Microbiology Press, USA.

Andreev, M. P. 2004. New taxonomic combinations for lecidioid lichens. *Novosti sistematiki nizshikh rasteniy* **37**: 188–191.

Arup, U., Ekman, S., Grube, M., Mattsson, J. E., & Wedin, M. 2007. The sister group relation of Parmeliaceae (Lecanorales, Ascomycota). *Mycologia* **99**(1): 42-49. https://doi.org/10.1080/15572536.2007.11832599.

Bendiksby, M., & Timdal, E. 2013. Molecular phylogenetics and taxonomy of Hypocenomyce sensu lato (Ascomycota: Lecanoromycetes): extreme polyphyly and morphological/ecological convergence. *Taxon* **62**: 940-956. https://doi.org/10.12705/625.18.

Bendiksby, M., Haugan, R., Spribille, T., & Timdal, E. 2015. Molecular Phylogenetics and Taxonomy of the *Calvitimela aglaea* complex (Tephromelataceae, Lecanorales). *Mycologia* **107**(1): 1172-1183. https://doi.org/10.3852/14-062.

Bivand, R. S., Pebesma, E. J., Gomez-Rubio, V., & Pebesma, E. J. 2013. *Applied spatial data analysis with R*. Vol. 2. New York: Springer.

Bouckaert, R., Vaughan, T. G., Barido-Sottani, J., Duchêne, S., Fourment, M., Gavryushkina, A., Heled, J., Jones, G., Kühnert, D., & De Maio, N. 2019. Beast 2.5: An Advanced Software Platform for Bayesian Evolutionary Analysis. *PLoS computational biology*, **15**(4): e1006650. https://doi.org/10.1371/journal.pcbi.1006650.

Brown, S. D., Collins, R. A., Boyer, S., Lefort, M. C., Malumbres-Olarte, J. A. G. O. B. A., Vink, C. J., & Cruickshank, R. H. 2012. Spider: an R package for the analysis of species identity and evolution, with particular reference to DNA barcoding. *Molecular ecology resources* **12**(3): 562-565. https://doi.org/10.1111/j.1755-0998.2011.03108.x.

Castresana, J. 2000. Selection of conserved blocks from multiple alignments for their use in phylogenetic analysis. *Molecular biology and evolution* **17**(4):540-552. https://doi.org/10.1093/oxfordjournals.molbev.a026334.

Chamberlain, S., Barve, V., Mcglinn, D., Oldoni, D., Desmet. P., Geffert, L., Ram, K. 2021. rgbif: Interface to the Global Biodiversity Information Facility API. R package version 3.5.2. https://CRAN.R-project.org/package=rgbif.

Chamberlain, S., Boettiger, C. 2017. R Python, and Ruby clients for GBIF species occurrence data (No. e3304v1). *PeerJ PrePrints*. https://doi.org/10.7287/peerj.preprints.3304v1.

Crespo, A., & Pérez-Ortega, S. 2009. Cryptic species and species pairs in lichens: a discussion on the relationship between molecular phylogenies and morphological characters. In *Anales del Jardín Botánico de Madrid* (Vol. 66, No. 1, p. 71-81). Consejo Superior de Investigaciones Científicas. https://doi:10.3989/ajbm.2225.

Crespo, A., & Lumbsch, H. T. 2010. Cryptic Species in Lichen-Forming Fungi. *IMA fungus* **1**(2): 167. https://doi.org/10.5598/imafungus.2010.01.02.09.

Culberson, C. F., & Johnson, A. 1982. Substitution of Methyl Tert. - Butyl Ether for Diethyl Ether in the Standardized Thin-Layer Chromatographic Method for Lichen Products. *Journal of Chromatography A*, **238**(2): 483-87. https://doi.org/10.1016/S0021-9673(00)81336-9.

Culberson, W. L. 1969. The Use of Chemistry in the Systematics of the Lichens. *Taxon* **18**(2): 152-166. https://doi.org/10.2307/1218673.

Culberson, C. F. 1972. Improved Conditions and New Data for Identification of Lichen Products by Standardized Thin Layer Chromatographic Method. *Journal of Chromatography A* **72**(1): 113-25. https://doi.org/10.1016/0021-9673(72)80013-X.

Culberson, C. F., & Kristinsson, H. D. 1970. A Standardized Method for the Identification of Lichen Products. *Journal of Chromatography A* **46**: 85-93. https://doi.org/10.1016/S0021-9673(00)83967-9.

Culberson, W. L. 1986. Chemistry and sibling speciation in the lichen-forming fungi: ecological and biological considerations. *Bryologist* 123-131. https://doi/10.2307/3242752.

Delsuc, F., Brinkmann, H., & Philippe, H. 2005. Phylogenomics and the reconstruction of the tree of life. *Nature Reviews Genetics* **6**(5): 361-375. https://doi.org/10.1038/nrg1603.

Dillman, K. L., Ahti, T., Björk, C. R., Clerc, P., Ekman, S., Goward, T., ... & Spribille, T. 2010. New records, range extensions and nomenclatural innovations for lichens and lichenicolous fungi from Alaska, USA. *Herzogia* **25**(2): 177-210. https://doi.org/10.13158/heia.25.2.2010.177.

Divakar, P. K., Crespo, A., Kraichak, E., Leavitt, S. D., Singh, G., Schmitt, I., & Lumbsch, H. T. 2017. Using a temporal phylogenetic method to harmonize family-and genus-level classification in the largest clade of lichen-forming fungi. *Fungal Diversity* **84**(1): 101-117. https://doi.org/10.1007/s13225-017-0379-z.

Dziak, J. J., Coffman, D. L., Lanza, S. T., Li, R., & Jermiin, L. S. 2020. Sensitivity and specificity of information criteria. *Briefings in bioinformatics* **21**(2): 553-565. https://doi.org/10.1093/bib/bbz016.

Edgar, R. C. 2004. Muscle: Multiple Sequence Alignment with High Accuracy and High Throughput. *Nucleic acids research* **32**(5): 1792-97. https://doi.org/10.1093/nar/gkh340.

Fjelde, M. O., & Melechin, A. M., Timdal, E. 2020. *Calvitimela talayana* new to Fennoscandia. *Graphis Scripta* **32**(5): 101-109.

Fries, T. M. 1874. *Lichenographia Scandinavica* 1, 2. Uppsala.

Frolov, I., Vondrák, J., Fernández-Mendoza, F., Wilk, K., Khodosovtsev, A., & Halıcı, M. G. 2016. Three new, seemingly-cryptic species in the lichen genus *Caloplaca* (Teloschistaceae) distinguished in two-phase phenotype evaluation. In *Annales Botanici Fennici* (Vol. 53. No. 3–4, p. 243-262). Finnish Zoological and Botanical Publishing Board. https://doi.org/10.5735/085.053.0413.

Fryday, A. M. 2011. New Species and Combinations in *Calvitimela* and *Tephromela* from the Southern Subpolar Region. *The Lichenologist* **43**(3): 225. https://doi:10.1017/S0024282911000065.

Ganley, A. R., & Kobayashi, T. 2007. Highly efficient concerted evolution in the ribosomal DNA repeats: total rDNA repeat variation revealed by whole-genome shotgun sequence data. *Genome research* **17**(2): 184-191. https://doi:10.1101/gr.5457707.

Garrido-Benavent, I., Pérez-Ortega, S., de Los Ríos, A., Mayrhofer, H., & Fernández-Mendoza, F. 2021. Neogene speciation and Pleistocene expansion of the genus *Pseudephebe* (Parmeliaceae, lichenized fungi) involving multiple colonizations of Antarctica. *Molecular Phylogenetics and Evolution* **155**: 107020. https://doi.org/10.1016/j.ympev.2020.107020.

GBIF Occurrence Download Accessed from R via rgbif (https://github.com/ropensci/rgbif) on 2021-05-14. https://doi.org/10.15468/dl.4y5sv6.

Guindon, S., Dufayard, J. F., Lefort, V., Anisimova, M., Hordijk, W., & Gascuel, O. 2010. New algorithms and methods to estimate maximum-likelihood phylogenies: assessing the performance of PhyML 3.0. *Systematic biology* **59**(3): 307-321. https://doi.org/10.1093/sysbio/syq010.

Hafellner, J. 1984. Studien in Richtung Einer Natürlicheren Gliederung Der Sammelfamilien Lecanoraceae Und Lecideaceae. *Beihefte zur Nova Hedwigia* (79): 241-371.

Haugan, R., & Timdal, E. 1994. *Tephromela perlata* and *T. talayana*, with notes on the *T. aglaea*- complex. *Graphis Scripta* **6**(1): 17-26.

Haugan, R., & Timdal, E. 2019. The morphologically cryptic lichen species *Parmelia ernstiae* and *P. serrana* new to Norway. *Graphis Scripta* **31**: 5-13.

Hafellner, J., & Türk, R. 2001. Die Lichenisierten Pilze Österreichs: Eine Checkliste Der Bisher Nachgewiesenen Arten Mit Verbreitungsangaben (Biologiezentrum d. Oberösterr. Landesmuseums).

Heethoff, M. 2018. Cryptic species–conceptual or terminological chaos? A response to Struck et al. *Trends in Ecology & Evolution* **33**(5): 310. https://doi.org/10.1016/j.tree.2018.02.006.

Hertel, H., & Rambold, G. 1985. *Lecidea* Sect. *armeniacae*: Lecideoide Arten Der Flechtengattungen *Lecanora* Und *Tephromela* (Lecanorales). *Botanische Jahrbucher fur Systematik, Pflanzengeschichte und Pflanzengeographie*.

Honegger, R., Edwards, D., & Axe, L. 2013. The earliest records of internally stratified cyanobacterial and algal lichens from the Lower Devonian of the Welsh Borderland. *New Phytologist* **197**(1): 264-275. https://doi.org/10.1111/nph.12009.

Huson, D. H., & Scornavacca, C. 2012. Dendroscope 3: an interactive tool for rooted phylogenetic trees and networks. *Systematic biology* **61**(6): 1061-1067. https://doi:10.1093/sysbio/sys062.

Kistenich, S., Rikkinen, J. K., Thüs, H., Vairappan, C. S., Wolseley, P. A., & Timdal, E. 2018. Three new species of Krogia (Ramalinaceae, lichenised Ascomycota) from the Paleotropics. *MycoKeys* **40**: 69. https://doi.org/10.3897/mycokeys.40.26025.

Kozlov, A. M., Darriba, D., Flouri, T., Morel, B., & Stamatakis, A. 2019. RAxML-NG: a fast, scalable and user-friendly tool for maximum likelihood phylogenetic inference. *Bioinformatics* **35(**21**)**: 4453-4455. https://doi.org/10.1093/bioinformatics/btz305.

LaGreca, S., Lumbsch, H. T., Kukwa, M., Wei, X., Han, J. E., Moon, K. H., ... & Leavitt, S. D. 2020. A molecular phylogenetic evaluation of the *Ramalina siliquosa* complex, with notes on species circumscription and relationships within *Ramalina*. *The Lichenologist* **52**(3):197-211. https://doi:10.1017/S0024282920000110.

Lamarck & De Candolle. 1805. *Flore française ou descriptions succinctes de toutes les plantes qui croissent naturellement en France*. ed. 3. Vol. 2 : 367.

Leavitt, S. D., Kraichak, E., Vondrak, J., Nelsen, M. P., Sohrabi, M., Perez-Ortega, S., ... & Lumbsch, H. T. 2016. Cryptic diversity and symbiont interactions in rock-posy lichens. *Molecular Phylogenetics and Evolution* **99**: 261-274. https://doi.org/10.1016/j.ympev.2016.03.030.

Leavitt, S. D., Grewe, F., Widhelm, T., Muggia, L., Wray, B., & Lumbsch, H. T. 2016. Resolving evolutionary relationships in lichen-forming fungi using diverse phylogenomic datasets and analytical approaches. *Scientific reports* **6**(1): 1-11. https://doi.org/10.1038/srep22262.

Lanfear, R., Calcott, B., Ho, S. Y., & Guindon, S. 2012. PartitionFinder: combined selection of partitioning schemes and substitution models for phylogenetic analyses. *Molecular biology and evolution* **29**(6): 1695-1701. https://doi.org/10.1093/molbev/mss020.

Lanfear, R., Frandsen, P. B., Wright, A. M., Senfeld, T., & Calcott, B. 2016. PartitionFinder 2: new methods for selecting partitioned models of evolution for molecular and morphological phylogenetic analyses. *Molecular biology and evolution* **34**(3): 772-773. https://doi.org/10.1093/molbev/msw260.

Larsson, A. 2014. Aliview: A Fast and Lightweight Alignment Viewer and Editor for Large Datasets. *Bioinformatics* **30**(22): 3276-78. https://doi.org/10.1093/bioinformatics/btu531.

Lemmon, E. M., & Lemmon, A. R. 2013. High-throughput genomic data in systematics and phylogenetics. *Annual Review of Ecology, Evolution, and Systematics* **44**: 99-121. https://doi.org/10.1146/annurev-ecolsys-110512-135822.

Lendemer, J. C., & Harris, R. C. 2016. Studies in Lichens and Lichenicolous Fungi–No. 20: Further notes on species from the eastern North America. *Opuscula Philolichenum* **15**: 105-131.

Lücking, R., Hodkinson, B. P., & Leavitt, S. D. 2017. The 2016 classification of lichenized fungi in the Ascomycota and Basidiomycota–Approaching one thousand genera. *The Bryologist* **119**(4): 361-416. https://doi.org/10.1639/0007-2745-119.4.361.

Lücking, R., Aime, M. C., Robbertse, B., Miller, A. N., Ariyawansa, H. A., Aoki, T., ... & Schoch, C. L. (2020). Unambiguous identification of fungi: where do we stand and how accurate and precise is fungal DNA barcoding? *IMA fungus* **11**(1): 1-32. https://doi.org/10.1186/s43008-020-00033-z.

Lumbsch, H. T., Ahti, T., Altermann, S., De Paz, G. A., Aptroot, A., Arup, U., ... & Lucking, R. 2011. One hundred new species of lichenized fungi: a signature of undiscovered global diversity. *Phytotaxa* **18**(1): 1-127. https://doi.org/10.11646/phytotaxa.18.1.1.

Lumbsch, H. T., & Leavitt, S. D. 2011. Goodbye morphology? A paradigm shift in the delimitation of species in lichenized fungi. *Fungal Diversity* **50**(1): 59-72. https://doi.org/10.1007/s13225-011-0123-z.

Maddison, W. P. 1997. Gene trees in species trees. *Systematic biology* **46**(3): 523-536. https://doi.org/10.1093/sysbio/46.3.523.

Magnusson, A. H. 1931. Studien ÜBer Einige Arten Der *Lecidea armeniaca*- Und *elata*-Gruppe. *Acta Horti Gothoburg* **6**:93–144.

Mann, D. G., & Evans, K. M. 2008. The species concept and cryptic diversity. In *Proceedings of the 12th International Conference on Harmful Algae* (p. 262-268). Copenhagen: International Society for the Study of Harmful Algae and Intergovernmental Oceanographic Commission of UNESCO.

Mattsson, J. E., & Lumbsch, H. T. 1989. The use of the species pair concept in lichen taxonomy. *Taxon* **38**(2): 238-241. https://doi.org/10.2307/1220840.

McCune, B. 2017. Microlichens of the Pacific Northwest. Volume 2: Key to the species. Corvallis. Wild Blueberry Media.

McCune, B., Arup, U., Breuss, O., Di Meglio, E., Di Meglio, J., Esslinger, T. L., ... & Walton, J. 2020. Biodiversity and ecology of lichens of Kenai Fjords National Park, Alaska. *Plant and Fungal Systematics* **65**(2): 586-619. https://doi.org/10.35535/pfsyst-2020-0032.

Menlove, J. E. 1974. Thin-Layer Chromatography for the Identification of Lichen Substances. *British Lichen Society Bulletin* **34**: 3-5.

Miadlikowska, J., Kauff, F., Hofstetter, V., Fraker, E., Grube, M., Hafellner, J., ... & Lutzoni, F. 2006. New insights into classification and evolution of the Lecanoromycetes (Pezizomycotina, Ascomycota) from phylogenetic analyses of three ribosomal RNA-and two protein-coding genes. *Mycologia* **98**(6): 1088-1103. https://doi.org/10.1080/15572536.2006.11832636.

Miadlikowska, J., Kauff, F., Högnabba, F., Oliver, J. C., Molnár, K., Fraker, E., ... & Stenroos, S. 2014. A multigene phylogenetic synthesis for the class Lecanoromycetes (Ascomycota): 1307 fungi representing 1139 infrageneric taxa, 317 genera and 66 families. *Molecular phylogenetics and evolution* **79**: 132-168. https://doi.org/10.1016/j.ympev.2014.04.003.

Muggia, L., Grube, M., & Tretiach, M. 2008. Genetic diversity and photobiont associations in selected taxa of the *Tephromela atra* group (Lecanorales, lichenised Ascomycota). *Mycological Progress* **7**(3): 147-160. https://doi.org/10.1007/s11557-008-0560-6.

Nelsen, M. P., Lücking, R., Boyce, C. K., Lumbsch, H. T., & Ree, R. H. 2020. No support for the emergence of lichens prior to the evolution of vascular plants. *Geobiology* **18**(1): 3-13. https://doi.org/10.1111/gbi.12369.

Næsborg, R. R., Ekman, S., & Tibell, L. 2007. Molecular phylogeny of the genus Lecania (Ramalinaceae, lichenized Ascomycota). *Mycological Research* **111**(5): 581-591. https://doi.org/10.1016/j.mycres.2007.03.001.

Paradis E. & Schliep K. 2019. ape 5.0: an environment for modern phylogenetics and evolutionary analyses in R. *Bioinformatics* **35**(3): 526-528. https://doi.org/10.1093/bioinformatics/bty633.

Paradis E. 2010. pegas: an R package for population genetics with an integrated-modular approach. *Bioinformatics* **26**(3): 419-420. https://doi.org/10.1093/bioinformatics/btp696.

Pebesma, E., & Bivand, R. S. 2005. S classes and methods for spatial data: the sp package. *R news* **5**(2): 9-13. https://cran.r-project.org/package=sp.

Pfeifer, B., Wittelsbürger, U., Ramos-Onsins, S. E., & Lercher, M. J. 2014. PopGenome: an efficient Swiss army knife for population genomic analyses in R. *Molecular biology and evolution* **31**(7): 1929-1936. https://doi.org/10.1093/molbev/msu136.

Philippe, H., Brinkmann, H., Lavrov, D. V., Littlewood, D. T. J., Manuel, M., Wörheide, G., & Baurain, D. 2011. Resolving difficult phylogenetic questions: why more sequences are not enough. *PLoS Biol* **9**(3): e1000602. https://doi.org/10.1371/journal.pbio.1000602.

Pizarro, D., Divakar, P. K., Grewe, F., Leavitt, S. D., Huang, J. P., Dal Grande, F., ... & Lumbsch, H. T. 2018. Phylogenomic analysis of 2556 single-copy protein-coding genes resolves most evolutionary relationships for the major clades in the most diverse group of lichen-forming fungi. *Fungal diversity* **92**(1): 31-41. https://doi.org/10.1007/s13225-018-0407-7.

Poelt, J. 1970. Das Konzept der Artenpaare bei den Flechten. *Deutsche Botanische Gesellschaft, neue Folge* **4**: 187-198.

Rambaut, A. 2012. Figtree v. 1.4.4 Retrieved from https://github.com/rambaut/figtree.

Rambaut, A., Drummond, A. J., Xie, D., Baele, G., & Suchard, M. A. 2018. Posterior Summarization in Bayesian Phylogenetics Using Tracer 1.7. *Systematic Biology* **67**(5): 901-04. https://doi.org/10.1093/sysbio/syy032.

R Core Team. 2020. R: A language and environment for statistical computing. R Foundation for Statistical Computing, Vienna, Austria. URL https://www.R-project.org/.

Ronquist, F., Teslenko, M., Van Der Mark, P., Ayres, D. L., Darling, A., Höhna, S., ... & Huelsenbeck, J. P. 2012. MrBayes 3.2: efficient Bayesian phylogenetic inference and model choice across a large model space. *Systematic biology* **61**(3): 539-542. https://doi.org/10.1093/sysbio/sys029.

Schneider, K., Resl, P., Westberg, M., & Spribille, T. 2015. A new, highly effective primer pair to exclude algae when amplifying nuclear large ribosomal subunit (LSU) DNA from lichens. *The Lichenologist* **47**(4): 269. https://doi:10.1017/S002428291500016X.

Schneider, K., Resl, P., & Spribille, T. 2016. Escape from the cryptic species trap: lichen evolution on both sides of a cyanobacterial acquisition event. *Mol Ecol* **25**(14): 3453-3468. https://doi.org/10.1111/mec.13636.

Schoch, C. L., Seifert, K. A., Huhndorf, S., Robert, V., Spouge, J. L., Levesque, C. A., ... & Fungal Barcoding Consortium. 2012. Nuclear ribosomal internal transcribed spacer (ITS) region as a universal DNA barcode marker for Fungi. *Proceedings of the National Academy of Sciences*, **109**(16): 6241-6246. https://doi.org/10.1073/pnas.1117018109.

Schwendener, S. 1869. *Die algentypen der Flechtengonidien*. C. Schultze.

Singh, G., Dal Grande, F., Werth, S., & Scheidegger, C. 2015. Long-term consequences of disturbances on reproductive strategies of the rare epiphytic lichen Lobaria pulmonaria: clonality a gift and a curse. *FEMS Microbiology Ecology* **91**(1): 1-11. https://doi:10.1093/femsec/fiu009.

Singh, G., Dal Grande, F., Divakar, P. K., Otte, J., Leavitt, S. D., Szczepanska, K., ... & Schmitt, I. 2015. Coalescent-based species delimitation approach uncovers high cryptic diversity in the cosmopolitan lichen-forming fungal genus *Protoparmelia* (Lecanorales, Ascomycota). *PLoS One* **10**(5): e0124625. https://doi.org/10.1371/journal.pone.0124625.

Soares, A. E., & Schrago, C. G. 2012. The influence of taxon sampling and tree shape on molecular dating: an empirical example from Mammalian mitochondrial genomes. *Bioinformatics and Biology Insights* **6**: BBI-S9677. https://doi.org/10.4137/BBI.S9677.

South, A. 2017. rnaturalearth: World map data from Natural Earth. R package version 0.1.0. *The R Foundation.* https://CRAN.R-project.org/package=rnaturalearth.

Spribille, T., Pérez-Ortega S., Tønsberg T., Schirokauer, D. 2010. Lichens and lichenicolous fungi of the Klondike Gold Rush National Historic Park, Alaska, in a global biodiversity context. *Bryologist* **113**(3): 439–515. https://doi.org/10.1639/0007-2745-113.3.439.

Spribille, T., Goffinet, B., Barbara, K., Muggia, L., Obermayer, W., & Mayrhofer, H. 2011a. Molecular Support for the Recognition of the *Mycoblastus fucatus* Group as the New Genus *Violella* (Tephromelataceae, Lecanorales). *The Lichenologist* **43**(5): 445-66. https://doi.org/10.1017/S0024282911000478.

Spribille, T., Klug, B., & Mayrhofer, H. 2011b. A phylogenetic analysis of the boreal lichen Mycoblastus sanguinarius (Mycoblastaceae, lichenized Ascomycota) reveals cryptic clades correlated with fatty acid profiles. *Molecular Phylogenetics and Evolution* **59**(3): 603-614. https://doi.org/10.1016/j.ympev.2011.03.021.

Spribille, T. 2018. Relative symbiont input and the lichen symbiotic outcome. *Current opinion in plant biology* **44**: 57-63. https://doi.org/10.1016/j.pbi.2018.02.007.

Struck, T. H., Feder, J. L., Bendiksby, M., Birkeland, S., Cerca, J., Gusarov, V. I., ... & Dimitrov, D. 2018a. Finding evolutionary processes hidden in cryptic species. *Trends in Ecology & Evolution* **33**(3): 153-163. https://doi.org/10.1016/j.tree.2017.11.007.

Struck, T. H., Feder, J. L., Bendiksby, M., Birkeland, S., Cerca, J., Gusarov, V. I., ... & Dimitrov, D. 2018b. Cryptic species–more than terminological chaos: a reply to Heethoff. *Trends in ecology & evolution* **33**(5): 310-312. https://doi.org/10.1016/j.tree.2018.02.008.

Swift, H. F., Daglio, L. G., & Dawson, M. N. 2016. Three routes to crypsis: stasis, convergence, and parallelism in the Mastigias species complex (Scyphozoa, Rhizostomeae). *Molecular Phylogenetics and Evolution* **99**: 103-115. https://doi.org/10.1016/j.ympev.2016.02.013.

Sætre, G. P., & Ravinet, M. 2019. *Evolutionary genetics: Concepts, analysis, and practice*. Oxford University Press, USA.

Talavera, G., & Castresana, J. 2007. Improvement of phylogenies after removing divergent and ambiguously aligned blocks from protein sequence alignments. *Systematic biology* **56**(4): 564-577. https://doi.org/10.1080/10635150701472164.

Taylor, J. W., Jacobson, D. J., Kroken, S., Kasuga, T., Geiser, D. M., Hibbett, D. S., & Fisher, M. C. 2000. Phylogenetic species recognition and species concepts in fungi. *Fungal genetics and biology* **31**(1): 21-32. https://doi:10.1006/fgbi.2000.1228.

Werth, S. 2010. Population genetics of lichen-forming fungi-a review. *The Lichenologist* **42**(5): 499-519. https://doi.org/10.1017/S0024282910000125.

White, T. J., Bruns, T., Lee, S. J. W. T., & Taylor, J. 1990. Amplification and direct sequencing of fungal ribosomal RNA genes for phylogenetics. In Innis, M.A., D.H. Gelfand, J.J. Sninsky, & T.J. White eds. *PCR protocols: a guide to methods and applications*. Academic Press, Inc., New York. p 315-322.

Wickham, H. 2016. ggplot2: Elegant Graphics for Data Analysis. Springer-Verlag, New York. https://ggplot2.tidyverse.org.

Widhelm, T. J., Grewe, F., Huang, J. P., Mercado-Díaz, J. A., Goffinet, B., Lücking, R., ... & Lumbsch, H. T. 2019. Multiple historical processes obscure phylogenetic relationships in a taxonomically difficult group (Lobariaceae, Ascomycota). *Scientific reports* **9**(1): 1-16. https://doi.org/10.1038/s41598-019-45455-x.

Zoller, S., Scheidegger, C., & Sperisen, C. 1999. PCR primers for the amplification of mitochondrial small subunit ribosomal DNA of lichen-forming ascomycetes. *The Lichenologist* **31**(5): 511-516. https://doi.org/10.1006/lich.1999.0220.

Supplementary information

Table S1. All taxa with fungarium and voucher numbers for the specimens used in this study. The table show sequence ID, country of origin and major lichen substances (if determined). Vouchers for which spores are measured are indicated with a black dot. Newly generated sequences are indicated with an asterix, and GenBank accession numbers for vouchers with already existing sequences. Sequences of ITS included in the phylogenetic analysis of the *C. melaleuca* populations are shown with a circle around the asterix. Two unpublished sequences from the DNA database at O were included and are indicated with PCR number and lane (51_19 and 293_11). The sequences included in the molecular dating analyses of the Tephromelataceae are highlighted in green.

Taxon	Fungarium and Voucher	Sequence ID	Country	Major substances	Spores (N = 15)	ITS	MCM7	TEF1-α	mtSSU	LSU	Genus
Calvitimela aglaea	**GZU Hafellner 72944**	**AGL2021_1**	**Austria**	**ATR, BOU, USN**		**JN009717**	**–**	**JN009683**	**–**	**–**	***CALVITIMELA***
C. aglaea	GZU Hafellner 70358	AGL2021_2	Austria	ATR, BOU, USN		JN009718	–	JN009684	–	–	
C. aglaea	GZU Nordin 6659 (UPS-183008)	AGL2021_3	Sweden	–		JN009719	–	JN009685	–	–	
C. aglaea	hb. Fryday 10101	AGL2021_4	USA	–		*	–	–	–	–	
C. aglaea	MSC Spribille 38382	AGL2021_5	USA	ATR, BOU, USN		KR303633	KR303669	KR704159	–	–	
C. aglaea	MSC Fryday & Spribille 39433	AGL2021_6	USA	ATR, BOU, USN		KR303635	KR303671	KR704158	–	–	
C. aglaea	MSC Spribille 38829	AGL2021_7	USA	ATR, BOU, USN		KR303634	KR303670	KR704160	–	–	
C. aglaea	O-L-225789	AGL2021_8	Norway	ATR, BOU, STI, USN	●	*	*	*	*	–	
C. aglaea	O-L-203822[1]	AGL2021_9	Spain	AL, ROC		*	–	*	–	–	
C. aglaea	O-L-225761	AGL2021_10	Norway	ATR, BOU, USN	●	*	–	–	–	–	
C. aglaea	O-L-225886	AGL2021_11	Norway	ATR, BOU, USN		*	–	–	–	–	
C. aglaea	O-L-210379	AGL2021_12	Japan	ATR, BOU, USN		*	*	*	–	–	
C. aglaea	O-L-228171	AGL2021_13	Norway	ATR, BOU, USN		*	–	–	–	–	
C. aglaea	O-L-228100	AGL2021_14	Norway	ATR, BOU, USN		*	*	*	–	–	
C. aglaea	O-L-228199	AGL2021_15	Norway	ATR, BOU, USN	●	*	–	*	–	–	
C. aglaea	O-L-228193[2]	AGL2021_16	Norway	ATR, NOR, STI		*	*	*	–	–	
C. aglaea	O-L-228189	AGL2021_17	Norway	ATR, BOU, USN		*	*	*	*	*	
C. aglaea	O-L-228145	AGL2021_18	Norway	ATR, BOU, USN		*	*	*	–	–	
C. aglaea	O-L-228075	AGL2021_19	Norway	ATR, BOU, USN	●	*	*	*	–	–	
C. aglaea	O-L-169281	AGL2021_20	Norway	ATR, BOU, USN		*	–	–	–	–	
C. aglaea	O-L-173528	AGL2021_21	Norway	ATR, BOU, USN		*	–	–	–	–	
C. aglaea	O-L-173831	AGL2021_22	Norway	ATR, BOU, USN		KR303630	KR303668	KR704161	–	–	
C. aglaea	O-L-163597	AGL2021_23	Norway	ATR, BOU, USN		KR303637	KR303672	KR704162	–	–	
C. aglaea	O-L-160708	AGL2021_24	Iceland	ATR, BOU, USN	●	KR303636	–	–	–	–	
C. aglaea	O-L-225848	AGL2021_26	Norway	ATR, BOU, USN		–	*	–	–	–	
C. aglaea	O-L-225758	AGL2021_27	Norway	ATR, BOU, USN, PSO		–	–	*	–	–	

C. aglaea	O-L-225845	AGL2021_28	Norway	ATR, BOU, USN		–	–	*	–	–
C. armeniaca	**GZU-000304515**	**ARM2021_1**	**Steiermark**	**ALE, ROC**	●	*	–	–	–	–
C. armeniaca	GZU SX-16647	ARM2021_2	Austria	ALE, PRO, ROC		*	–	–	–	–
C. armeniaca	GZU Hafellner 71304[3]	ARM2021_3	Austria	ALE, ROC		JN009709	JN009739	JN009678	–	–
C. armeniaca	GZU Perez-Ortega 1322	ARM2021_4	Spain	–		JN009711	JN009741	–	–	–
C. armeniaca	GZU Perez-Ortega 1321	ARM2021_5	Spain	–		JN009710	JN009740	–	–	–
C. armeniaca	hb. Arup U. Arup L97797	ARM2021_6	Italy	–		AY541278	–	–	–	–
C. armeniaca	O-L-204648	ARM2021_7	Slovakia	ALE, ROC	●	*	–	*	–	–
C. armeniaca	O-L-225775	ARM2021_8	Norway	ALE, ROC	●	*	*	*	–	–
C. armeniaca	O-L-224526	ARM2021_9	Norway	ALE, ROC		–	*	*	–	–
C. armeniaca	O-L-204644	ARM2021_10	Slovakia	ALE, ROC		*	*	*	–	–
C. armeniaca	O-L-225800	ARM2021_11	Norway	ALE, ROC		*	–	–	–	–
C. armeniaca	O-L-204644	ARM2021_12	Slovakia	ALE, ROC		*	–	*	–	*
C. armeniaca	O-L-225781	ARM2021_13	Norway	ALE, ROC	●	*	*	*	–	–
C. armeniaca	O-L-204918	ARM2021_14	Switzerland	ALE, PRO, ROC		*	*	*	–	–
C. armeniaca	O-L-204901	ARM2021_15	Switzerland	PROT, PSO, ROC		*	*	–	–	–
C. armeniaca	O-L-228173	ARM2021_16	Norway	ALE, ROC		⊛	*	*	–	*
C. armeniaca	O-L-228137	ARM2021_17	Norway	ALE, ROC	●	*	*	*	–	–
C. armeniaca	O-L-195811	ARM2021_18	Norway	ALE, ROC		*	–	–	–	–
C. armeniaca	O-L-228197	ARM2021_19	Norway	ALE, ROC		*	–	–	–	–
C. armeniaca	O-L-228180	ARM2021_20	Norway	ALE, ROC		⊛	*	*	–	–
C. armeniaca	O-L-170675	ARM2021_21	Norway	ALE, ROC		KR303638	KR303673	KR704163	–	–
C. armeniaca	O-L-170644	ARM2021_22	Norway	ALE, ROC		KR303639 ⊛	KR303674	KR704164	–	–
C. armeniaca	QFA-0635917[4]	ARM2021_23_S3	Canada	ROC	●	*	–	–	–	–
C. armeniaca	QFA-0635924[5]	ARM2021_24	Canada	ALE, RAN		*	–	–	–	–
C. armeniaca	hb. McCune 362853[6]	ARM2021_26_S3	USA	–		MN906274	–	–	–	–
C. armeniaca	GZU hb. 80890	ARM2021_27	**Austria**	–		*	–	–	–	–

C. armeniaca	O-L-195741 (OLICH2348)	ARM2021_28	Norawy	ALE		KY266899 ⊛	–	–	–	–
C. cuprea	**O-L-225862**[7]	**CUP2021_1**	**Norway**	**ATR, STI**		*	–	–	–	–
C. cuprea	O-L-225833[8]	CUP2021_2	Norway	ATR, NOR, STI		*	*	*	*	*
C. cuprea	O-L-179566 (HOLOTYPE)	CUP2021_3	Norway	ATR, NOR, STI		KR303663	KR303690	KR704174	KR303701	–
C. cuprea	O-L-174230	CUP2021_4	Norway	ATR, NOR, STI		KR303659	KR303686	KR704171	KR303698	–
C. cuprea	O-L-175695	CUP2021_5	Norway	ATR, NOR, STI		KR303660	KR303687	–	–	–
C. cuprea	O-L-179616	CUP2021_6	Norway	ATR, NOR, STI		KR303661	KR303688	KR704172	KR303699	–
C. cuprea	O-L-173292	CUP2021_7	Norway	ATR, NOR, STI		KR303662	KR303689	KR704173	KR303700	–
C. livida	**O-L-228165**	**LIV2021_1**	**Norway**	**ATR, STI**		*	–	–	–	–
C. livida	O-L-228169[9]	LIV2021_2_AGL	Norway	ATR, STI		*	*	*	*	*
C. livida	O-L-228182	LIV2021_3	Norway	ATR, STI		*	*	*	–	–
C. livida	O-L-228168[10]	LIV2021_4_CUP	Norway	ATR, NOR, STI		*	*	–	–	–
C. livida	O-L-228124[11]	LIV2021_5_CUP	Norway	ATR, STI		*	–	–	–	–
C. livida	O-L-228138	LIV2021_6	Norway	ATR, NOR, STI		*	–	–	–	–
C. livida	O-L-228126	LIV2021_7	Norway	ATR, STI		*	–	–	–	–
C. livida	O-L-163835 (HOLOTYPE)	LIV2021_8	Norway	ATR, STI		KR303627	–	–	–	–
C. livida	O-L-174237	LIV2021_9	Norway	ATR, STI		KR303654	KR303681	KR704167	KR303693	–
C. livida	O-L-170759	LIV2021_10	Norway	ATR, STI		KR303655	KR303682	KR704168	KR303694	–
C. livida	O-L-180011	LIV2021_11	Norway	ATR, STI		KR3036571	KR303684	KR704170	KR303696	–
C. livida	O-L-170703	LIV2021_12	Norway	ATR, STI		KR303658	KR303685	–	KR303697	–
C. livida	UPS-L-520818	LIV2021_13	Sweden	ATR, STI		KR303656	KR303683	KR704169	KR303695	–
C. melaleuca	**GZU Spribille s.n. 2010**	**MEL2021_1_S2**	**USA**	**ALE, ROC**		**JN009712**	**JN009742**	**JN009679**	**–**	**–**
C. melaleuca	GZU Spribille 27965-B	MEL2021_2_S2	USA	ALE, ROC		JN009714	JN009744	–	–	–
C. melaleuca	GZU Spribille 28707	MEL2021_3_S2	Canada	–		JN009708	JN009738	JN009677	–	–
C. melaleuca	hb. KLGO Spribille 26952	MEL2021_4_S1	USA	PSO, ROC		JN009713	JN009743	JN009680	–	–
C. melaleuca	O-L-184315	MEL2021_5_S1	Norway	PSO, ROC		*	–	–	–	–
C. melaleuca	O-L-195669	MEL2021_6_S1	Sweden	PSO	●	*	–	–	–	–

C. melaleuca	O-L-223736	MEL2021_7_S2	Canada	ALE		*	–	*	–	–	
C. melaleuca	O-L-225948	MEL2021_8_S2	Norway	PSO		*	–	*	–	–	
C. melaleuca	O-L-225855	MEL2021_9_S1	Norway	PSO		*	*	*	–	–	
C. melaleuca	O-L-225813	MEL2021_10_S2	Norway	NOR, ROC	●	*	*	–	–	–	
C. melaleuca	O-L-225777	MEL2021_11_S2	Norway	PSO		*	*	*	–	–	
C. melaleuca	O-L-225773	MEL2021_12_S2	Norway	PSO		*	*	*	–	–	
C. melaleuca	O-L-225783	MEL2021_13_S2	Norway	NOR, PSO		*	*	–	–	–	
C. melaleuca	O-L-225950	MEL2021_14_S2	Norway	NOR, ROC		*	–	*	–	–	
C. melaleuca	O-L-225811	MEL2021_15_S2	Norway	ROC		–	*	*	–	–	
C. melaleuca	O-L-225808	MEL2021_16_S2	Norway	NOR, ROC		*	*	*	–	–	
C. melaleuca	O-L-225834[12]	MEL2021_17_S1	Norway	NOR, ROC		*	*	*	–	–	
C. melaleuca	O-L-225780	MEL2021_18_S2	Norway	PSO	●	*	*	*	–	–	
C. melaleuca	O-L-225814	MEL2021_19_S1	Norway	PSO, ROC		*	–	*	–	*	
C. melaleuca	O-L-225776	MEL2021_20_S2	Norway	PSO	●	*	*	*	–	–	
C. melaleuca	O-L-225949	MEL2021_21_S2	Norway	NOR, ROC		*	*	*	*	–	
C. melaleuca	O-L-225759	MEL2021_22_S2	Norway	ALE, NRA, RAN, PSO		*	*	*	–	–	
C. melaleuca	O-L-225809	MEL2021_23_S1	Norway	PSO		*	*	*	–	*	
C. melaleuca	O-L-225760	MEL2021_24_S2	Norway	ALE, PSO		*	–	*	–	–	
C. melaleuca	O-L-225805	MEL2021_25_S2	Norway	ALE, NOR, ROC		*	–	–	–	–	
C. melaleuca	O-L-225778	MEL2021_26_S2	Norway	PSO		*	*	*	–	–	
C. melaleuca	O-L-225889	MEL2021_27_S2	Norway	ALE, PSO		*	*	*	–	–	
C. melaleuca	O-L-225763	MEL2021_28_S2	Norway	ALE, PSO		*	–	–	–	–	
C. melaleuca	O-L-223724	MEL2021_29_S2	Canada	ALE		*	*	*	–	–	
C. melaleuca	O-L-195518	MEL2021_30_S1	Norway	PSO		*	*	–	–	*	
C. melaleuca	O-L-225748	MEL2021_31_S1	Svalbard	PSO		*	–	–	–	–	
C. melaleuca	O-L-203814[13]	MEL2021_32_ARM	Spain	ALE, ROC		*	–	–	–	–	
C. melaleuca	O-L-160366	MEL2021_33_S2	Norway	ALE		*	–	–	–	–	

CALVITIMELA

C. melaleuca	O-L-228149	MEL2021_34_S1	Norway	PSO, ROC	●	*	–	–	–	–	*CALVITIMELA*
C. melaleuca	O-L-227934[14]	MEL2021_35_AGL	Norway	ATR		*	*	*	–	–	
C. melaleuca	O-L-228170	MEL2021_36_S2	Norway	ALE, NOR, ROC		*	*	*	–	–	
C. melaleuca	O-L-228187	MEL2021_37_S1	Norway	–		*	–	*	–	–	
C. melaleuca	O-L-228175	MEL2021_38_S1	Norway	PSO, ROC		*	–	*	–	–	
C. melaleuca	O-L-228117	MEL2021_39	Norway	ATR, PSO, ROC	●	–	–	–	–	–	
C. melaleuca	O-L-228077	MEL2021_40_S2	Norway	ALE, RAN, PSO		*	–	*	–	–	
C. melaleuca	O-L-228122	MEL2021_41_S3	Norway	ROC	●	*	–	*	–	–	
C. melaleuca	O-L-228123	MEL2021_42_S1	Norway	PSO, ROC		*	–	–	–	–	
C. melaleuca	O-L-228095	MEL2021_43_S1	Norawy	PSO, ROC	●	*	–	–	–	–	
C. melaleuca	O-L-141654 (OLICH394)	MEL2021_44_S1	Norway	PSO, ROC		KR303640	–	–	–	–	
C. melaleuca	O-L-163829 (OLICH403)	MEL2021_45_S1	Norway	PRO, PSO, ROC	●	KR303641	–	–	–	–	
C. melaleuca	O-L-89218 (OLICH396)	MEL2021_46_S1	Norway	PSO, ROC		KR303642	–	–	–	–	
C. melaleuca	O-L-170490	MEL2021_47_S2	Norway	ALE, ROC		KR303643	KR303675	KR704166	**51_19**	–	
C. melaleuca	O-L-159803	MEL2021_48_S2	Norway	ALE, RAN		KR303644	KR303676	KR704165	–	–	
C. melaleuca	O-L-159804 (OLICH395)	MEL2021_49_S2	Norway	ALE, RAN		KR303645	–	–	–	–	
C. melaleuca	O-L-228131[15]	MEL2021_50_CUP	Norway	ATR, NOR, STI	●	*	–	–	–	–	
C. melaleuca	QFA-0623869[16]	MEL2021_51_S1	Canada	ALE, RAN		*	–	–	–	–	
C. melaleuca	QFA-0635918	MEL2021_52_S2	Canada	NOR, ROC	●	*	–	–	–	–	
C. melaleuca	hb. McCune 36870	MEL2021_53_S1	USA	–		MN906284	–	–	–	–	
C. melaleuca	O-L-195711	–	Norway	ALE, ATR	●	–	–	–	–	–	
C. perlata	**hb. Spribille 26544**	**PER2021_1**	**USA**	**NRA, RAN, UN1, UN2**		**KR303647**	–	**KR704154**	**–**	**–**	
C. perlata	hb. Spribille 29105	PER2021_2	USA	NRA, RAN, UN1, UN2		KR303648	–	–	–	–	
C. perlata	hb. KLGO Spribille 29312	PER2021_3	USA	NRA, RAN, UN1, UN3		KR303649	KR303678	KR704155	–	–	
C. perlata	MSC Spribille 39024	PER2021_4	USA	RAN, UN1, UN2		*	*	*	–	–	
C. perlata	O-L-225810[17]	PER2021_5_SP	Norway	ATR, STI	●	*	*	*	*	*	
C. perlata	O-L-225859[18]	PER2021_6_AGL	Norway	ATR, BOU, USN		*	*	*	–	–	

C. perlata	O-L-225740	PER2021_7	Norway	RAN		*	*	*	–	*	*CALVITIMELA*
C. perlata	O-L-225172	PER2021_8	Norway	NRA, RAN, ZEO	●	*	*	–	–	*	
C. perlata	O-L-200938 (OLICH 3933)[19]	PER2021_9_SP	Norway	ATR, STI	●	*	*	–	*	*	
C. perlata	O-L-195661	PER2021_10	Sweden	NRA, RA U1, U2	●	*	–	–	–	–	
C. perlata	O-L-170830	PER2021_11	Norway	NRA, RAN, UN1, UN2	●	*	*	*	*	–	
C. perlata	O-L-163770	PER2021_12	Norway	NRA, RAN UN1, UN2	●	KR303650	KR303679	KR704156	–	–	
C. septentrionalis	**hb. McCune (SX-15820)**	**SEP2021_1**	**USA**	**ATR, STI**		**293_11**	**–**	**–**	–	**–**	
Calvitimela sp.	O-L-228085[20]	SP_AGL2021_2	Norway	ATR, STI	●	*	*	–	*	–	
Calvitimela sp.	O-L-228094[21]	SP_AGL2021_3	Norway	ATR, STI	●	*	*	–	–	–	
C. talayana	**Herm. 14958**	**TAL2021_1**	**Russia**	**–**		**KR303666**	**–**	**–**	**–**	**–**	
C. talayana	O-L-225288	TAL2021_2	Russia	ATR, NRA, RAN, USN		⊛	*	–	*	–	
C. talayana	O-L-225289	TAL2021_3	Russia	ATR, NRA, RAN, USN		⊛	*	–	*	–	
C. talayana	O-L-126 (HOLOTYPE)	TAL2021_4	Russia	ATR, NRA, RAN, USN		KR303665	–	–	–	–	
C. talayana	O-L-19175	TAL2021_5	Russia	ATR, NRA, RAN, USN		KR303664	–	–	KR303702	–	
C. talayana	QFA-0635921	TAL2021_6	Canada	ATR, BOU, NRA, RAN		*	–	–	*	–	
C. uniseptata	**UPS-L-838893 (ISOTYPE)**	**UNI2021_1**	**Antarctica**	**No subst.**		**–**	**–**	**–**	*	**–**	
Mycoblastus affins	**GZU Spribille 30126 (379)**	**AFF2021_1**	**USA**			**JF744980**	**JF744795**	**JF744898**	**–**	**–**	*MYCOBLASTUS*
M. affinis	GZU Spribille 32102 (AFF465)	AFF2021_2	Austria			JF744977	JF744801	JF744902	–	–	
M. alpinus	**GZU Spribille and Clayden s.n. 2009 (ALP537)**	ALP2021_1	Canada			JF744976	JF744805	JF744901	–	–	
M. alpinus	KGLO Spribille 26781 (468)	ALP2021_2	USA			–	JF744803	JF744904	**–**	–	
M. glabrescens	**GZU Spribille 29848 (GLA92)**	GLA2021_1	USA			JF744967	JF744810	JF744894	–	–	
M. glabrescens	GZU Spribille 30024 (352)	GLA2021_2	USA			JF744985	JF744816	JF744893	–	–	
M. japonicus	UPS Thor 20551 (JAP802)	JAP2021_1	South Korea			JF744983	–	JN009688	–	–	
M. sanguinarioides	**GZU Ohmura 6740 (502)**	**SANO2021_1**	**Japan**			**JN009723**	**JN009748**	**JN009689**	**–**	**–**	
M. sanguinarioides	GZU Spribille & Wagner s.n. (542)	SANO2021_2	Canada			JF744981	JF744806	JF744888	–	–	
M. sanguinarioides	GZU Kantvilas 1/09 (582)	SANO2021_3	Australia			JF744972	JF744819	JF744889	–	–	
M. sanguinarius	**GZU Spribille 31959 and Yakovchenko (772)**	SANG2021_1	Russia			JN009727	JN009751	JN009695	–	–	

M. sanguinarius	UPS Wedin 6932	SANG2021_2	Sweden	—	—	—	AY756403	—	
M. sanguinarius	DUKE 0047513; Lutzoni and Miądlikowska (AFTOL-ID196)	SANG2021_3	Canada	—	—	—	DQ912276	—	
M. sanguinarius	GZU Ohmura 6746 (493)	SANG2021_4	Japan	JF744953	JF744786	JF744866	—	—	
M. sanguinarius	GZU Spribille 30237-I (170)	SANG2021_5	Norway	JF744905	JF744765	JF744843	—	—	
Tephromela atra	**TSB 37924 (L415)**	**ATRA2021_1**	**Greece**	**EU558688**	**JN009753**	**JN009697**	**—**	**—**	
T. atra	GZU Bjork 18057 (TEPH629)	ATRA2021_3	Canada	JF744986	JF744821	JF744875	—	—	
T. atra	GZU Spribille 31797 (850; pertusarioides)	ATRA2021_4	Russia	JN009730[1]	JN009761	JN009701	—	—	
T. atra	TSB 37124 (L228)	ATRA2021_5	Italy	EU558650[1]	JN009755	JN009699	—	—	
T. atra	TSB 37119 (L223)	ATRA2021_7	Italy	EU558648	JN009754	JN009698	—	—	
T. atra	O-L-170530 (342)	ATRA2021_9	Norway	—	KR303691	KR704175	KR303704	—	
T. atra	BG Ekman 3105	ATRA2021_10	Sweden	—	—	—	AY300915	—	
T. atra	DUKE 0047688; Hudson and Hafellner (AFTOL-ID1328)	ATRA2021_11	USA	HQ650607	—	—	DQ986875	—	
T. atra var. calcarea	**GZU Spribille 15951 (628)**	**ATCL2021_1**	**Greece**	**JN009729**	**JN009758**	**JN009700**	**—**	**—**	
T. atra var. calcarea	TSB Muggia (TSB-37912)	ATCL2021_2	Greece	EU558681	JN009759	—	—	—	
T. atra var. calcarea	TSB Muggia (TSB-37461)	ATCL2021_3	Italy	EU558660	JN009760	—	—	—	
T. atra var. calcarea	TSB 37939 (C15)	ATCL2021_4	Italy	EU558608	—	—	—	—	
T. atra var. calcarea	TSB 37914 (L405)	ATCL2021_5	Greece	EU558682	—	—	—	—	
T. atra var. calcarea	TSB 37937 (C14)	ATCL2021_6	Italy	EU558606	—	—	—	—	
T. atra var. torulosa	**TSB 38695 (T1)**	**ATTR2021_1**	**Italy**	**EU558616**	**—**	**—**	**—**	**—**	
T. atra var. torulosa	TSB 38699 (T5)	ATTR2021_2	Italy	EU558620	—	—	—	—	
T. grumosa	**TSB 38686 (G2)**	**GRUM2021_1**	**Italy**	**EU558625**	**—**	**—**	**—**	**—**	
T. grumosa	TSB 37079 (G20)	GRUM2021_2	Italy	EU558635	—	—	—	—	
T. grumosa	TSB 37081 (G22)	GRUM2021_3	Italy	EU558637	—	—	—	—	
T. grumosa	O-L-184061 (327)	GRUM2021_4	Sweden	KR303667	KR303692	—	KR303705		
T. grumosa	MSC Fryday 9429 (MSC-0050468)	GRUM2021_5	Scotland	KF712223	KF730347	—	—	—	
T. grumosa	hb. Soun 141	GRUM2021_6	Check Republic	KF712220	KF730345	—	—	—	

TEPHROMELA

Violella fucata	**GZU Spribille 30276 (835)**	**FUC2021_1**	**Austria**	**JN009733**	**JN009763**	**–**	**–**	**–**	***VIOLELLA***
V. fucata	GZU Spribille 32161 and Wagner (FUC600)	FUC2021_2	Slovenia	JF744968	JF744818	JN009703	–	–	
V. wangii	**GZU Goffinet 10029 (796)**	**WAN2021_1**	**USA**	**JN009734**	**JN009764**	**JN009704**	**–**	**–**	
V. wangii	KUN Spribille 31621 (840)	WAN2021_2	China	JN009736	JN009766	JN009705	–	–	
Alectoria sarmentosa	GZU Spribille s.n. (638)	AS2021_OG1	Canada	JN009706	JN009737	JN009675	–	–	***OUTGROUP***
Cetraria sepenicola	GZU Spribille 32131 & Wagner	CS2021_OG3	Slovakia	JN009715	JN009745	JN009681	–	–	
Hypogymnia physodes	hb. MA-21075	HP2021_OG4	Austria	MT396099	MT416167	MT416180	–	–	
Japewia subaurifera	GZU Spribille & Wagner s.n. (764)	JS2021_OG5	USA	JN009716	–	JN009682	–	–	
Parmelia saxatilis	hb. MA-21076	PS2021_OG6	Austria	MT396100	MT416170	MT416186	–	–	
Protoparmelia badia	GZU Spribille s.n. 2010 (853)	PB2021_OG7	USA	JN009728	JN009752	JN009696	–	–	
Usnea intermedia	GZU Obermayer 11839 (609)	UI2021_OG9	Austria	JN009731	JN009762	JN009702	–	–	

Based on the molecular results the following specimens were wrongly determined: [1]O-L-203822 det: *C. aglaea*, res: *C. armeniaca*. [2]O-L-228193 det: *C. aglaea*, res: *C. cuprea*. [3]Hafellner 71304 det: *C. armeniaca*, res: *C. melaleuca* I. [4]QFA-0635924 det: *C. armeniaca*, res: *C melaleuca* III. [5]QFA-0635924 det: *C. armeniaca*, res: *C. melaleuca* II. [6]McCune 362853 det: *C. armeniaca*, res: *C. melaleuca* III (specimen not seen). [7]O-L-225862 det: *C. cuprea*, res: *C. livida*. [8]O-L-225833 det: *C. cuprea*, res: *C. livida*. [9]O-L-228169 det: *C. livida*, res: *C. aglaea*. [10]O-L-228168 det: *C. livida*, res: *C. cuprea*. [11]O-L-228124 det: *C. livida*, res: *C. cuprea*. 12 O-L-225834 det: *C. melaleuca* I, res: *C. melaleuca* II. [13]O-L-203814 det: *C. melaleuca*, res: *C. armeniaca*. [14]O-L-227934 det: *C. melaleuca*, res: *C. aglaea*. [15]O-L-228131 det: *C. melaleuca*, res: *C. cuprea*. [16]QFA-0623869 det. *C. melaleuca* I, res: *C. melaleuca* II. [17]O-L-225810 det: *C. perlata*, res. *C. sp*. 18 O-L-225859 det: *C. perlata*, res: *C. aglaea*. [19]O-L-200938 det: *C. perlata*, res: *C. sp*. [20]O-L-228085 det: *C. aglaea*, res: *C. sp*. [21]O-L-228094 det: *C. aglaea*, res: *C. sp*. The specimen Spribille 31797 is labeled *Tephromela atra* but is a *T. pertusarioides* as indicated in the table.

Table S2. All individual samples from the four populations of *C. melaleuca* in Norway showing the sequence ID, extraction number, locality information, habitat information, and chemotypes for all samples. The samples that were excluded from calculation of population statistics are indicated in bold and with asterix'.

Identity	ID	SEQ HEADER	Extr nr	Province	District	Locality	Latitude N	Longitude E	Altitude	Habitat	Chemotype
Population 1	1_1	POP1_132_1	10166	**Oppland**	**Dovre**	**Snøhetta**	**62.3197333**	**9.2851833**	**2079 m**	**Exposed in alpine rock**	PSO, RAN, UNF1, UNF2
	1_2	POP1_132_2	10167							**outcrop on moutain rigde**	PSO, UNF1, UNF2
	1_3*	**POP1_132_3***	**10168***							**of Snøhetta**	PSO, RAN
	1_4	POP1_132_4	10169								NOR, NRA, PSO, RAN, UNF1, UNF2
	1_5	POP1_132_5	10170								NOR, NRA, PSO, RAN, UNF1, UNF2
	1_6	POP1_132_6	10171								NRA, PSO, RAN, UNF1, UNF2
	1_7	POP1_132_7	10172								RAN, PSO, UNF1, UNF2
	1_9	POP1_132_9	10174								NRA, PSO, RAN, UNF1, UNF2
	1_10	POP1_132_10	10175								NOR, NRA, PSO, RAN, UNF1, UNF2
	1_11	POP1_132_11	10176								NOR, ROC, UNF1, UNF2
	1_12	POP1_132_12	10177								PSO, RAN, UNF1, UNF2
	1_13	POP1_132_13	10178								PSO, UNF1, UNF2
	1_14*	**POP1_132_14***	**10179***								PSO, RAN, UNF1, UNF2
	1_15	POP1_132_15	10180								PSO, RAN, UNF1, UNF2
	1_16	POP1_132_16	10181								NRA, PSO, RAN, UNF1, UNF2
	1_17	POP1_132_17	10182								NOR, NRA, RAN, UNF1, UNF2
	1_18	POP1_132_18	10183								NRA, PSO, RAN, UNF1, UNF2
	1_19	POP1_132_19	10184								NRA, PSO, RAN, UNF1, UNF2
	1_20*	**POP1_132_20***	**10185***								PSO, RAN, UNF1, UNF2
Population 2	2_2	POP2_184_2	10211	**Trøndelag**	**Bjung**	**Kopparen**	**63.8016333**	**9.7339333**	**285 m**	**Oceanic heath/**	PSO, ROC, UNF1
	2_3	POP2_184_3	10212							**rock outcrop**	PSO, ROC, UNF1
	2_4	POP2_184_4	10213								PSO, ROC, UNF1
	2_5	POP2_184_5	10214								ATR, PSO, ROC, UNF1
	2_6	POP2_184_6	10215								PSO, ROC, UNF1
	2_7	POP2_184_7	10216								ATR, PSO, ROC, UNF1
	2_9	POP2_184_9	10218								PSO, ROC, UNF1
	2_10	POP2_184_10	10219								PSO, ROC, UNF1
	2_11	POP2_184_11	10220								PSO, ROC, UNF1
	2_13	POP2_184_13	10222								PSO, ROC, UNF1
	2_14	POP2_184_14	10223								ATR, PSO, ROC, UNF1
	2_15	POP2_184_15	10224								PSO, ROC, UNF1
	2_16	POP2_184_16	10225								ATR, NOR, PSO, ROC, UNF1
	2_17	POP2_184_17	10226								PSO, ROC, UNF1
	2_18	POP2_184_18	10227								PSO, ROC, UNF1
	2_19	POP2_184_19	10228								ATR, PSO, ROC, UNF1
Population 3	3_1	POP3_276_1	10617	**Norland**	**Saltdal**	**Storengdalen,**	**66.9165**	**15.5418333**	**610 m**	**Boulders in low**	PSO, ROC
	3_2	POP3_276_2	10618			**N slope of Mt**				**alpine heath**	PSO, ROC
	3_3	POP3_276_3	10619			**Satertind,**					PSO, ROC
	3_4	POP3_276_4	10620			**Kvitbekkhumpen**					NRA, ROC, PSO

	3_5	POP3_276_5	10621							PSO, ROC
	3_6	POP3_276_6	10622							ATR, ROC, PSO, U, U
	3_7*	**POP3_276_7***	**10623***							PSO, ROC
	3_8	POP3_276_8	10624							PSO, ROC
	3_9	POP3_276_9	10625							PSO, ROC
	3_10*	**POP3_276_10***	**10626***							PSO, ROC
	3_11	POP3_276_11	10627							PSO, ROC
	3_12	POP3_276_12	10628							ATR, ROC, PSO
	3_13	POP3_276_13	10629							PSO, ROC
	3_14	POP3_276_14	10630							PSO, ROC
	3_15	POP3_276_15	10631							PSO, ROC
	3_16	POP3_276_16	10632							ATR, ROC, PSO
	3_17	POP3_276_17	10633							PSO, ROC
	3_18	POP3_276_18	10634							PSO, ROC
	3_19	POP3_276_19	10635							NRA, ROC, PSO, U
	3_20	POP3_276_20	10636							PSO, ROC
Population 4	4_1	POP4_320_1	10641	**Finnmark**	**Tana**	**Dárjohčohkka, S of and by the foot of Mt Rásttigáisá**	**69.9621333**	**26.3982833**	**375 n**	**Boulders in alpine heath/rock outcrop**	PSO, ROC
	4_2	POP4_320_2	10642								PSO, ROC
	4_3	POP4_320_3	10643								PSO, ROC
	4_4	POP4_320_4	10644								PSO, ROC
	4_5	POP4_320_5	10645								PSO, ROC
	4_6	POP4_320_6	10646								PSO, ROC
	4_7	POP4_320_7	10647								PSO, ROC
	4_8	POP4_320_8	10648								PSO, ROC
	4_9	POP4_320_9	10649								PSO, ROC
	4_10	POP4_320_10	10650								NOR, RA, ROC
	4_11	POP4_320_11	10651								ATR, ROC, PSO
	4_12	POP4_320_12	10652								PSO, ROC
	4_13	POP4_320_13	10653								PSO, ROC
	4_14	POP4_320_14	10654								ATR, ROC, PSO
	4_15	POP4_320_15	10655								PSO, ROC
	4_16	POP4_320_16	10656								ATR, ROC, PSO
	4_17	POP4_320_17	10657								PSO, ROC
	4_18	POP4_320_18	10658								PSO, ROC
	4_19	POP4_320_19	10659								PSO
	4_20	POP4_320_20	10660								PSO

ITS

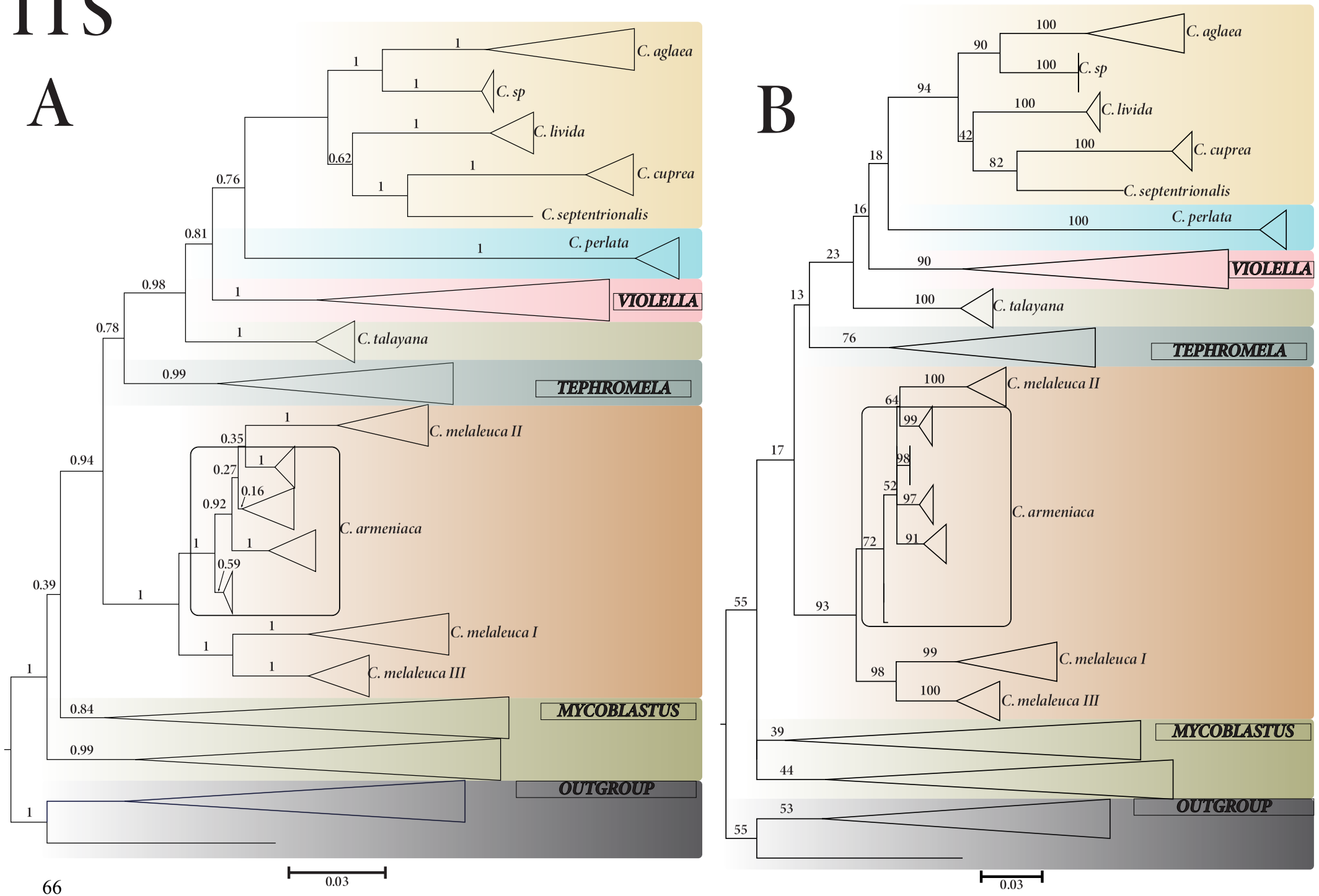
A
C. aglaea
C. sp
C. livida
C. cuprea
C. septentrionalis
C. perlata
VIOLELLA
C. talayana
TEPHROMELA
C. melaleuca II
C. armeniaca
C. melaleuca I
C. melaleuca III
MYCOBLASTUS
OUTGROUP
0.03
B
C. aglaea
C. sp
C. livida
C. cuprea
C. septentrionalis
C. perlata
VIOLELLA
C. talayana
TEPHROMELA
C. melaleuca II
C. armeniaca
C. melaleuca I
C. melaleuca III
MYCOBLASTUS
OUTGROUP
0.03

MCM7

C

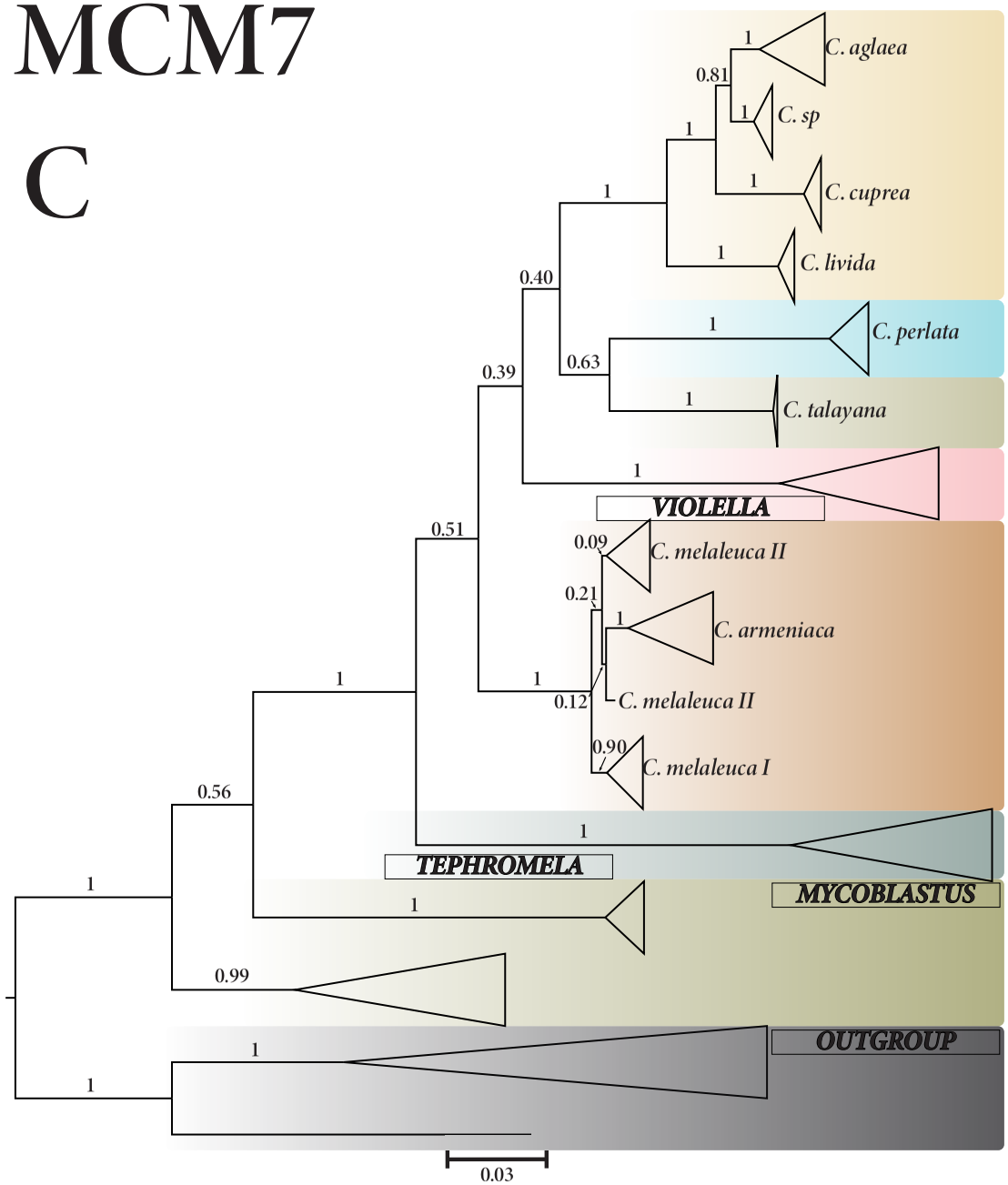
C. aglaea
C. sp
C. cuprea
C. livida
C. perlata
C. talayana
VIOLELLA
C. melaleuca II
C. armeniaca
C. melaleuca II
C. melaleuca I
TEPHROMELA
MYCOBLASTUS
OUTGROUP
0.03

D

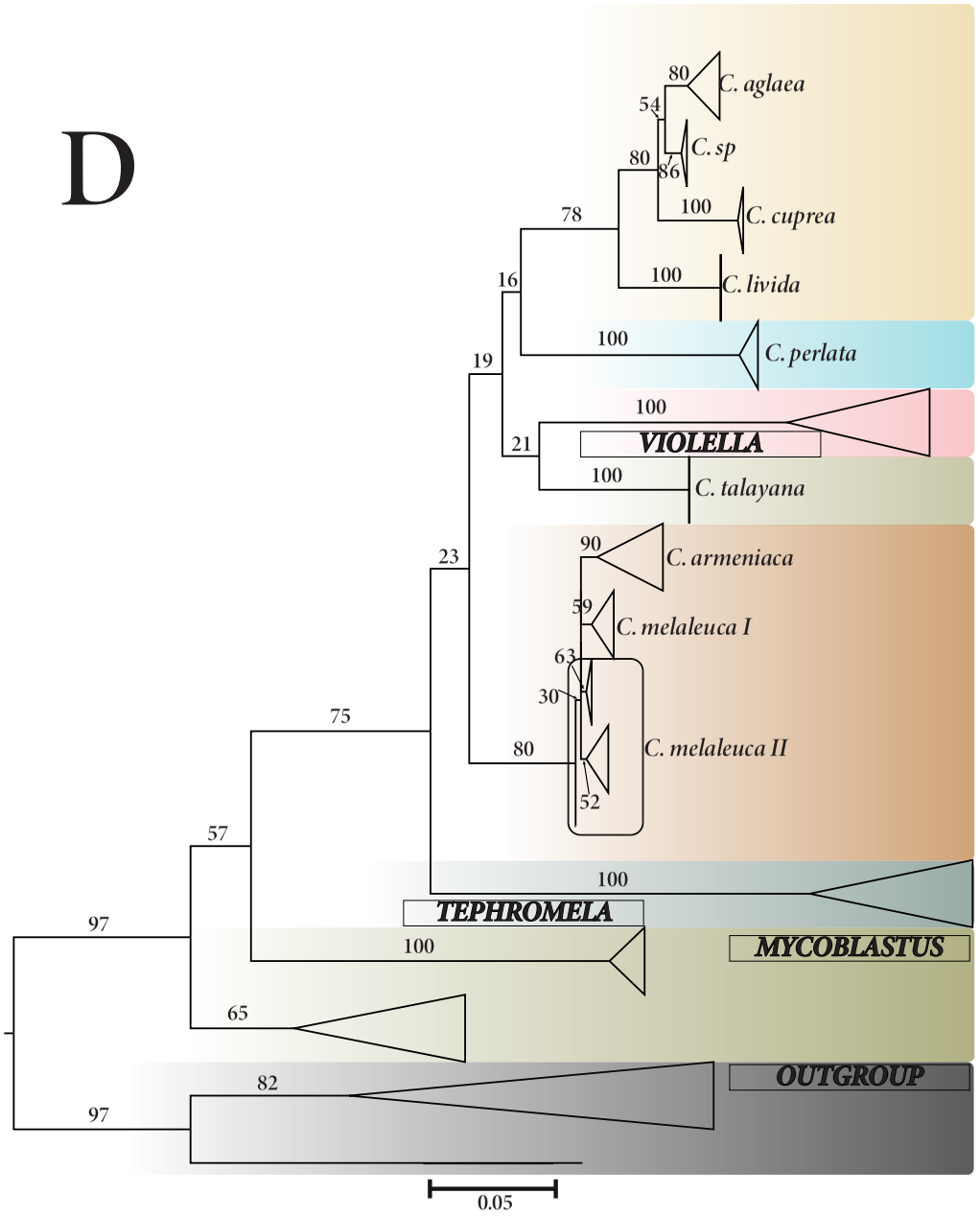
C. aglaea
C. sp
C. cuprea
C. livida
C. perlata
VIOLELLA
C. talayana
C. armeniaca
C. melaleuca I
C. melaleuca II
TEPHROMELA
MYCOBLASTUS
OUTGROUP
0.05

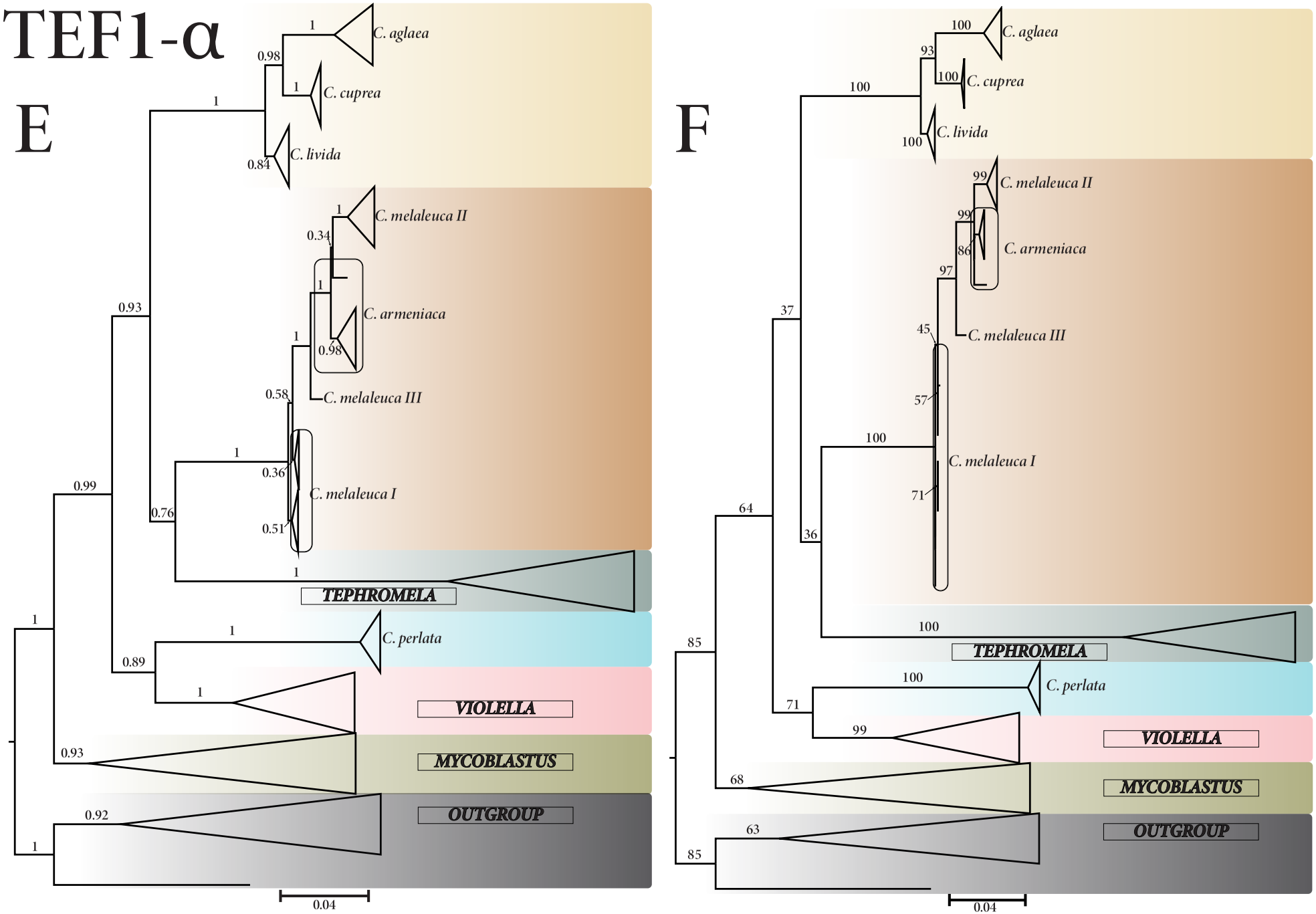

Figure S1. Bayesian consensus phylograms of three nuclear markers: (**A**) ITS, (**C**) MCM7 and (**E**) TEF1-α, with posterior probabilities shown above branches or indicated with an arrow. Maximum likelihood phylograms of (**B**) ITS, (**D**) MCM7 and (**F**) TEF1-α, with bootstrap values from 1000 replicates shown above branches or indicated with an arrow. The same colors as used throughout the thesis indicate the genera and subgenera of the Tephromelataceae. Scale bar representing the number of substitutions per site.

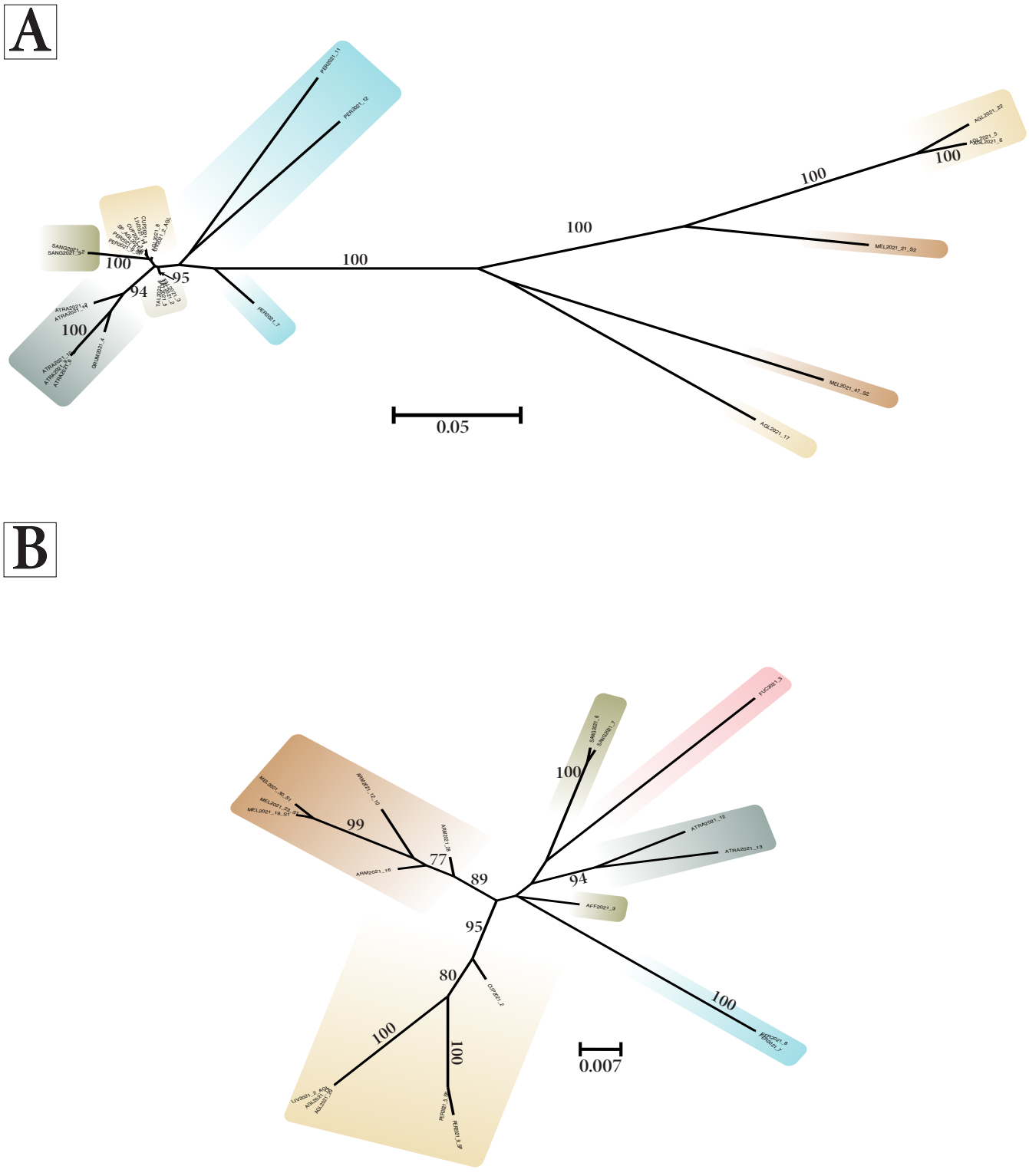

Figure S2. Unrooted Maximum likelihood (ML) topologies from 1000 bootstrap replicates of (**A**) mtSSU and (**B**) LSU. The LSU alignment consisted of 20 accessions and 762 characters, and the mtSSU consisted of 29 accessions and 757 characters. The alignments were partitioned according to the entire fragment lengths and the best fitting substitution model selected using PartitionFinder2 (Lanfear et al. 2016) and the corrected Akaike Information Criterion (AICc) was GTR+I+G for LSU, and GTR+G for mtSSU.

Figure S3. Maximum likelihood topology (ML) from 1000 bootstrap replicates of mtSSU sequences from the genus *Lecania* and *Calvitimela uniseptata* (UPS-L-838893). Sequences were mined from GenBank (All sequences included are labeled with GB accession numbers) and aligned using Muscle (Edgar 2004) in Aliview (Larson 2014), and further trimmed using Gblocks (Castresana, 2000; Talavera & Castresana, 2007). The alignment was partitioned according to the entire fragment length and the best fitting substitution model selected using PartitionFinder2 (Lanfear et al. 2016) and the corrected Akaike Information Criterion (AICc) was TVM+I+G.

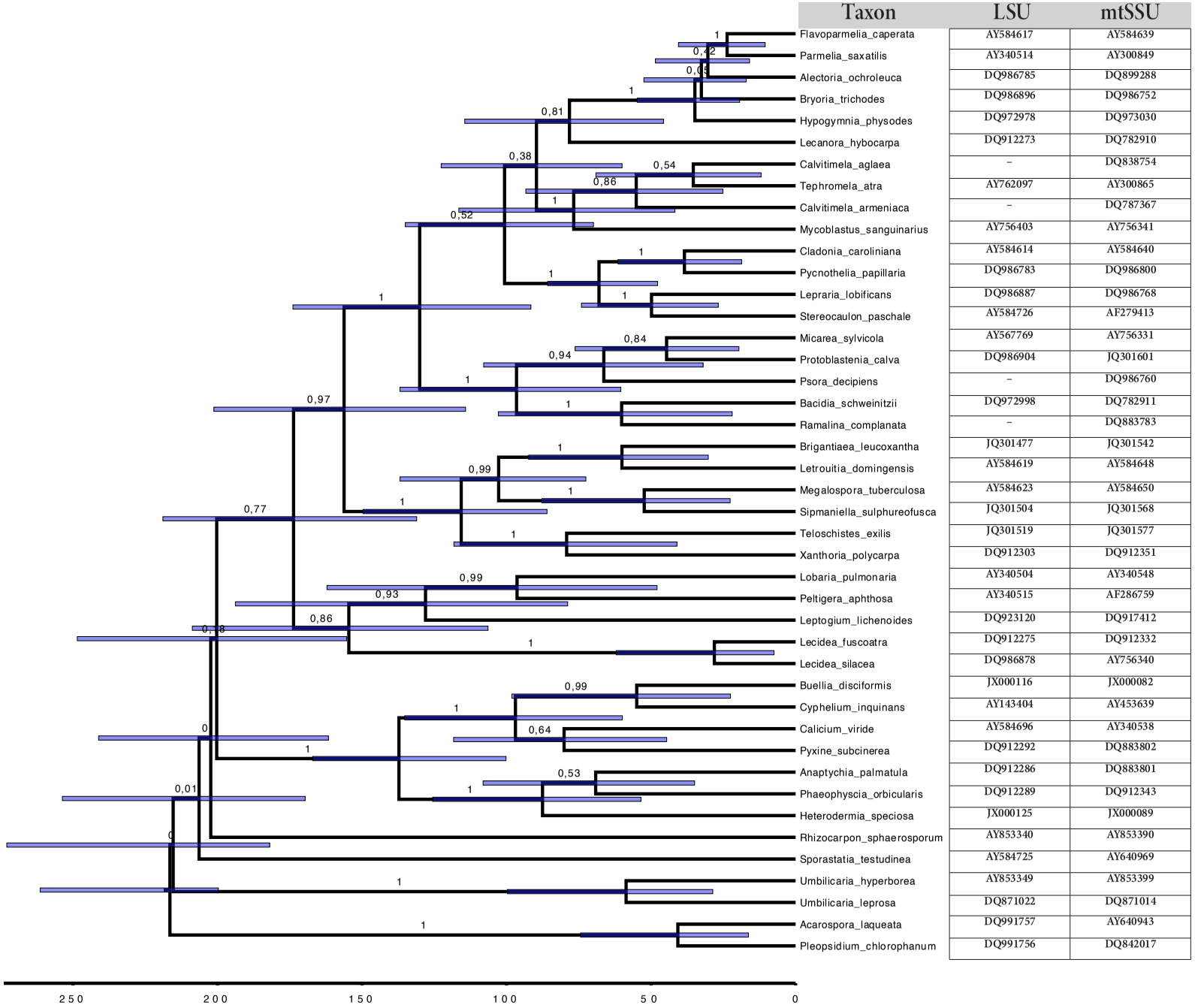

Taxon	LSU	mtSSU
Flavoparmelia_caperata	AY584617	AY584639
Parmelia_saxatilis	AY340514	AY300849
Alectoria_ochroleuca	DQ986785	DQ899288
Bryoria_trichodes	DQ986896	DQ986752
Hypogymnia_physodes	DQ972978	DQ973030
Lecanora_hybocarpa	DQ912273	DQ782910
Calvitimela_aglaea	–	DQ838754
Tephromela_atra	AY762097	AY300865
Calvitimela_armeniaca	–	DQ787367
Mycoblastus_sanguinarius	AY756403	AY756341
Cladonia_caroliniana	AY584614	AY584640
Pycnothelia_papillaria	DQ986783	DQ986800
Lepraria_lobificans	DQ986887	DQ986768
Stereocaulon_paschale	AY584726	AF279413
Micarea_sylvicola	AY567769	AY756331
Protoblastenia_calva	DQ986904	JQ301601
Psora_decipiens	–	DQ986760
Bacidia_schweinitzii	DQ972998	DQ782911
Ramalina_complanata	–	DQ883783
Brigantiaea_leucoxantha	JQ301477	JQ301542
Letrouitia_domingensis	AY584619	AY584648
Megalospora_tuberculosa	AY584623	AY584650
Sipmaniella_sulphureofusca	JQ301504	JQ301568
Teloschistes_exilis	JQ301519	JQ301577
Xanthoria_polycarpa	DQ912303	DQ912351
Lobaria_pulmonaria	AY340504	AY340548
Peltigera_aphthosa	AY340515	AF286759
Leptogium_lichenoides	DQ923120	DQ917412
Lecidea_fuscoatra	DQ912275	DQ912332
Lecidea_silacea	DQ986878	AY756340
Buellia_disciformis	JX000116	JX000082
Cyphelium_inquinans	AY143404	AY453639
Calicium_viride	AY584696	AY340538
Pyxine_subcinerea	DQ912292	DQ883802
Anaptychia_palmatula	DQ912286	DQ883801
Phaeophyscia_orbicularis	DQ912289	DQ912343
Heterodermia_speciosa	JX000125	JX000089
Rhizocarpon_sphaerosporum	AY853340	AY853390
Sporastatia_testudinea	AY584725	AY640969
Umbilicaria_hyperborea	AY853349	AY853399
Umbilicaria_leprosa	DQ871022	DQ871014
Acarospora_laqueata	DQ991757	AY640943
Pleopsidium_chlorophanum	DQ991756	DQ842017

Figure S4. Time calibrated phylogeny of the Lecanoromycetes. A Bayesian maximum clade credibility (MCC) chronogram, from the relaxed clock molecular dating analyses of the nuclear loci LSU, and the mitochondrial mtSSU. The scale axis at the bottom represent age in millions of years (Ma). Node bars indicate the 95% highest density posterior interval (95% HPD) for estimated node ages (Ma). Branch support values are shown above branches as posterior probabilities (PP). All taxa included are indicated with taxon names and their respective GenBank accession numbers for LSU and mtSSU.